Influence of Precipitation, Temperature, and Climate Change on Landslide Hazards in Western Canada

by

Seyed Nima Mirhadi

A thesis submitted in partial fulfillment of the requirements for the degree of

Doctor of Philosophy

in

Geotechnical Engineering

Department of Civil and Environmental Engineering

University of Alberta

Abstract

Canada experiences a significant number of landslides each year, posing substantial risks to safety, infrastructure, economic activities, and the environment. Over the last two and a half centuries, Canada has witnessed approximately 800 fatalities attributed to landslides, which has made landslides the nation's deadliest geological hazard. Furthermore, landslides are estimated to cost the country CA$200 - CA$400 million annually.

This research aims to investigate the relationship between weather conditions (past and future), in particular precipitation, which has shown a high correlation with landslides in Canada from previous studies and landslides in western Canada. Due to the impact of various factors on landslides, such as geological and geotechnical conditions, the relationship between weather and landslides is unique in every region. This relationship has been studied in three locations: (1) The Transportation and Economic Corridors (TEC)’s C018 site, (2) The Yale subdivisions of the Canadian National (CN) Railway network in the Canadian Cordillera, and (3) Parts of the Battle, Red Deer, and Bow Rivers that are located within the Bearpaw Formation in Alberta,

Different approaches and methodologies have been applied for each part of this study. In the first study at the C018 site, which is explained in Chapter 3, the antecedent weather signature that led to each recorded landslide has been investigated. Results show that antecedent precipitation, freeze-thaw cycles, and short-term temperature fluctuations play a significant role in landslide occurrences at the C018 site, and their effect can be quantified from a probabilistic

approach. A clear weather signature has been identified for landslides occurring in the winter months. Moreover, statistical analyses on landslides occurring in spring and summer showed that if there is more than 20 mm of rainfall in 14 days, there is a 6% probability of a landslide, with a 0.1% probability of a landslide if there is less than 20 mm of rainfall in the preceding 14 days. This probabilistic approach provides a means to identify periods when the landslide hazard is 60 times higher than the other periods in spring and summer.

In Chapter 4, I studied the cumulative effects of precipitation on the volume of landslides at the C018 site. The study looks at the correlation between precipitation and landslides between 2018 and 2022. The results show that a linear relationship can be approximated between the annual precipitation and the annual volume of landslides. This relationship is then used to estimate the annual volume of landslides by considering the projected annual precipitation based on the climate change models for the region.

In the next step of understanding the relationship between landslides and weather, a statistical approach is applied to quantify the relationship between monthly precipitation and freeze-thaw cycles and rock fall frequencies for a section of a transportation corridor along the Fraser River in British Columbia, Canada (Chapter 5). von Mises distributions are used to find the best-fitted models to the monthly precipitation and freeze-thaw cycles, and proper relative weights are applied to the models to calibrate them to the rock fall monthly frequency. The calibrated model is then used with the climatic predictions for 2041-2070 and 2071-2100 to see how rock fall distribution will be affected due to climate change in the future decades. Results show that between 9% and 19% more rock fall is anticipated in future winters. Rock falls are expected to decrease in other months, especially in October, November, March, and April.

Finally, in order to evaluate the relationship between climate conditions and landslide activity at a regional scale, I mapped the landslides on parts of the Battle, Red Deer, and Bow Rivers that are located within the Bearpaw Formation in southern Alberta, Canada, and compared their characteristics (Chapter 6). Further investigations into the long-term impact of climate on the formation of river valleys and the Bearpaw Formation reveal that climate is the main factor in causing variations in landslide occurrences across the study areas.

This research enhances our understanding of landslide processes, and importantly, provides a means for predicting landslide frequency and volumes in the next decades as a consequence of climate change. This can prove to be very important information for agency resource allocation towards increasing resiliency in the built environment in the coming decades and promoting sustainable development.

Preface

This thesis is an original work by Seyed Nima Mirhadi and has been written according to the guidelines for the paper-format thesis of the Faculty of Graduate Studies and Research at the University of Alberta under the supervision and guidance of Dr. Renato Macciotta.

As of January 2024, Chapters 3, 4, 5, and 6 of this thesis have been submitted or published in peer-reviewed journals as listed below.

The research presented in Chapter 3 was submitted to the Natural Hazards journal in November 2022 with the following citation:

Mirhadi N, Macciotta R, Gräpel C, Skirrow R, Tappenden K, Probabilistic approach for quantifying weather conditions for landslide occurrences at a 60 m-high weathered rock slope in western Canada. Submitted to "Natural Hazards" on November 21, 2022

The research presented in Chapter 4 was submitted to the Natural Hazards journal in November 2023 with the following citation:

Mirhadi N, Macciotta R, Gräpel C, Assessing the Influence of Precipitation on Landslide Volume in Alberta, Canada: Implications for Climate Change-Driven Landslide Hazards. Submitted to "Natural Hazards" on November 24, 2023

The research presented in Chapter 5 has been published in the Landslides journal in June 2023 with the following citation:

Mirhadi N, Macciotta R (2023) Quantitative correlation between rock fall and weather seasonality to predict changes in rock fall hazard with climate change. Landslides. https://doi.org/10.1007/s10346-023-02105-8

The research presented in Chapter 6 was submitted to the Canadian Geotechnical Journal in August 2023 with the following citation:

Mirhadi N, Macciotta R, Regional scale evaluation of landslide activity and its relation to climate in southern Alberta, Canada. Submitted to "Canadian Geotechnical Journal" on August 28, 2023

For Romina & Manny

Acknowledgements

I extend my heartfelt gratitude to all those who have contributed significantly to the completion of this research and the successful culmination of my Ph.D. journey.

First and foremost, I am deeply indebted to Dr. Renato Macciotta, who has been more than a supervisor to me. His unwavering support and invaluable guidance have been instrumental throughout this research endeavour. Dr. Macciotta's dedication and willingness to always be available for meetings and discussions have not only enriched this work but also shaped my growth as a researcher. Thank you, Renato.

I would like to express my sincere appreciation to Drs. Michael Hendry and Nicholas Beier, the esteemed members of my Ph.D. committee, for their thoughtful comments and guidance throughout the entire journey. Their expertise and constructive feedback have played a pivotal role in shaping the direction and refining the outcomes of this research. Special thanks to Drs. Mustafa Gül and Scott McDougall, the external examiners, for their positive feedback and comments during the final oral exam.

I am also grateful to Mr. Chris Gräpel, for his dedicated time and effort in attending numerous meetings and meticulously reading through the manuscripts. His constructive comments and valuable insights, particularly on the works presented in Chapters 3 and 4 have been incredibly valuable in elevating the quality of this research.

I am also grateful to Dr. Kristen Tappenden and Mr. Roger Skirrow for their insightful comments on the work presented in Chapter 3. Their feedback has significantly enriched the depth and scope of this thesis.

On a personal note, a very special thanks to my wife, Romina, for her unconditional love and support throughout this journey. Her constant encouragement and faith in me have been my

sources of strength, helping me navigate through the challenges that came along the way. Without your support, this would not have been possible, and for that, I am eternally grateful.

Table of Contents

List of Tables

List of Figures

List of Abbreviations

Abbreviation	Extended Form
ACIS	Alberta Climate Information Service
AGDM	Agricultural Drought Monitoring
AGS	Alberta Geological Survey
AT	Alberta Transportation
C2C	Closest Point Method
cal yr B.P.	Calibrated Years Before Present
CN	Canadian National Railway
DEM	Digital Elevation Model
GCM	Global Circulation Model/Global Climate Model
GIS	Geographic Information System
GRMP	Geohazard Risk Management Program
GSC	Geological Survey of Canada
IPCC	Intergovernmental Panel on Climate Change
LiDAR	Light Detection and Ranging
M3C2	Multiscale Model-to-Model Cloud Comparison
PCA	Principal Component Analysis
RCP	Representative Concentration Pathway
TEC	Transportation and Economic Corridors
TESLEC	Temporal Stability and Activity of Landslides in Europe with Respect to Climatic Change
UAV	Unmanned Aerial Vehicle
WMO	World Meteorological Organization

CHAPTER 1

Introduction

Population is increasing in most of the world today and has resulted in rapid urbanization and development around the world. These pressures have not only increased exposure to areas that were already prone to landslides but have also expanded the extent and distribution of landslide-prone regions in several ways. Deforestation and the necessary construction required for the development of the cities are the main causes of landslide-prone areas expansion.

Also, construction in the vicinity of the landslide-prone areas creates several problems for linear infrastructure like roads, railways, power lines, and pipelines. The annual economic impact of prairie landslides is approximately CA$100 to CA$148 million in some parts of the western Canadian sedimentary basin, which includes parts of Manitoba, Saskatchewan, Alberta, British Columbia, and Northwest Territories (Porter et al. 2019). According to Porter et al. (2019), CA$9 to CA$17 million of this amount is estimated direct damage to the railways, and CA$16 to CA$22 million is the estimated damage to the provincial transportation network.

Several reasons may contribute to the occurrence of landslides. Cruden and Varnes (1996) classified these causes into four groups: geological, morphological, physical, and human causes. Each of these causes may increase shear stresses, reduce material strength, or contribute to low strength. In most cases, only one trigger, which is an external stimulus, is needed to cause a near-immediate response in the form of a landslide by increasing the stresses or by reducing the strength of slope materials. These external factors could be intense rainfall, earthquake shaking, volcanic eruption, storm waves, or rapid stream erosion (Wieczorek 1996). In some cases, landslides may occur due to a combination of several causes that gradually bring the slope to a state of failure. In these cases, no apparent attributable trigger can be identified. The most common natural landslide triggers are precipitation, freeze-thaw cycle, shrink-swell cycle, rapid snowmelt, earthquake, and volcanic eruption (Cruden and Varnes 1996; Wieczorek 1996).

High-magnitude earthquakes and volcanic activities are not common in the Canadian Interior Plains and therefore have the least effect on the landslide activity in western Canada. A number of examples of rock falls triggered by strong earthquakes — greater than Richter magnitude (M) 6 — are presented in Wieczorek (1996) and Wyllie (2014). In a study on rock falls and their triggers in the Canadian Cordillera, Macciotta et al. (2015a) found no meaningful relationship between the recorded rock fall events in their database (constrained to a 60 km section of railway) and the low-magnitude (less than M 5) seismic events. This, and the low frequency of large earthquakes, suggest that weather-related factors are the main triggering factors in landslide occurrences in western Canada.

Landslides affect transportation corridors. Managing risks associated with potential landslide events becomes a requirement for economic sustainability as provided by safe and efficient transportation systems. In this regard, adequate knowledge of landslide mechanisms, kinematics, and precursory factors and triggers is necessary for a robust risk management strategy.

1.1 Problem Statement

The effects of climate change are becoming more apparent (IPCC 2021). However, evaluating the potential changes in landslide activity in light of climate change is in the preliminary stages, and the published literature reflects the work needed to understand the potential change in landslide hazard. Due to the impact of various factors on landslides, such as geological and geotechnical conditions, the relationship between weather and landslides is unique in every region. This relationship needs to be quantified to forecast the increase in risks associated with changes in weather due to climate change. Climate change will lead to changes in weather conditions, therefore potentially changing the modes of failure, volumes, and frequencies of landslides, which will impact landslide hazards in a given region. Without this understanding, planning for resiliency in infrastructure and economic activities to manage the increasing risk of landslides becomes guess work.

Despite many studies, which are reviewed in Chapter 2, there is still a knowledge gap in quantifying the relationship between weather and landslides in western Canada. The relationship

between weather data — especially precipitation and freeze-thaw cycle — and landslides in Alberta and British Columbia is investigated in this research program to help close this gap and to be able to plan for risk management. This thesis focuses on the potential change of landslide hazards due to climate change, and not changes in population or infrastructure exposure that could lead to changes in the consequence of landslide events.

1.2 Research objectives

The general objective of this study is to analyze the role of weather conditions, particularly precipitation and temperature, on landslides as the main triggering factor and to assess the effects of climate change on landslide activity in western Canada. To achieve this goal, the following specific objectives are defined:

- Develop methodologies to quantify the change in landslide hazard as a response to changes in weather conditions (precipitation and temperature) at a local scale. These methodologies are illustrated in case studies in southern Alberta and the Canadian Cordillera.
- Develop methodologies to forecast changes in landslide hazard as a response to climate change. These methodologies are illustrated in case studies in southern Alberta and the Canadian Cordillera.
- Develop a methodology to evaluate the changes in regional landslide hazards due to different climate conditions. This methodology is illustrated in a region in southern and central Alberta.

It should be noted that due to the impact of other factors on landslides, the quantitative results of this study could be used only for the study sites and the neighbouring areas where geology, weather conditions, failure mechanisms, and other related characteristics are similar. However, the developed methodologies could be adopted elsewhere.

This research aims to evaluate the correlation between antecedent precipitation and freeze-thaw cycle, as the main triggering factors for landslide activity at local and regional scales in Alberta and British Columbia, Canada.

At the local scale, this research consists of two analyses on landslide activity at a 60 m-high weathered rock slope in Alberta, Canada. A statistical study is done to quantify the correlation between antecedent precipitation and freeze-thaw cycles and landslide activity that allows identifying periods of time in which landslide probability is significantly higher. In the other study, the relationship between the annual volume of the recorded landslides and precipitation is investigated and a climate change model is used to estimate the annual volume of landslides based on the annual predicted precipitation.

A similar study is conducted on the recorded rock falls in a section of the CN's Yale subdivision in the Canadian Cordillera to provide a framework to estimate changes in landslide risk as a response to climate change. This framework can be used by decision-makers to develop risk mitigation plans for the CN railway network in the region.

At the regional scale, landslides on parts of the Battle, Red Deer, and Bow Rivers that are located within the Bearpaw Formation in southern Alberta are mapped by reviewing digital elevation models (DEM), aerial photos, and satellite images, and their characteristics are compared using a geographic information system (GIS) software. In order to find a relationship between the climate conditions and the mapped landslides, 30-year annual precipitation and other factors such as aspect and geology are compared between the river valleys.

The potential changes in landslide probabilities are evaluated for all of the study areas, given the current climate change models and predictions, and based on the previous quantitative correlations between weather and landslides.

1.3 Overview of the study sites

Three study areas have been selected for this research: (1) Transportation and Economic Corridors (TEC)'s C018 site, (s) The Yale subdivision of the Canadian National (CN) Railway network in

the Canadian Cordillera, and (3) parts of the Battle, Red Deer, and Bow Rivers in Alberta that are located within the Bearpaw Formation.

In this section, a general description is provided for each study site. Specific details about each of the study sites are provided in other chapters of this thesis.

1.3.1 C018 site

The C018 site is a 60 m-high rock slope adjacent to Highway 837 on the Red Deer River valley near Drumheller, Alberta, Canada. Figure 1-1 and Figure 1-2 show the location and the south view of the site. The name of the site comes from the geohazard nomenclature used by TEC as part of their Geohazard Risk Management Program (GRMP) (Tappenden and Skirrow 2020).

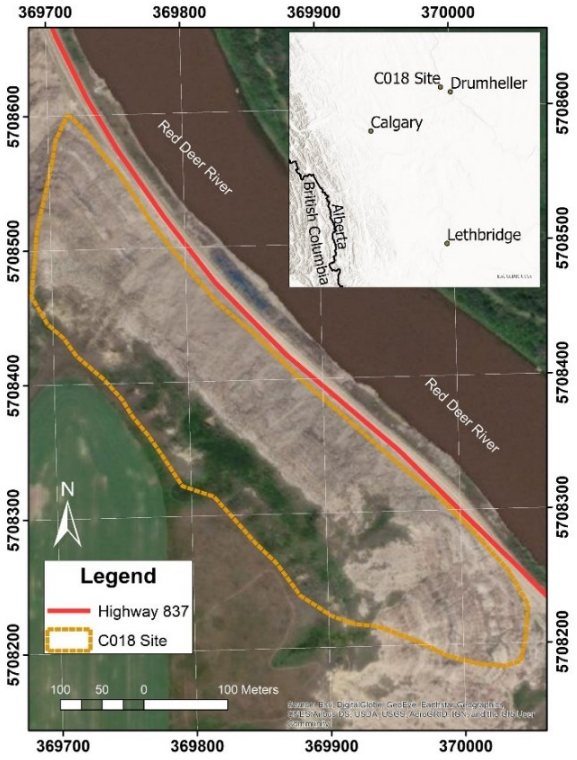

Figure 1-1: Location of the C018 rock slope

Figure 1-2: C018 site south view

The geology of the area corresponds to the Horseshoe Canyon Formation, which includes all strata between the Bearpaw and the distinctive Whitemud sandstone (Hamblin 2004). The Horseshoe Canyon Formation comprises varicolored, sub-horizontal thinly interbedded fine-grained sandstone, siltstone, mudstone, and coal and is well-exposed in the valley of the Red Deer River in the vicinity of the City of Drumheller (Hamblin 2004). Siltstone, sandstone, and coal make up approximately 60%, 30%, and 10% of the strata, respectively (Hamblin 2004). The steep-walled valleys of the Red Deer River are a result of the erosion of meltwater streams and of rivers cutting new channels after diversion from their earlier valleys (Stalker 1973). Consolidated sandstone, ironstone bands, and coal seams make the beds more resistant to weathering, and these commonly form steep valley walls (Stalker 1973).

Previous site investigations at the C018 site revealed that the slide material appears to consist of fine-grained clay-rich soil-like material, a product of bedrock weathering, which is highly erodible and becomes very soft when wet (Klohn Crippen Berger 2000). The types and characteristics of the recorded landslides at this site are explained in Chapters 3 and 4.

1.3.2 CN's Yale subdivision (CN site)

The Yale subdivision is a section of the CN rail network that begins near Boston Bar and continues south along the east bank of the Fraser River, terminating in Vancouver. The study area in this section lies between Boston Bar and Hope and is located along the east bank of the Fraser River Valley. The location of the study site is shown in Figure 1-3.

The study site is located in the Canadian Cordillera, and the geology along this corridor is characterized by the presence of rock units of volcanic, volcaniclastic, sedimentary, and plutonic origin. Several thrust faults associated with mountain building trend northwest-southeast and regional faults and lineaments are also observed with a northeast-southwest trend (Macciotta et al. 2017a). Yale's study area features a north-south oriented fault zone known as the Fraser River fault zone, which creates a highly foliated metamorphosed rock zone (Pratt et al. 2019). The types and characteristics of the recorded landslides at this site are explained in Chapter 5.

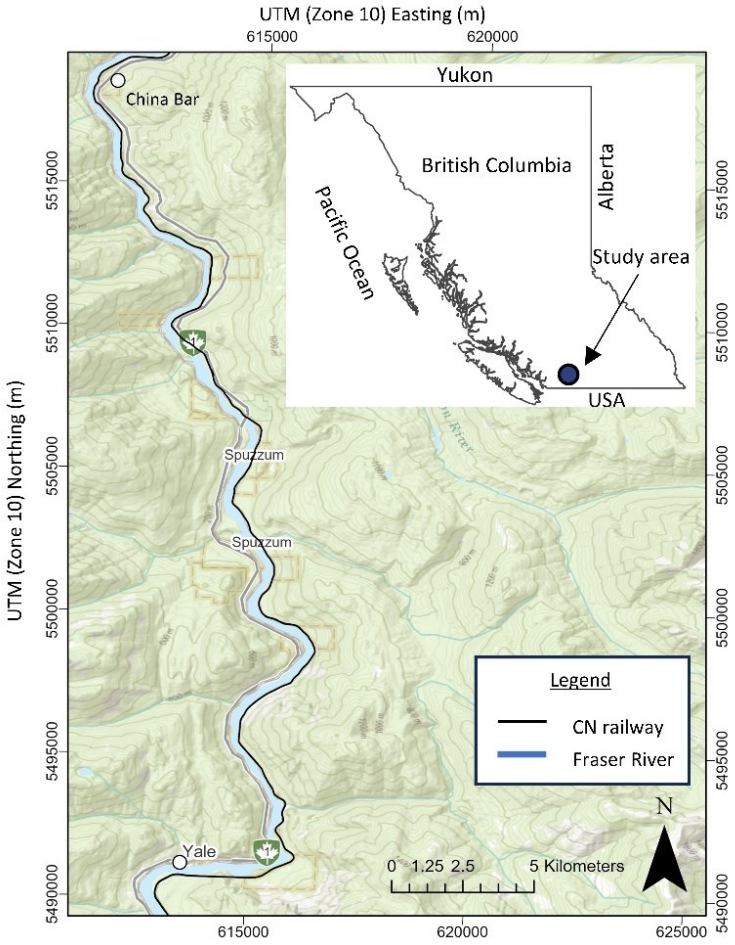

Figure 1-3: CN's Yale subdivision

1.3.3 Regional study area

The regional study area includes parts of the Battle, Red Deer, and Bow Rivers that are located within the Bearpaw Formation in Alberta. The extent of the Bearpaw formation in Alberta and the locations of the study areas are shown in Figure 1-4.

To study the effect of weather and climate on landslides, it is necessary to normalize the impact of other factors affecting landslides, such as bedrock geology. In the regional study of this research (Chapter 6), the selected river valleys are located within the same geological formation and have a similar postglacial history.

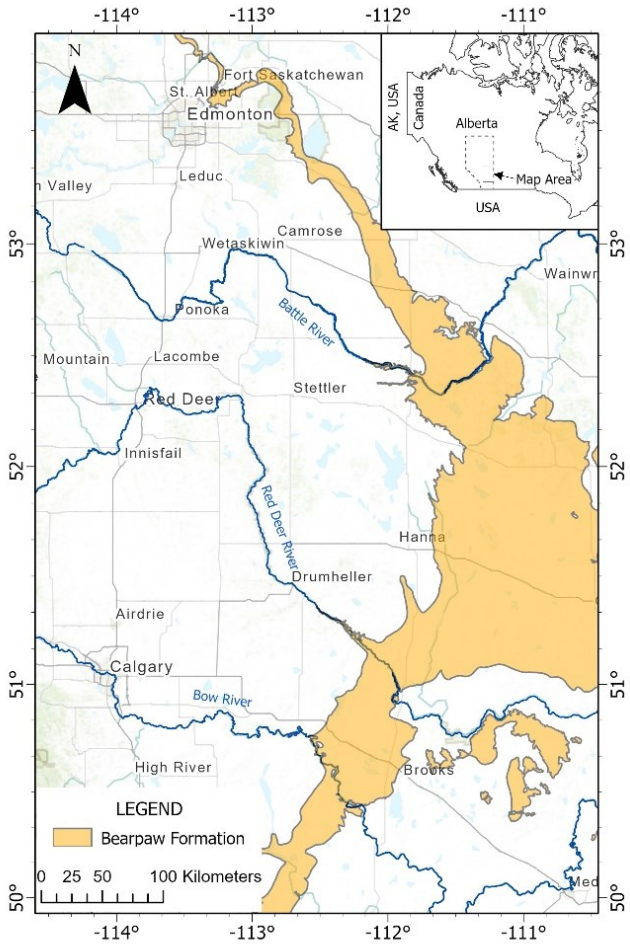

Figure 1-4: Bearpaw Formation and the location of the study areas

The Bearpaw Formation is of marine origin and covers a vast area in Canada and the United States (Allan and Sanderson 1945) and is composed almost exclusively of shale (Russell and Landes 1940). The shale is sub-horizontal dark grey or brownish grey, not very plastic, and tends to weather into small angular fragments or flakes. The weathered shale commonly takes on stains of a rusty colour, less commonly yellowish or indigo blue (Russell and Landes 1940). Stalker (1973) states that the Bearpaw Formation consists of bentonitic green, brown, dark grey, or black shale and minor sandstone. The Bearpaw Formation is less resistant to erosion, and districts underlain by it are typically low and flat (Stalker 1973). The types and characteristics of the mapped landslides in the study areas are explained in Chapter 6.

1.4 Methodology

The specific methodology applied in each study is explained in the corresponding chapter in detail. The following are the general steps followed in order to study the effect of weather and climate on landslides at the *C018 and CN sites:*

- Analysis of the geological and geomorphological conditions of the sites. This is done with the help of the available resources provided by the Alberta Geological Survey (AGS), Geological Survey of Canada (GSC), reports from Transportation and Economic Corridors, the Government of Alberta (TEC) and their consultants, and other published papers. Geological reports and maps are used to extract data about the geological condition of the sites. The procedure of extracting data and drawing the geological section of the local study site in Alberta is described in detail in Chapters 3 and 4.
- Evaluation of the failure modes of the sites. Failure modes and landslide characteristics are evaluated using data available publicly for the provinces of Alberta and British Columbia. Rock fall data are provided by CN for the study site in the Canadian Cordillera. Landslide photos available in the inspection reports are used along with weather data at the time of the landslide to study the failure modes. More details are given in Chapters 3, 4, and 5.
- Evaluation of the current and antecedent weather conditions of the sites. Current and historical weather data are collected from Environment Canada, Alberta Climate Information Service (ACIS), and the ClimateData.ca database. The closest weather stations to the C018 site are selected, and a comprehensive and representative weather database for the site is built based on the correlation coefficients, the number of days with available data, and the distance from the C018 site. The procedure of building a weather database from the eight stations close to the site in Alberta is described in detail in Chapter 3.

Historical weather information at the CN site is collected from the ClimateData.ca database. Details are given in Chapter 5.

- Forward modelling of climate prediction changes and quantifying their effects on the calculated landslide probabilities. Weather predictions are calculated through ClimateAB and ClimateWNA software and ClimateData.ca using different climate models and Representative Concentration Pathways (RCP). Weather databases are generated using the daily or annual precipitations and temperatures predicted by the selected climate model(s) to evaluate the change of landslide probability until 2100. More details are provided in Chapters 3, 4, and 5.
- Statistical analysis of weather and failure conditions. This is done using general statistical methods to calculate the landslide probabilities and changes in the probabilities in light of climate change. The quantitative approaches used in this study include: (1) the ratio of landslides that occurred for a given set of conditions over the total number of times the conditions were present, providing an estimate of the conditional probability of landslide occurrence for a given set of weather conditions, (2) binomial analyses on the relative frequency of landslides and specified thresholds for current and expected weather conditions, and (3) von Mises distributions to find the best-fitted distribution to the monthly normalized weather data. More detailed information is provided in Chapters 3 and 5.
- Change detection analysis is done at the C018 site using DEMs generated from photos taken with an unmanned aerial vehicle (UAV). The UAV has been used since 2017 to collect images for generating surface point clouds. After constructing the point clouds, CloudCompare v2.10.2 (a 3D point cloud processing software) is used to calculate the difference between subsequent point clouds.

For the *regional study area*, the following steps are followed:

- Analysis of the geological and geomorphological conditions of the area. This is done with the help of the available resources provided by the Alberta Geological Survey (AGS), Geological Survey of Canada (GSC), reports, and published papers. Landcover data, geological maps, bedrock geology, and other required data are available in GIS formats. This information is used along with weather data and other landslide characteristics to compare the landslide activity between study areas using ArcGIS.
- Locating and mapping landslides in the river valleys. DEMs are generated from LiDAR data and are used with aerial photos and satellite images to identify landslides in three river valleys based on observable morphological features. More details are presented in Chapter 6.
- Evaluation of the current and antecedent weather conditions of the region. Future and historical weather data are collected from ClimateData.ca. ArcGIS is used to interpolate weather data. The reader is encouraged to refer to Chapter 6 for more information.
- ArcGIS software is used to calculate weather averages and geometrical properties of river valleys and landslides. Characteristics of the river valleys such as slope, height, and aspect are compared. Calculations are made on rasters generated from LiDAR and weather data.
- Statistical evaluation of the landslide characteristics, including frequency, size, and location along the three river valleys. The possible relationship between precipitation and the mapped landslides is evaluated using ArcGIS. Detailed information is available in Chapter 6.

1.5 Thesis Outline

This thesis is structured into seven chapters, including this introductory chapter.

Chapter 2 provides a summary of previous studies with an emphasis on landslides and their relationship with weather and climate in Western Canada. Since this thesis is structured in a paper-based format, each chapter includes its relevant literature review.

Chapter 3 presents the study conducted to quantify weather conditions contributing to landslide occurrences at the C018 rock slope in Alberta. The study also investigates the impact of climate change on the landslides at this site over the next decades.

Chapter 4 investigates the relationship between landslide volumes and precipitation at the C018 site. Climate change models are used to predict landslide volumes in the next decades.

Chapter 5 presents a quantitative correlation between rock fall and weather seasonality to predict changes in rock fall hazard with climate change at the CN site in the Canadian Cordillera.

Chapter 6 evaluates the relationship between landslide activity and climate on a regional scale for three different study areas in Southern Alberta.

Finally, Chapter 7 provides a summary of the conclusions drawn from this research program, along with recommendations for future research.

CHAPTER 2

Literature Review

This chapter reviews the previous studies on landslides and their relationship with weather, especially precipitation and freeze-thaw cycle. The first part of this chapter discusses the triggering factors of landslides. The chapter then continues by exploring the relationship between landslides and weather, along with a discussion of the various approaches used in the literature to study this relationship. Finally, the landslide activity and current climate change situation in Canada and its potential effects on the future of landslides are reviewed.

2.1 Landslide triggering mechanisms

Any factor or cause that changes the slope to an actively unstable state is considered a trigger (Varnes 1978). Some researchers such as Sowers and Sowers (1970) as cited in Varnes (1978) have defined a landslide trigger as the final action that initiates the failure of a marginally stable slope. As McColl (2022) described, this can be likened to the idiom ‘the straw that broke the camel’s back’.

Table 2-1 shows some examples of the triggering factors and processes involved in the occurrence of landslides (Varnes 1978; Popescu 1994). Processes have been categorized into geomorphological, physical and human processes following the classification of Popescu (1994). The triggers listed in Table 2-1 can reduce the factor of safety of the slope either by reducing the shear strength or increasing the shear stresses.

Table 2-1: Examples of triggering factors and the processes involved in landslides (after McColl 2022)

	Process		
Triggers	Geomorphological	Physical	Human
Rapid increase in porewater pressures		• Rainfall • Thaw of snow/ice	• Undrained loading from rapid emplacement of fill or heavy loads • Artificial reservoir filling
Drawdown of groundwater	• Natural dam breach	• River flood recession	• Rapid lowering of reservoir level
Transitory applied stresses	• Passage of rock avalanche	• Earthquake • Wind	• Machinery vibrations
Reduction in strength		• Permafrost degradation • Weathering • Stress-induced fatigue	
Loading of the slope	• Other landslides	• Vegetation • Precipitation	• Construction materials • Snow sports (snow loading)

In this short literature review section, only those triggers that are related to weather are discussed.

2.1.1 Weathering

Weathering reduces the material strength of a hillslope over time. Weathering happens in all slopes and causes the growth of fractures or the development of a failure surface. In some cases, strength degradation, caused by weathering or other processes such as fatigue and permafrost degradation, can be a possible cause of failure (Wieczorek and Jäger 1996).

According to Durgin (1977), the engineering properties of granite change as weathering continues. Their study shows a relationship between the degree of weathering in granite and the dominant types of landslides. For example, rock falls and rock slides are more common in fresh granitoid, as these landslides are controlled by factors related to jointing. On the other hand, debris flows, debris avalanches, and debris slides are more common in decomposed granitoid – a rock that has undergone granular disintegration. The final stage of weathering of granitic rocks is saprolite, which is a residual granitic rock that is vulnerable to rotational slides and slumps.

Weathering can affect sedimentary formations both physically and chemically. The C018 site and Bearpaw are weathered sedimentary formations in which weathering and other physicochemical reactions can cause several changes (Varnes 1978). For example, water absorption by clay minerals and swelling of montmorillonitic clays decrease the cohesion of clayey soils. Moreover, cracks may appear in clayey soils upon drying, resulting in a loss of cohesion and allowing more water to infiltrate the soil. Drying of shales creates cracks on bedding and shear planes, reducing shale to chips or smaller particles. The removal of cement by solution, frost, and thermal expansion which physically disintegrate sandstone, softening of fissured clays, and the migration of water to the weathering front under electrical potential are other examples of changes that can be caused by weathering (Varnes 1978).

2.1.2 Freeze-thaw processes

The weathering process associated with repeated freezing and melting of moisture and trapped fluid in rock pores is another strength reduction factor in jointed rock masses (Matsuoka and Murton 2008). Pressures generated during the expansion of water upon freezing (ice-wedging) and movement of water towards the freezing point (ice segregation) could be sufficient for fracture propagation. Theoretically, if the water completely fills the spaces in the rock, volumetric

expansion of water during the freezing phase can generate pressures up to 207 MPa inside cracks (Matsuoka and Murton 2008). This pressure can easily fracture any rock.

While ice formation may generate and propagate micro- and macro fractures in rocks, the subsequent warming and thawing may loosen and weaken the fractured rock. This repeated process, known as freeze-thaw cycle, promotes the disintegration of rock and creates favourable conditions for landslides. Freeze-thaw cycle is one of the main preparatory factors contributing to many landslides in regions where temperatures fluctuate around the water freezing point (Macciotta et al. 2015a).

2.1.3 Precipitation

Precipitation especially in the form of rainfall is a major trigger of landslides (Cruden and Varnes 1996; Crozier 2017). Precipitation alters the stress state within a slope by adding weight and changing the groundwater regime. It can also reduce the slope material strength by weakening the bonds holding the slope material and washing away the slope material through internal flow pathways (Cruden and Varnes 1996).

While rainfall is often associated with initiating shallow landslides, it can also cause the failure or movement of deep-seated landslides. However, this typically occurs through longer-duration or seasonal rainfall patterns rather than individual rainfall events (McColl 2022). This distinction arises from the lower permeability and less sensitivity of bedrocks to moisture compared to thin surface soils (McColl 2022). The long-term effects of precipitation on landslide activity on a regional scale are investigated in Chapter 6.

2.2 Different approaches to study the relationship between landslides and weather conditions

This section will review the available approaches for studying landslide hazards and their relationship with weather. In the first part of this section, the qualitative approaches available to study the effects of weather conditions on landslides and their applicability to the current study

will be discussed. The next part will focus on the quantitative methods, and the relevant statistical approaches will be reviewed.

2.2.1 Qualitative approaches to study the effect of weather conditions on landslides

Landslide-weather relationships can be studied through qualitative or quantitative statistical approaches. While quantitative approaches are based on numerical expressions, in qualitative methods, a descriptive outcome provides information about the existing relationship between the occurrence of landslides and antecedent weather conditions.

In direct heuristic methods, the landslide susceptibility or hazard zonation map can be prepared directly in the field by expert geomorphologists or can be created in the office with the help of a geomorphological map (Corominas et al. 2014). In an indirect heuristic method, the landslide susceptibility or hazard zonation map is created using GIS software by combining several factor maps such as lithology, the density of water paths, land use, slope degrees, aspect, etc. that are considered to be important for landslide occurrence (Corominas et al. 2014).

Wolter et al. (2010) investigated the landslides' characteristics and bedrock geology of mass movements located in tributary valleys of the Chilliwack River Valley, BC (Figure 2-1), using qualitative observations and simple statistical tests to study the influence of logging on the landslide type and frequency. They made a landslide inventory by digitizing landslides identified on aerial photos dating from 1941 to 2002 and measured the slope, type, initiation location, aspect, rate, bedrock geology, and size of the landslides. The location of the landslides in the watersheds chosen for their study is shown in Figure 2-1. They concluded that logging had a definite and significant impact on the Chilliwack Valley geography, including the increase in open-slope failures, and landslide rates, an average of nine times greater than natural rates. Although the subject of the Wolter et al. (2010) work is different from this research program, the methodology used in their work is similar to what is employed in Chapter 6 of this research.

In another qualitative study, Reid and Page (2003) studied the sediment budget for the Waipaoa catchment in New Zealand and evaluated the long-term rates of landslide activity for six landslide-prone areas in the catchment. They used sequential aerial photographs to calculate the number of landslides per unit area that were generated by several storms. They combined these

results with rainfall records to estimate a long-term magnitude-frequency relationship for landslide activity in the region.

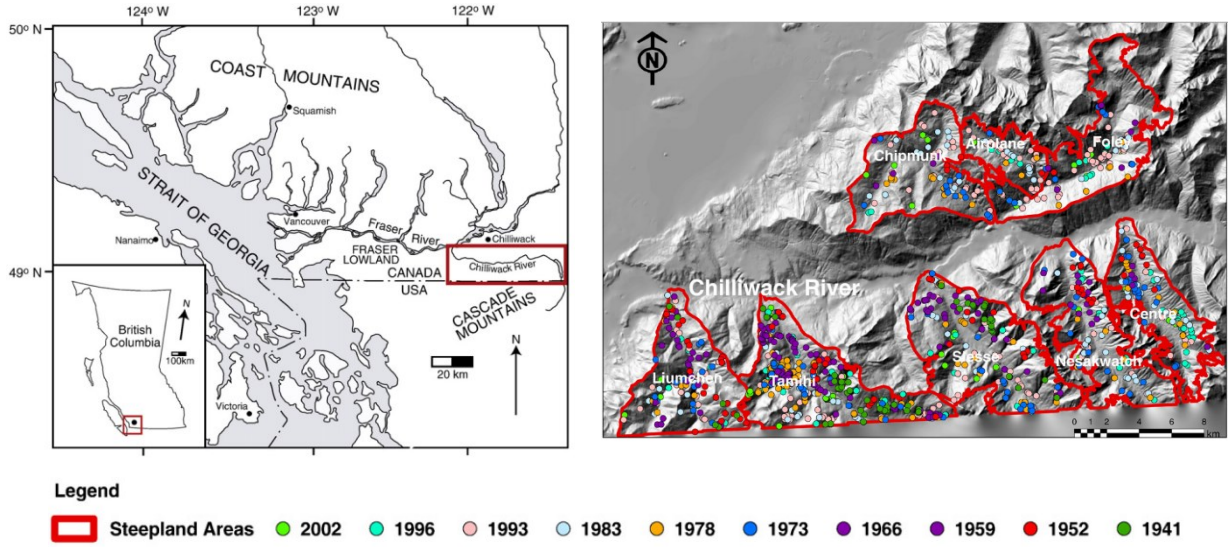

Figure 2-1: Location map of the Chilliwack study area (Left) and landslide locations in different watersheds (Right). Points indicate landslide initiation locations of different airphoto time periods, with respective years given in the legend. (Wolter et al. 2010 with permission).

Kayastha et al. (2013) used the analytical hierarchy process method, which is a semi-quantitative method to generate a landslide susceptibility map for the Tinau watershed in Nepal. They showed that the model's predicted susceptibility levels are in good agreement with past landslides.

Zhu et al. (2018) compared an expert knowledge-based model with a logistic regression model and an artificial neural network model to test their respective performance in mapping landslide susceptibility in two study areas in China. Their comparison, which is shown in Figure 2-2, indicates that the artificial neural network model tends to overestimate and produce maps with higher susceptibility values, while the logistic regression model produces maps with lower susceptibility values. They concluded that the expert knowledge-based method gives better results for landslide susceptibility mapping over large areas.

2.2.2 Quantitative approaches to study the effect of weather conditions on landslides

Several statistical data-driven methods have been used widely for landslide susceptibility mapping or to find the correlations between landslide occurrences and weather conditions.

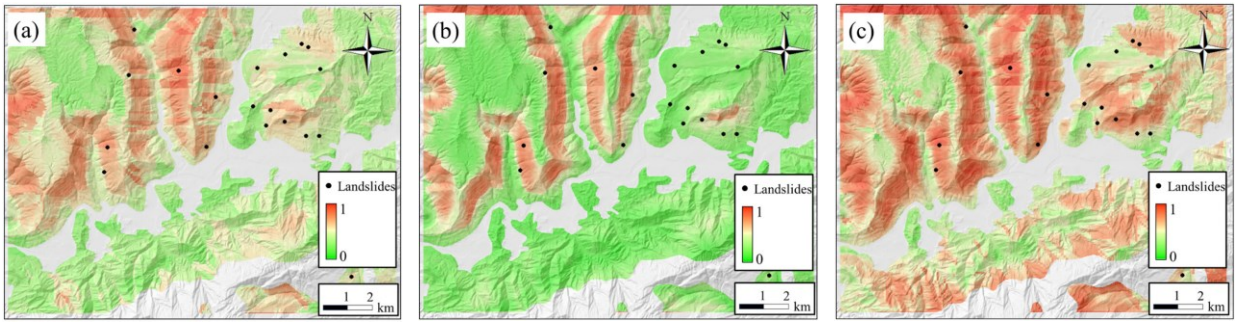

Figure 2-2: Landslide susceptibility maps in the Kaixian study area using different models developed in the Three Gorges area: (a) Expert knowledge-based model; (b) Logistic regression model; (c) Artificial neural network model (Zhu et al. 2018 with permission).

Many researchers have studied the effect of precipitation as a precursory factor and trigger for landslide activity, including rock falls, by defining rainfall thresholds associated with defined periods of time (Iverson and Major 1987; Iverson 2000; Rahardjo et al. 2001; Godt et al. 2006; Guzzetti et al. 2008; Huang et al. 2012; Macciotta et al. 2015a; Rosi et al. 2016; Macciotta et al. 2017a; Brunetti et al. 2018; Martinović et al. 2018; Bhardwaj et al. 2019; Macciotta 2019; Pratt et al. 2019; Weidner et al. 2019; Leyva et al. 2022).

Martinović et al. (2018) used an empirical method to develop rainfall thresholds for the landslides that occurred on engineered slopes on the Irish Rail network earthworks. They analyzed a database including 35 landslides and observed that a ten-day antecedent rainfall exhibits a strong relation with critical event rainfall and is suited for determining landslide-triggering conditions.

In another study, Bhardwaj et al. (2019) studied the June 2013 series of landslides that occurred following a two-day extreme rainfall event in Mandakini Catchment, India. They used the two-day total precipitation and 515 landslides that occurred after the monsoon rainfall to provide a landslide susceptibility map for the region. They found that the antecedent six-day

rainfall prior to the extreme rainfall event had greater impacts on the failures that occurred during the subsequent extreme rainfall. They also found that except for the aspect of slopes, all other factors including elevation, slope, lithology, river buffer, road buffer, and rainfall were statistically significant in causing landslides in the catchment.

Godt et al. (2006) introduced an empirical method to quantify the antecedent moisture conditions and the intensity and duration of the rainstorms in Seattle, WA that led to shallow landslides based on 25 years of hourly rainfall data and recorded landslide events. They designed a decision tree for assigning warnings to the rainstorms based on the antecedent and threshold-exceeding rainfall, and classified rainstorms into three landslide-warning classes. They observed evidence of shallow landslides in 61.5 percent of rainstorms classified within the landslide-warning class.

Guzzetti et al. (2008) established global minimum rainfall intensity-duration thresholds for the initiation of rainfall-induced shallow landslides and debris flows by analyzing 2626 landslide events covering the 89-year period between 1917 and 2005, with the majority of the events (97.5%) occurring between 1950 and 2005. Their findings indicated that antecedent rainfall and soil moisture conditions may become important for the initiation of shallow slope failures when rainfall events exceed approximately 48 hours. Additionally, they found that for the same rainfall duration, higher mean rainfall intensity is required to initiate landslides in areas with mountain climate than in areas characterized by mid-latitude climate.

In a similar attempt to set a series of thresholds for the initiation of the landslides, Mateos et al. (2012) studied the effects of rainfall and freeze-thaw cycles on 34 landslides recorded between 2008 and 2018 at the Tramuntana Range in Majorca, Spain. Based on the daily rainfall and temperature collected from 36 weather stations, they found that the recorded rock falls took place under two circumstances: (1) after occurrences of intense rain >90 mm/24 h, regardless of the temperature, and (2) they started in saturated rocky massifs (accumulated rain >800 mm) when there were several freeze-thaw cycles in the days prior to the failure, regardless of whether the maximum daily rainfall was overly intense (around 30 mm).

2.3 Landslides in western Canada

Numerous landslides happening every year in Canada pose significant risks to safety, economic activity, and the environment. According to Blais-Stevens (2020), a total of 774 individuals have died in 157 events between 1771 and 2018 across Canada which makes it the most deadly geological hazard in the country historically. Moreover, landslides are estimated to cost (direct and indirect) the country CA$200 - CA$400 million annually (Natural Resources Canada 2017). Porter et al. (2019) estimated that the annual financial impact of landslides in the western Canadian sedimentary basin ─ which includes parts of Manitoba, Saskatchewan, Alberta, British Columbia, and Northwest Territories ─ is approximately CA$100 to CA$148 million, of which CA$9 to CA$17 million is estimated direct damage to the railways, and CA$16 to CA$22 million is the estimated damage to the provincial transportation network. Examples of the landslides in western Canada that affected the transportation corridors are shown in Figure 2-3.

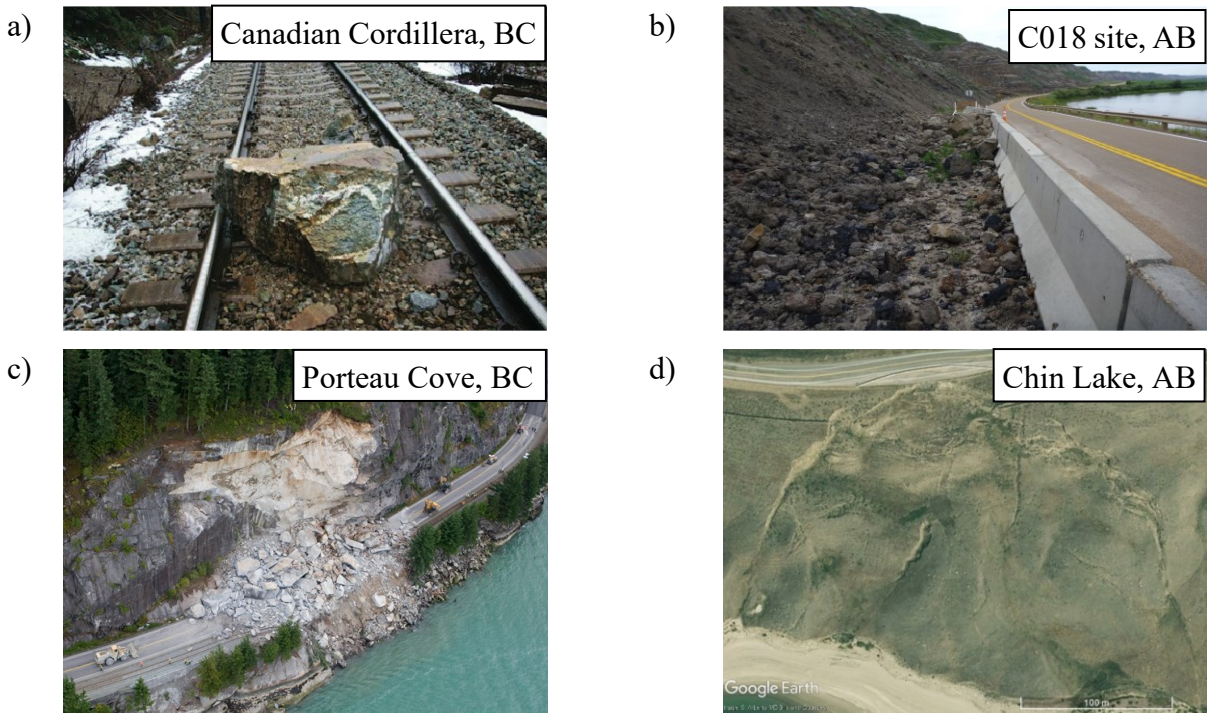

Figure 2-3: Examples of landslides in western Canada. A rock fall in Canadian Cordillera impacting CN railway (Macciotta et al. 2015b - with permission) (a), Rock fall on a river valley near Drumheller, Alberta (Klohn Crippen Berger 2019) (b), 2008 rock fall incidence north of Porteau Cove in British Columbia (Natural hazards learning resources at EOAS 2022) (c), and Chin Coulee landslide in Alberta undermining Highway 36 (d)

Figure 2-4 shows the landslide susceptibility map of Alberta provided by Pawley et al. (2017) by considering predisposing factors, including mean annual precipitation. This map shows higher landslide susceptibility along the walls of major river valleys and their tributary channels across Alberta. Although most of these zones are less than 1 km wide, they can extend along one or both valley walls for hundreds of kilometres. Landslide-susceptible terrain along valley walls presents a particular challenge to the development of linear infrastructure such as roads, rail lines, and pipelines (Pawley et al. 2017).

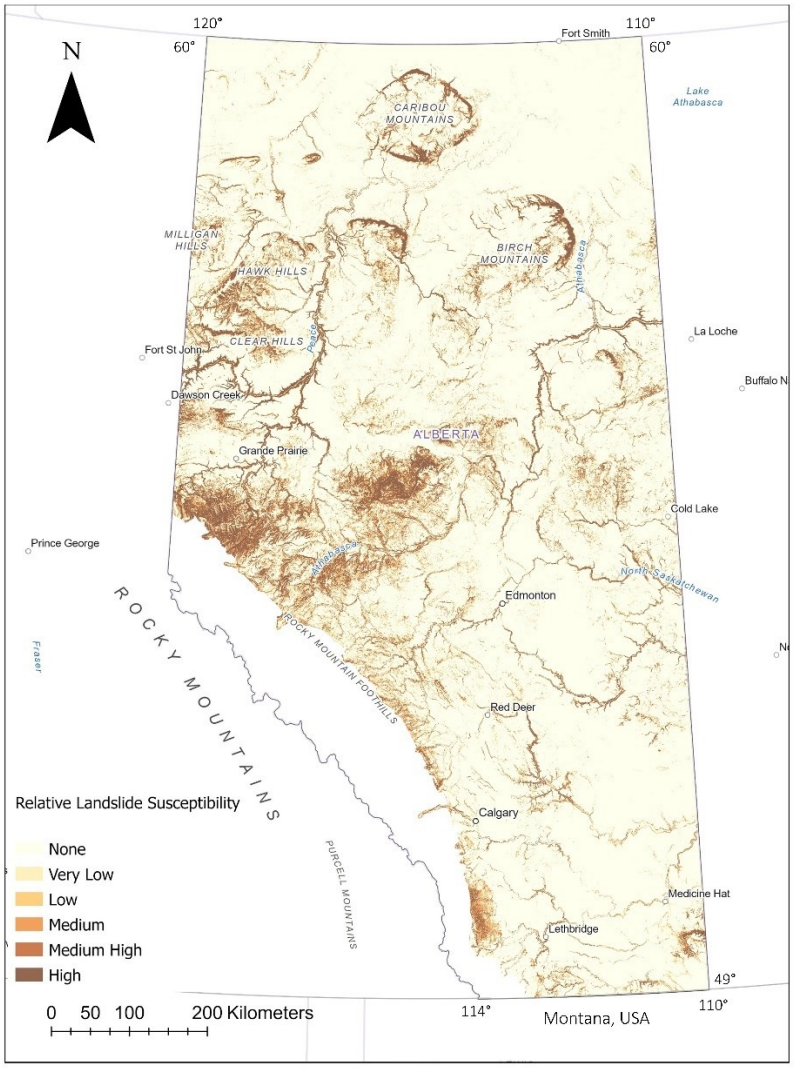

Figure 2-4: Relative landslide susceptibility map of Alberta (after Pawley et al. 2017)

Liang (1999) studied the landslide incidences on the Battle, Red Deer, and Bow Rivers in the Bearpaw Formation in Alberta (same as the study area selected in Chapter 6 of this thesis) to find a relationship between the landslide incidences and microclimate in the region. They compared the north- and south-facing slopes and showed that the landslide incidence is significantly higher on north-face slopes than on south-face slopes in the sections of the Red Deer and Bow Rivers due to the difference in moisture caused by solar radiation. However, in their study, they did not investigate the effect of weather, especially precipitation, on the landslides directly.

The characteristics and geotechnical properties of the Upper Cretaceous argillaceous bedrock in the Interior Plains have been extensively documented by various researchers, including Brooker and Scott (1968) and Thomson and Morgenstern (1979). Preconsolidated clay shales, overconsolidated clays, and overconsolidated plastic clay and clay shales are the most abundant materials of the argillaceous bedrock (Hardy 1957; Bjerrum 1967). Geologists refer to them as poorly indurated argillaceous bedrock, but mostly as shale and silty shale (Mollard 1977). According to Brooker and Scott (1968), the marine Bearpaw Formation contributes significantly to landslides in the Interior Plains. They reported that most shale in the Bearpaw Formation contains 30% to 60% clay and 40% to 70% silt, has a plasticity index between 40% and 80%, and a liquid limit between 65% and 100%.

According to Mollard (1977), retrogressive slope failures in the Interior Plains occur mostly in Upper Cretaceous bentonitic marine clay shale, silty shale, and claystone, commonly with siltstone and sandstone interbeds. These slope failures result in a gradual flattening of the slopes to gradients as low as 4° to 9.5° due to slow movements. These slope failures can be easily identified in air photos or satellite images due to their large dimensions and elongated ridge-and-depression topography. Samples of these slope failures which were identified along the Battle River are shown in Chapter 6 of this thesis. In another study, Thomson and Morgenstern (1979) stated that bentonite seams and the presence of bentonite admixtures are the most important geologic factors affecting the shearing resistance of Upper Cretaceous argillaceous rocks in Alberta, and therefore, one of the main factors in the occurrence of landslides in Alberta.

2.4 Climate change and its effect on landslides in Canada

Climate change has had measurable effects on rainfall and temperature in the last decades, and these effects are forecasted to increase in intensity (Bush and Lemmen 2019; IPCC 2021). Extreme climate events frequently result in costly climate impacts. For example, the 2013 flood in southern Alberta, caused by extraordinary precipitation over three days, resulted in damage valued at billions of dollars (Pomeroy et al. 2016).

Climate change can alter precipitation patterns, temperature, and wind speed and duration (Crozier 2010). According to Bush and Lemmen (2019), warming in Canada is, on average, about double the magnitude of global warming regardless of the emission scenario. Annual and seasonal mean temperatures across Canada have increased, with the greatest warming occurring in winter. According to Figure 2-5, between 1948 and 2012, the best estimate of the mean annual temperature increase was 1.7 °C for Canada as a whole and 2.3 °C for northern Canada (Vincent et al. 2015).

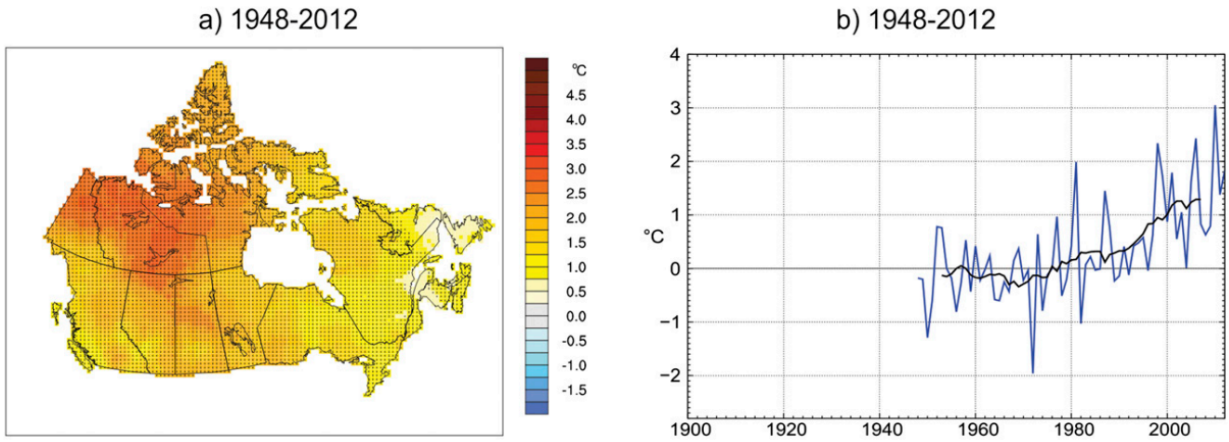

Figure 2-5: Trends in annual mean temperature in Canada for 1948–2012 (a), and Annual mean temperature anomalies (b) (Vincent et al. 2015 with permission)

Bush and Lemmen (2019) showed that most of Canada is expected to experience a general increase in precipitation, with some exceptions where summer rainfall may decrease in specific regions. Many areas across Canada have already witnessed an increase in precipitation, and there has been

a shift toward less snowfall and more rainfall. Projections show an increase in annual and winter precipitation throughout Canada over the 21st century along with some decreases in summer rainfall for parts of southern Canada under a high-emission scenario (Bush and Lemmen 2019).

Figure 2-6 shows the changes in annual total precipitation in Canada during 1948-2012. This figure shows that the northern regions including Yukon, Northwest Territories, Nunavut, and northern Quebec have experienced more increase in annual total precipitation compared to the rest of the country. Meanwhile, some areas in the south including eastern Manitoba, western and southern Ontario, and Atlantic Canada have also experienced significant increasing trends. The anomalies averaged over the country indicate a significant increase of 19% [15%–22%] between 1948 and 2012 (Vincent et al. 2015).

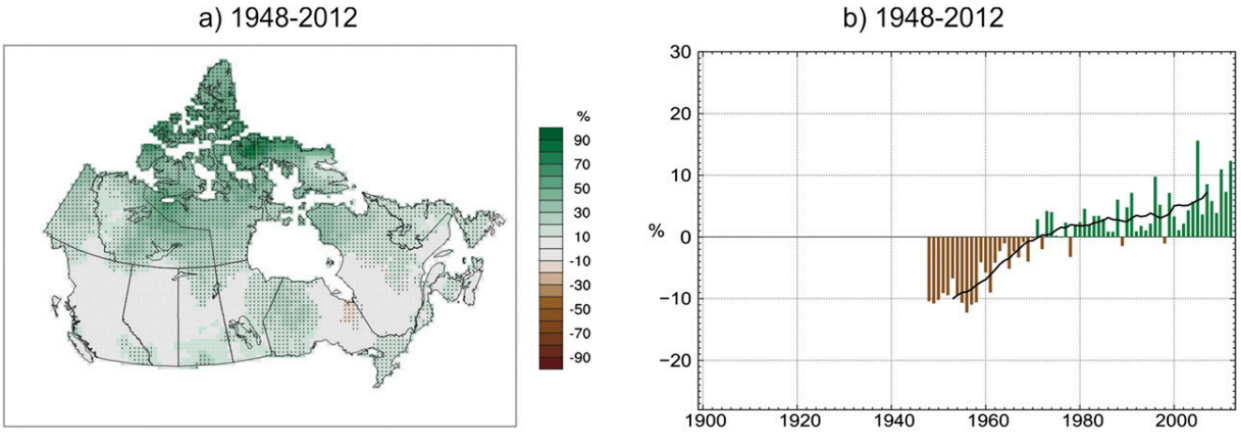

Figure 2-6: Trends in annual total precipitation in Canada for 1948–2012 (a), and Annual total precipitation anomalies (b) (Vincent et al. 2015 with permission)

An enhanced and quantified understanding of how landslide activity is affected by antecedent weather becomes important as the continued change in climate is expected to lead to changes in landslide activity.

Dikau and Schrott (1999) presented the results of the "Temporal Stability and activity of Landslides in Europe with respect to Climatic Change (TESLEC)" project. The project was focused on three main objectives: (1) developing criteria for the recognition of landslides, (2)

reconstructing past distributions of landslide incidents and their relationship to climatic change parameters, and (3) developing a hydrological and slope stability modelling framework using different test sites. Eight study sites in Europe were investigated in the period 1850-2000 to achieve the study objectives. They concluded that due to the complexity of the problem, and the heterogeneity of the available data set, it was not feasible to establish "universal laws" for landslide activity in Europe.

Coe and Godt (2012) identified fourteen technical approaches used in the literature to assess the impact of climate change on landslide activity and placed them in one of three categories: (1) long-term monitoring of climate change and the accompanying landslide response, (2) retrospective approaches that establish links between climate and landslide activity from historical or prehistoric data, and (3) prospective approaches that establish patterns between historical landslide activity and climate records and then use these patterns with downscaled climate projections to predict future landslide activity. Coe and Godt (2012), after reviewing the literature, concluded that because of the difficulty in predicting the frequency and magnitude of short-term extreme storms, studies that attempted to predict the activity of precipitation-triggered shallow landslides and debris flows have the greatest uncertainty. On the other hand, studies that predict landslide activity using air temperature or annual/seasonal precipitation exhibit less uncertainty because there is less difficulty in predicting these variables.

Based on the literature reviewed, the following points can be extracted:

- There are different landslide triggers in western Canada among which geology and weather conditions historically have the greatest impact on landslides. Among the factors related to weather conditions, precipitation plays the predominant role and causes landslides more than the other factors.
- Because of the susceptibility of the geological formation in western Canada to landslides and the annual costs that landslides impose on infrastructure, the region is a suitable location for studying the relationship between landslides and influencing factors.
- One of the most important points in the reviewed literature is the lack of studies on the effects of climate change on landslides. This is while the reality climate change is undeniable and previous studies show that with the current greenhouse gas emissions, the

average annual precipitation in western Canada is expected to increase in the future. Therefore, considering the effect of precipitation on the intensity and frequency of landslides, it is expected that more studies will be conducted in this field.

CHAPTER 3

Effect of Antecedent Precipitation and Freeze-Thaw Cycles on Landslide Occurrences

Contribution of this chapter to the overall study

The geometry, geology, and susceptibility of the C018 slope material to moisture make it susceptible to landslides. Signs of landslides are evident in aerial photos dating back to the 1960s. Due to its proximity to Highway 837 and reports of falling rocks on the highway, the Government of Alberta has been monitoring the slope since 2000. This chapter focuses on the first and second objectives of this thesis, which involve developing a methodology to quantify changes in landslide hazard in response to weather conditions and forecasting changes in landslide hazard as a response to climate change at a local scale. Specifically, this chapter investigates the effects of antecedent precipitation, freeze-thaw cycles, and temperature fluctuations on the landslide occurrences recorded since 2000. This study also evaluates the influence of climate change on landslide activity through a probabilistic approach. The methodology developed in this chapter includes the following steps in general:

- Create a complete weather database that represents the weather conditions at the study site using data available from different weather stations.
- Investigate the relationship between the antecedent weather conditions and the recorded landslides.
- Define different weather thresholds and calculate the probability of occurring a similar landslide over the selected time period for when the weather thresholds are exceeded.
- Use binomial analysis to calculate the annual probability of occurring an exact number of landslides over the selected time period and generate the landslide probability distribution.

- Create new weather databases using available climate models for selected time periods in the future.
- Recalculate the landslide probabilities for the same weather criteria defined earlier in the analysis and generate new landslide probability distributions.
- Study the effects of climate change on landsides by comparing the predicted probability distributions with the distribution generated for the current climate conditions.

A modified version of this chapter was submitted to the Natural Hazards journal in November 2022 with the following citation:

Mirhadi N, Macciotta R, Gräpel C, Skirrow R, Tappenden K, Probabilistic approach for quantifying weather conditions for landslide occurrences at a 60 m-high weathered rock slope in western Canada. Submitted to "Natural Hazards" on November 21, 2022

Abstract

A 500 m long, 60 m high rock slope adjacent to Highway 837 in Alberta, Canada (C018 site) has a long history of landslides, with multiple occurrences of fallen material reaching and blocking the highway. Since 2000, 11 landslides have been reported. Previous studies have shown that a relationship exists between weather conditions and three distinct failure modes at this site: slides of frozen slabs of heavily weathered material, earthflows, and rock falls. Weather data have been analyzed for each recorded landslide, and the corresponding weather signature that led to each landslide has been investigated. Results show that antecedent precipitation, seasonal thawing, and short-term temperature fluctuations all play a significant role in landslide occurrences, and their effect can be quantified from a probabilistic approach. A clear weather signature has been identified for landslides occurring in the winter months. These landslides have occurred after episodes of precipitation that were followed by a decrease in temperature into freezing values with a duration of several days to weeks, and subsequently followed by thawing with temperatures fluctuating around 0°C. Moreover, statistical analyses on landslides occurring in spring and summer showed that if there is more than 20 mm of rainfall in a 14-day period, there is a 6% probability of a landslide, with a 0.1% probability of a landslide if there is less than 20 mm of

rainfall in the preceding 14 days. This probabilistic approach provides a means to identify periods when landslide hazard is 60 times higher than the other time periods in spring and summer. Furthermore, the paper illustrates how this knowledge can be used to enhance our understanding of the potential effects of climate change on landslide risk and quantify the increase in landslide hazard based on climatic predictions.

3.1 Introduction

Landslides can have several causes, including geological and morphological predisposing factors, natural external factors, and human activity (Cruden and Varnes 1996). Among the natural external causes, intense rainfall, rapid snowmelt, prolonged precipitation, ground thaw, freeze-and-thaw weathering, and shrink-and-swell weathering are related to weather conditions that can lead to a landslide event (Cruden and Varnes 1996). Generally, weather-related factors can increase destabilizing forces (e.g., precipitation or thawed water filling open cracks) or decrease the strength of soils and rocks through different mechanisms. These factors can trigger the onset of accelerated movement when excess unbalanced driving forces are present or lead to the detachment of rock blocks from rock slopes.

Many researchers have studied the effect of precipitation as a precursory factor and trigger for landslide activity, including rock falls, by defining rainfall thresholds associated with defined periods of time (Iverson and Major 1987; Iverson 2000; Rahardjo et al. 2001; Godt et al. 2006; Guzzetti et al. 2008; Huang et al. 2012; Macciotta et al. 2015a; Rosi et al. 2016; Macciotta et al. 2017a; Brunetti et al. 2018; Martinović et al. 2018; Bhardwaj et al. 2019; Macciotta 2019; Pratt et al. 2019; Weidner et al. 2019; Leyva et al. 2022). For example, Macciotta et al. (2015a) investigated the relationship between weather conditions and rock fall occurrences on hard rock slopes along a railway section through the Canadian Cordillera. They found that 90% of rock falls could be predicted by the 3-day antecedent precipitation and freeze-thaw cycles. They also noticed that some rock falls not predicted by this 3-day antecedent approach occurred during the first two weeks of the spring thaw.

Freeze-thaw cycle is a cause for physical weathering that weakens the rock structure over time and can occur many times between late fall and early spring when the temperature fluctuates around the water freezing point (i.e., 0°C). During the freezing phase, moisture and trapped water in rock pores undergo a phase transformation from liquid to solid. When water freezes, its volume expands by 9% and therefore opens and expands existing micro- and macro-fractures in the rock matrix. Over time, the repetitive process of freezing and thawing leads to cyclic opening and closing of these fractures, which eventually decreases the rock strength and promotes the occurrence of landslides. Many researchers have studied the effect of freeze-thaw cycles as a landslide trigger on rock slopes (Krautblatter and Moser 2009; Mateos et al. 2012; Arosio et al. 2013; Guo et al. 2014; Macciotta et al. 2015a; Macciotta et al. 2017a; Pratt et al. 2019). Yuan et al. (2021) investigated the degree of soil damage under freeze-thaw cycles and showed that the voids are expanded and further inter-connected as the number of freeze-thaw cycles increases. An experimental study done by Guo et al. (2014) showed that soil cohesion in their samples decreased by about 75% after 5 freeze-thaw cycles. Also, the internal friction angle of their soil samples increased after the first freeze-thaw cycle, then decreased during subsequent cycles by 22% after 5 freeze-thaw cycles.

Krautblatter and Moser (2009) presented a nonlinear model that relates rock fall to rainfall intensity in the German Alps. They observed that rock fall deposition increased by 2 to 218 times during wet freeze-thaw cycles. In another example, Fahey and Lefebure (1988) monitored the bedrock freeze-thaw at an actively eroding site on the Niagara Escarpment in southern Ontario. They concluded that assuming an adequate moisture supply, long periods of comparatively intense freezing followed by temperatures well above 0°C represent the most favourable conditions for debris production. According to Fahey and Lefebure (1988), the duration of the freeze and the intensity are two important factors in a freeze-thaw cycle's effect, where intensity refers to the magnitude of the freezing temperature. They also stated that shorter, more frequent freeze-thaw events, even when accompanied by quite severe freezing intensities, produce less debris. Fahey and Lefebure (1988) concluded that the duration of the freeze is more important than its intensity.

Statistical evaluation of weather conditions can be used as a tool to estimate the probability of a landslide in rock slopes that are actively eroding (Macciotta et al. 2017a; Macciotta 2019). The statistical approaches become more robust when reliable landslide inventories and weather data are available for the study area, and the mechanistic relationship between the landslide activity

and weather conditions is well understood. These approaches become attractive for allocating risk management resources throughout a portfolio of geohazards associated with different risk levels, where more expensive stabilization and protection methods can be suitable for a subset of geohazards, and weather-based hazard warnings can inform decision-making regarding exposure to other geohazards (Macciotta et al. 2017b; Pratt et al. 2019). Bias in landslide records is common, where recorded landslides correspond to volumes large enough to be noticed or consequential (e.g. debris captured behind protective structures as opposed to small individual rock falls) or those affecting infrastructure (e.g. damaging buildings or blocking roads and rail tracks). It is important to leverage the available information, however with the understanding that the recorded phenomena represent an incomplete inventory of landslide activity, favouring events with characteristics that facilitate being noticed and reported.

There are several statistical, data-driven methods that have been widely used for landslide susceptibility mapping, or for correlating landslide occurrences to weather conditions. These models include heuristic models (Barredo et al. 2000; Shu et al. 2019), general statistical models (Macciotta et al. 2015a; Chen et al. 2017; Macciotta et al. 2017a; Huang et al. 2018; Arabameri et al. 2019; Chen et al. 2019; Pratt et al. 2019), and machine-learning models (Song et al. 2012; Kavzoglu et al. 2014; Dehnavi et al. 2015; Hong et al. 2016; Aditian et al. 2018; Chen et al. 2019; Huang et al. 2020). Among these methods, statistical and machine-learning models have been reported more widely in the literature than the heuristic models. Statistical methods such as principal component analysis (PCA) or machine-learning techniques such as neural networks, regression methods, and classification methods have been shown to provide more reliable results when large databases are available (Jolliffe and Cadima 2016).

An enhanced and quantified understanding of how landslide activity is affected by antecedent weather becomes important as the continued change in climate is expected to lead to changes in landslide activity and associated risk. Climate change has had measurable effects on rainfall and temperature in the last decades, and these effects are forecasted to increase in intensity (Bush and Lemmen 2019; IPCC 2021). According to Crozier (2010), climate change can cause an increase in precipitation totals and intensity, temperature, wind speed and duration, and shift in cyclone tracks and other rain-bearing weather systems. Also, shallow failures can be triggered by heavy rainfall due to a reduction in cohesion through decreased capillary suction, or an increase in

porewater pressure, as a result of the formation of shallow perched water tables (Brooks et al. 2004). This suggests that quantifying the relationships between antecedent weather and landslide activity provides an opportunity to understand the potential changes in landslide probabilities, frequencies, and intensity (i.e., landslide volumes) because of climate change. This becomes more important for metastable dormant, or very slowly moving slope failures, which have undergone movement-related strain weakening (Crozier 2010).

I present an analysis of landslide activity at a 60 m-high rock slope adjacent to Highway 837 in Alberta, Canada. The site is known as C018, following the geohazard nomenclature used by Alberta Transportation (AT) as part of their Geohazard Risk Management Program (GRMP) (Tappenden and Skirrow 2020). A statistical approach is presented to quantify the correlation between antecedent weather conditions and landslide activity, to identify time periods in which landslide likelihood is significantly higher, thereby facilitating a risk-based approach for implementing highway warning systems. The paper further evaluates the potential changes in landslide activity given the current climate change models and predictions for the region.

3.2 The C018 site

3.2.1 Location and geologic context

The C018 site is a rock slope located 12 km northwest of the city of Drumheller in central Alberta, Canada, parallel to the Red Deer River valley along Highway 837 (Figure 3-1).

The regional geology corresponds to the Horseshoe Canyon Formation of the Western Canada Sedimentary Basin, which includes all strata between the Bearpaw and the Battle Formations (Hamblin 2004). The Horseshoe Canyon Formation comprises varicolored, thinly interbedded sub-horizontal fine-grained sandstone, siltstone, mudstone, and coal and is well-exposed in the valley of the Red Deer River in the vicinity of the City of Drumheller (Hamblin 2004). Siltstone, sandstone, and coal make up approximately 60%, 30%, and 10% of the strata, respectively (Hamblin 2004). The steep-walled valleys of the Red Deer River are a result of the erosion of meltwater streams and of rivers cutting new channels after diversion from their earlier

valleys (Stalker 1973). Consolidated sandstone, ironstone bands, and coal seams make the beds more resistant to weathering, and these commonly form steep valley walls (Stalker 1973).

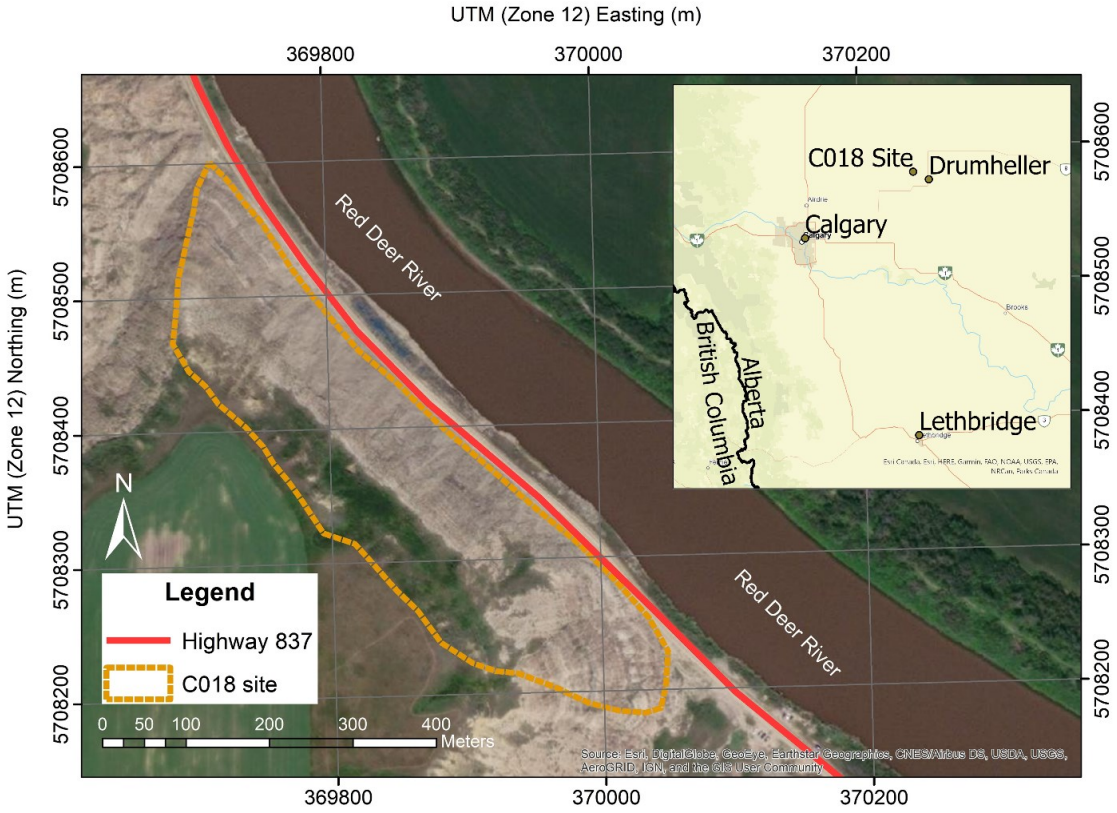

Figure 3-1: Location of the C018 rock slope

Previous investigations at the C018 site revealed that the landslide material (between highway and elevation 725 m) appears to consist of fine-grained, clay-rich, soil-like material, a product of bedrock weathering, which is highly erodible and becomes very soft when wet (Klohn Crippen Berger 2000). Roustaei et al. (2020) investigated the susceptibility of the materials to moisture conditions by performing water reaction tests, slake durability tests, and wetting-drying cycles on rock samples collected from the site. Their study showed significant disaggregation of the samples after being immersed in water for six days and a loss of 11% and 18% of the weight of the samples containing weak sandstones and weak dispersive siltstone after five wetting-drying cycles (Roustaei et al. 2020).

Figure 3-2 presents the geological model for the C018 site, developed from available information and site observations. Geological data below elevation 725 m were transposed from a study done by Hamblin (2004) at the Orkney Hill section, 2.5 km north of the C018 site and adjacent to Highway 837. Stratigraphy from the Orkney Hill study was mapped onto a section of the C018 slope at their corresponding elevations (Figure 3-2).

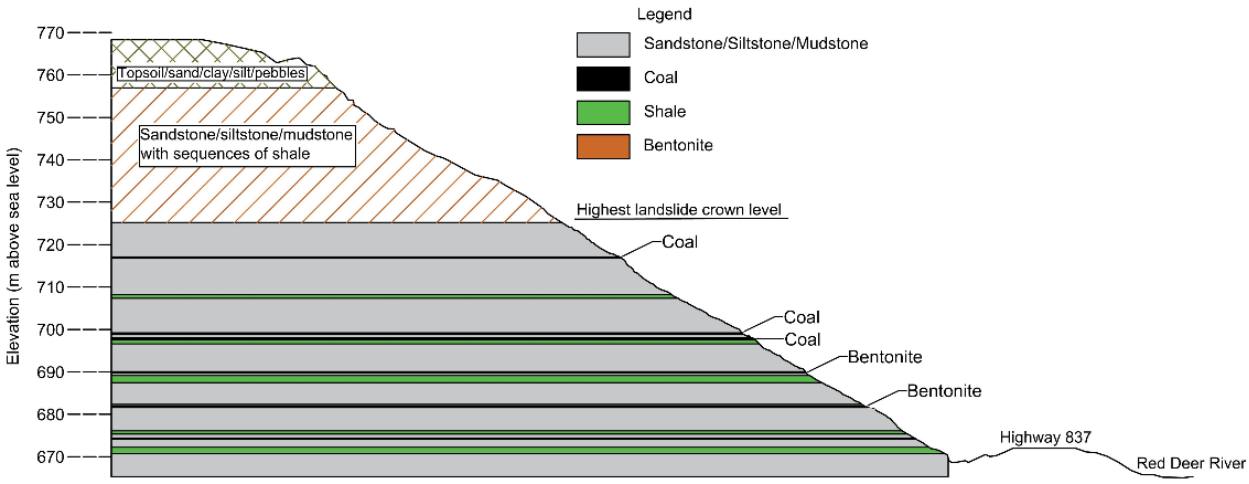

Figure 3-2: Geological section representative of the C018 rock slope

The Orkney Hill section provides geological data below elevation 725 m, which capture the elevations of the recorded landslides at the C018 slope and are consistent with the site observations and previous studies (Klohn Crippen Berger 2000; Roustaei et al. 2020). According to this geological section, sandstone, siltstone, and mudstone make up most of the slope. Thin layers of coal, bentonite, and shale are also evident throughout the slope.

The upper 11 m of the C018 site (above elevation 757 m) consists of topsoil, sand, clay, silt, and pebbles (Curtis Engineering Associates 2009). The middle 32 m (above elevation 725 m and below elevation 757 m) consists of sandstone, siltstone, and mudstone with sequences of shale. No coal or bentonite layer could be identified for the middle 32 m of the C018 site (above elevation 725 m and below elevation 757 m) from the remote information or field observations from the highway level.

3.2.2 Weather

According to the Morrin Agricultural Drought Monitoring (AGDM) station (22 km from the C018 site), and the Drumheller East weather station (16 km from the C018 site) historical databases, the temperatures near the C018 site range from a monthly average low of -15.9°C in February to a monthly average high of 25.0°C in July, with annual extreme temperatures surpassing this range (Figure 3-3). The annual average precipitation is 370 mm of combined snow and rainfall. A summary of the weather conditions, including the minimum, average, and maximum monthly temperatures and precipitation, is provided in Figure 3-3. This figure shows that an average of approximately 170 mm of rain falls from June to August, and the average temperature is below 0˚C from November to the following March. The temperature and precipitation averages are based on the recorded data between 2000 to 2021.

3.2.3 Recorded landslide activity

On July 18, 2000, a site inspection was undertaken at the site following slope and road embankment instabilities on July 14 of that year. The inspection report stated that the landslides had been observed shortly after a period of heavy rainfalls (Klohn Crippen Berger 2000).

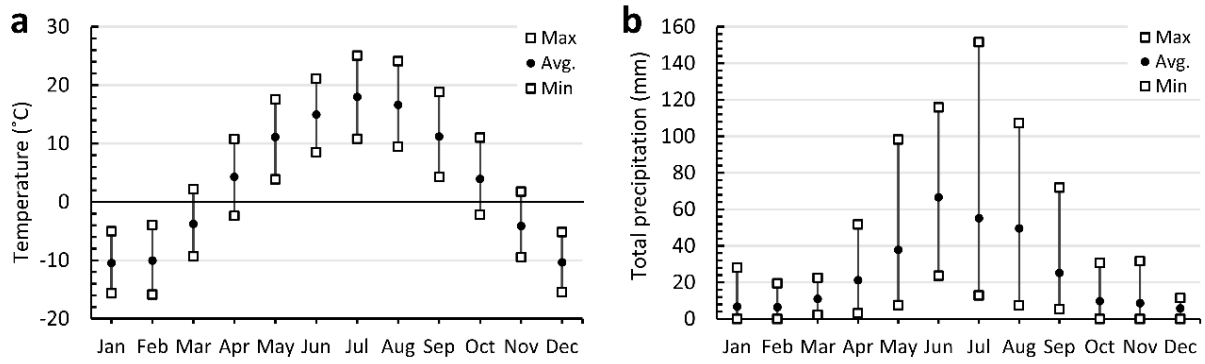

Figure 3-3: Weather summary representative of the C018 area from 2000 to 2021: monthly temperature (a), and total monthly precipitation (b)

A series of annual site inspections were carried out after the July 14, 2000 landslide, to assess the ongoing condition of the highway, the adjacent rock slope, and the riverbank. Since then, AT has recorded 11 landslides at this site, including earthflows, rock falls, and slides of frozen slabs (Alberta Transportation 2021).

According to Roustaei et al. (2020), the continuous weathering of the surficial rock materials, mainly due to precipitation, freeze-thaw cycles, and swelling-shrinking processes of the clay fraction, generates a surficial layer of soil-like materials that experience a continuous process of cohesion loss. They stated that once a critical strength loss is reached, increases in moisture content of the weathered materials in response to infiltration during rainfall and snowmelt events would weaken the weathered soil-like materials, leading to the development of earthflow events with thicknesses corresponding to the penetration of the weathering front into the slope. The type and date of the recorded landslides at the C018 site are shown in Table 3-1.

Table 3-1: Recorded landslides

Date	Type
14-Jul-00	Earthflow
09-May-03	Earthflow
12-Jul-05	Earthflow
01-Jun-07	Earthflow
14-Jun-12	Earthflow
16-May-13	Earthflow
09-Jun-17	Earthflow
13-Dec-17	Slides of frozen slabs of weathered material
22-May-18	Rock fall
10-Jun-18	Rock fall
04-Jan-21	Earthflow

It is noted that this record is biased towards landslide events of enough volume to be noticed and reported by AT maintenance crews, or that generate enough debris to disrupt the highway operations; smaller landslide volumes captured within the highway ditch, which is about two meters wide and half a meter deep, would not typically be reported. Therefore, the weather correlations presented in this paper are derived based on landslide events that impacted highway operations and would not necessarily be representative of smaller-volume landslides. This limitation is acceptable for a study that is intended to inform risk management of the highway. It is worth noting that based on the available data, the annual volume of the recorded landslides between 2018 and 2021 is about 630 m^3.

Figure 3-4a shows a summary of weather data and landslides annual frequency for the C018 site. The monthly frequency of the recorded landslides is provided in Figure 3-4b, which shows that nine of the recorded landslides occurred in spring and summer, and two occurred in winter (December 2017 and January 2021). It is postulated that the winter landslides had different failure mechanisms, factors, and triggers than those that occurred in spring and summer.

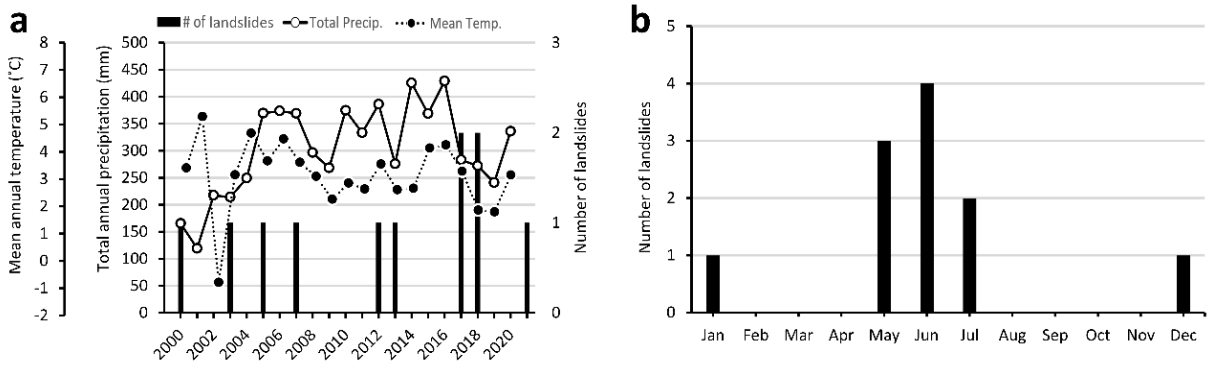

Figure 3-4: Summary of weather data and landslide annual frequency (a), and Landslide monthly frequency (b)

Figure 3-5 shows an elevation view of the site and the location of the recorded landslides, captured via UAV drone photogrammetry. Evidence of scattered landslide events throughout the slope is visible in Figure 3-5. However, most of the recorded landslides have taken place in the northwest portion of the slope.

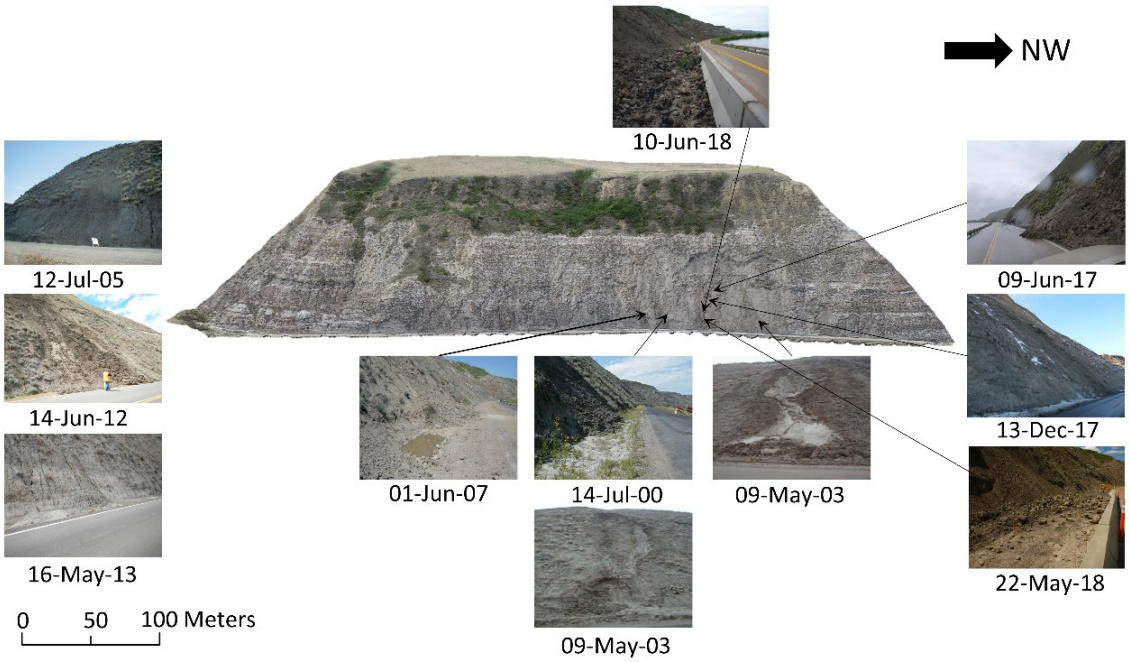

Figure 3-5: Landslides' location. The slope front view is shown from the photogrammetry taken in May 2021. Most of the landslides occurred near the northwest end of the slope. All of the landslides shown in this figure were large enough to reach the highway. After the May 2018 rock fall, jersey barriers were installed to reduce, but not fully mitigate, the potential for debris reaching the highway. Accurate locations of the July 2005, June 2012, and May 2013 landslides were not recorded.

3.3 Methods and materials

3.3.1 Weather database

The eight nearest weather stations to the C018 site were selected to quantify the weather conditions at the site (Figure 3-6). Weather data include hourly and daily temperature and precipitation, which can be accessed through the Alberta Climate Information Service (ACIS) and the Department of Environment and Natural Resources of Canada. Databases available corresponded to the period between January 2000 and December 2021 for daily and hourly weather data (Alberta Climate Information Service 2020; Government of Canada 2020). Data from multiple weather stations needed to be compiled to overcome data gaps. For this purpose, data were compared through

Pearson's correlation coefficient to evaluate the consistency of data among stations and build a comprehensive and representative weather database for the site based on the correlation coefficients, the number of days with available data, and distance from the study site. Pearson's correlation coefficient, which is a number between -1 and +1, describes the linear relationship between two sets of data and is calculated by dividing the covariance of the two variables by the product of their standard deviations. The closer the value of the coefficient is to either -1 or +1, the stronger the relationship between the two variables is (Witte and Witte 2016). The weather stations with the highest Pearson correlation coefficient would be considered the "most consistent" among the full set of data.

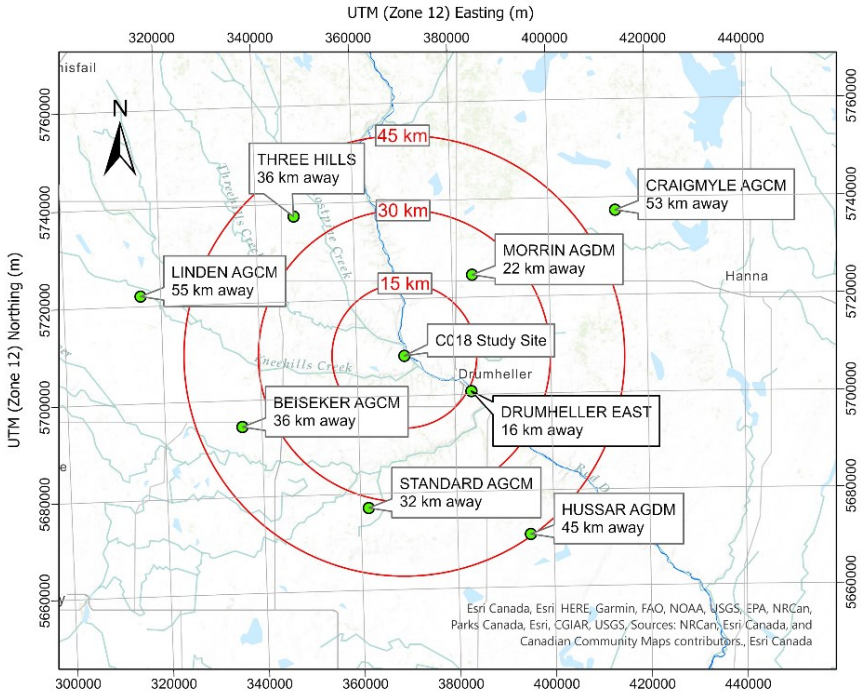

Figure 3-6: Weather stations used in this study

Cumulative precipitation and freeze-thaw cycles

Cumulative precipitation and freeze-thaw cycles were calculated for the periods of 3, 7, 14, 30, 45, 60, and 90 days before each landslide event. Freezing and thawing points were set to -2˚C and +2˚C, respectively, and hourly temperatures were used to determine the occurrence of freeze-thaw

cycles. The -2˚C was chosen to ensure that the freezing front could penetrate into the slope materials, and +2˚C was selected to ensure that the frozen material had enough time to thaw. This approach is consistent with previous studies on rock fall mechanisms (McGreevy and Whalley 1982; Macciotta et al. 2015a; Pratt et al. 2019). One freeze-thaw cycle is counted when the hourly temperature drops below -2˚C (freezing) and then rises above +2˚C (thawing).

3.3.2 Statistical analysis and relevant definitions

Eleven landslides have been recorded at the C018 site with a mean of 0.5 landslides per year. Only those landslides that were large enough to reach the highway and disrupt traffic, or large enough to be noticed filling the ditch were recorded, meaning that several smaller events are likely undocumented. The quantitative approaches used in this study include: (1) the ratio of landslides that occurred for a given set of conditions, over the total number of times the conditions were present, providing an estimate of the conditional probability of landslide occurrence for a given set of weather conditions, and (2) binomial analyses on the relative frequency of landslides and specified thresholds for current and expected weather conditions.

The following definitions are used in this paper:

- Landslide conditional probability - thresholds exceeded: The probability that a landslide occurs if the weather threshold is exceeded.
- Landslide conditional probability - thresholds not exceeded: The probability that a landslide occurs if the weather threshold is not exceeded.
- No-landslide conditional probability - thresholds exceeded: The rate of days when the weather threshold was exceeded but no landslide has occurred (False Alarm).

The analyses on landslides occurring in the spring and summer focused on precipitation. Precipitation thresholds are defined in the results section based on the quantitative evaluation of antecedent precipitation for all recorded landslides. Freeze-thaw cycles are identified as precursory factors, setting the conditions for landslide events in the spring and summer that would be triggered by accumulation of precipitation over the medium and short terms.

Binomial distribution fit

The binomial distribution is a discrete distribution that calculates the probability of exactly x number of successes occurring in n trials and can be described by the following equation (Rhinehart and Bethea 2021):

$$f(x|n) = \binom{n}{x} p^x (1-p)^{n-x},\ x = 0, 1, 2, \ldots, n \quad (3\text{-}1)$$

Where, $f(x|n)$ is the probability of events that are observed in n number of observations, and p is the probability of success in one observation. In my study, p can be the daily probability of a landslide or the daily probability of exceeding a precipitation threshold from January 2000 to December 2021. Occurrence of a landslide, and exceeding precipitation thresholds are two distinct steps considered in this study for quantifying landslide probability.

Pearson's chi-squared (χ^2) test

The χ^2 goodness-of-fit test is used to compare a measured probability distribution to a hypothesized distribution using the following formula (Rhinehart and Bethea 2021):

$$\chi^2 = \sum_{i=1}^{N} \frac{(E_i - O_i)^2}{E_i} \quad (3\text{-}2)$$

Where, χ^2 is the calculated statistic between the recorded and the fitted distributions, E_i is the expected number of observations in the ith histogram bin, O_i is the number of actual observations in the same bin, and N is the number of bins in the histogram. The calculated χ^2 is compared to an upper critical value in the χ^2 distribution considering a selected confidence level, adopted as 95% in this study. Degrees of freedom are equal to $N - k$, where k is the number of model

coefficients or characterizations used in the comparison (Rhinehart and Bethea 2021). In this study, degrees of freedom are considered $N - 2$ which is consistent with the study done by Macciotta et al. (2017a). The hypothesis, that deviations of the data histogram from the probability density function are small, is rejected if the calculated χ^2 exceeds the critical value.

3.3.3 Climate-change models

The ACCESS1.0 GCM, which was developed by Bi et al. (2013) at the Australian Community Climate and Earth System Simulator, and the Representative Concentration Pathway (RCP)4.5 scenario were selected to generate climate-change influenced weather data predictions for the decade 2050-2059 (2050s) and 2080-2089 (2080s). ACCESS1.0 GCM uses atmospheric and land surface components such as radiation scheme, turbulent fluxes of heat and moisture, convection scheme, precipitation microphysics, and cloud schemes to predict the global climate change with a horizontal resolution of 1.25˚ (≈140 km) latitude by 1.875˚ (≈130 km) longitude (calculated at latitude 51 degrees where the study site is located), and 38 vertical levels in the atmosphere (Bi et al. 2013).

The RCPs describe four different 21st century pathways of greenhouse gas emissions and atmospheric concentrations, air pollutant emissions, and land use (IPCC 2014). The Intergovernmental Panel on Climate Change (IPCC) describes RCP4.5 as an intermediate scenario that needs intermediate efforts to constrain the emissions (IPCC 2014). This scenario is within the probable future CO2 emissions and is in line with future fossil fuel productions (Laherrère 2019), which is the reason I selected this scenario in my study. In RCP4.5, emissions peak around 2040 and then decline (Meinshausen et al. 2011). According to the RCP4.5 scenario, the global mean surface temperature is expected to increase by 1.4 ˚C in 2046-2065 and 1.8 ˚C in 2081-2100 relative to the reference period of 1986-2005 (Collins et al. 2013).

The 65-year weather forecast at the C018 site was generated with the ClimateAB v3.21 software package (Wang et al. 2008). ClimateAB is an open-source software based on the methodology described by Mbogga et al. (2010) that uses a 30 arcsecond (approximately 1 km) resolution. This software generates interpolated climate change projections for the 21st century using 23 models including ACCESS1.0-RCP4.5 (Mbogga et al. 2010).

Synthetic weather databases were generated using the seasonal precipitations predicted by the ACCESS1.0-RCP4.5 model to evaluate the change of landslide probability in the 2050s and 2080s. First, a 365-day database was created by averaging daily precipitation (for each date) from January 2000 to the end of December 2021. Second, the difference in total seasonal precipitation between the predicted values and the average database was calculated and then divided by the number of days of each season. Finally, the calculated differences were added to the corresponding values in the original recorded 22-year daily database. The result is a synthetic 22-year database in which the total seasonal precipitation values are equal to those predicted in the ACCESS1.0-RCP4.5 GCM. A limitation of this approach is that it does not capture the increased frequency of extreme precipitation events beyond the 22-year period observed, and that magnitudes of precipitation storm events are only increased by an average estimate over the entire season. This approach, however, does provide a quantified means of evaluating increases in landslide risk that reflects the results of the climatic models available and provides a framework for scenario testing of increased frequency and magnitude of extreme precipitation events.

I adopted the ACCESS1.0 model to develop the methodology presented in this study. Another approach is the integration of multi-models for forecasting climate, which could allow capturing more possible scenarios.

3.4 Results and discussion

3.4.1 2000-2021 Weather database

The average correlation coefficients of the daily mean temperature and daily total precipitation for the period between January 2000 and December 2021 are presented in Table 3-2 for each station. According to Table 3-2, the correlation coefficients of daily mean temperature are 0.99 for both Weather Canada and ACIS databases which suggests that relying solely on temperature records may not suffice when studying the correlation between weather stations.

Table 3-2: Results of weather stations analysis (Pearson's correlation coefficients)

	Database	Data time period	Data type	Database	Data time period	Data type
	Weather Canada	2000-01 to 2020-12	Daily	ACIS	2005-04 to 2020-12	Daily
Weather station	Daily mean temperature	Daily total precipitation		Daily mean temperature	Daily total precipitation	
BEISEKER AGCM	0.991	0.648		0.993	0.687	
CRAIGMYLE AGCM	0.991	0.615		0.993	0.660	
DRUMHELLER EAST	0.987	0.673		0.987	0.707	
HUSSAR AGDM	0.988	0.656		0.989	0.696	
LINDEN AGCM	0.990	0.616		0.991	0.645	
MORRIN AGDM	0.992	0.656		0.993	0.692	
STANDARD AGCM	0.990	0.652		0.991	0.690	
THREE HILLS	0.991	0.674		0.993	0.709	

Based on the highest average correlation coefficient of precipitation with other weather stations (Table 3-2), the number of days with available data at each station (to maximize completeness of data), and its distance from the study site (to maximize how representative the data are), as presented in Table 3-3, the final database was formed by combining the data of Drumheller East and Morrin AGDM weather stations. These two weather stations are the closest ones to the site. The Drumheller East weather station is 16 km away from the C018 site, with average Pearson's correlation coefficients of 0.71 and 0.67 for precipitation in the ACIS and Weather Canada databases, respectively. At 678 m, it is located at a similar elevation to the C018 site (the site's uppermost elevation is 769 m). The Morrin AGDM weather station is 22 km away with average Pearson's correlation coefficients of 0.69 and 0.66 for precipitation in the ACIS and Weather Canada databases, respectively, and is located at a relatively higher elevation of 836 m.

Table 3-3: Availability of weather stations data

			ACIS database		Weather Canada database	
Weather station	Station elevation (m)	Distance to the site (km)	Availability of precipitation (%)	Availability of temperature (%)	Availability of precipitation (%)	Availability of temperature (%)
BEISEKER AGCM	896	36	89.6	89.7	58.5	62.7
CRAIGMYLE AGCM	845	53	88.3	88.4	57.0	62.4
DRUMHELLER EAST	678	16	82.7	99.8	58.2	96.5
HUSSAR AGDM	971	45	99.8	99.8	81.5	86.7
LINDEN AGCM	914	55	88.8	89.7	55.5	61.9
MORRIN AGDM	836	22	99.9	99.8	74.3	83.9
STANDARD AGCM	901	32	89.0	89.1	53.4	61.1
THREE HILLS	857	36	76.4	99.7	71.2	96.6

3.4.2 C018 landslide events and their relationship to weather

The 4-month antecedent average daily air temperature and total daily precipitation are shown in Figure 3-7. Except for the May 2013 landslide and the two events that occurred during winter (December 2017 and January 2021), the other eight landslides occurred shortly after periods of rainfall. This is consistent with the general observation that many landslide occurrences and episodes of landslide acceleration are triggered by precipitation events over timescales ranging from minutes to years (Coe and Godt 2012). Figure 3-7 shows that some landslides occurred immediately or within a few days after a rainfall event (July 2000, May 2003, July 2005, June 2007, June 2012, June 2017, May 2018, and June 2018), corresponding to spring and summer

conditions. Other landslides occurred a couple of weeks after a rainfall event (December 2017 and January 2021) and during winter conditions.

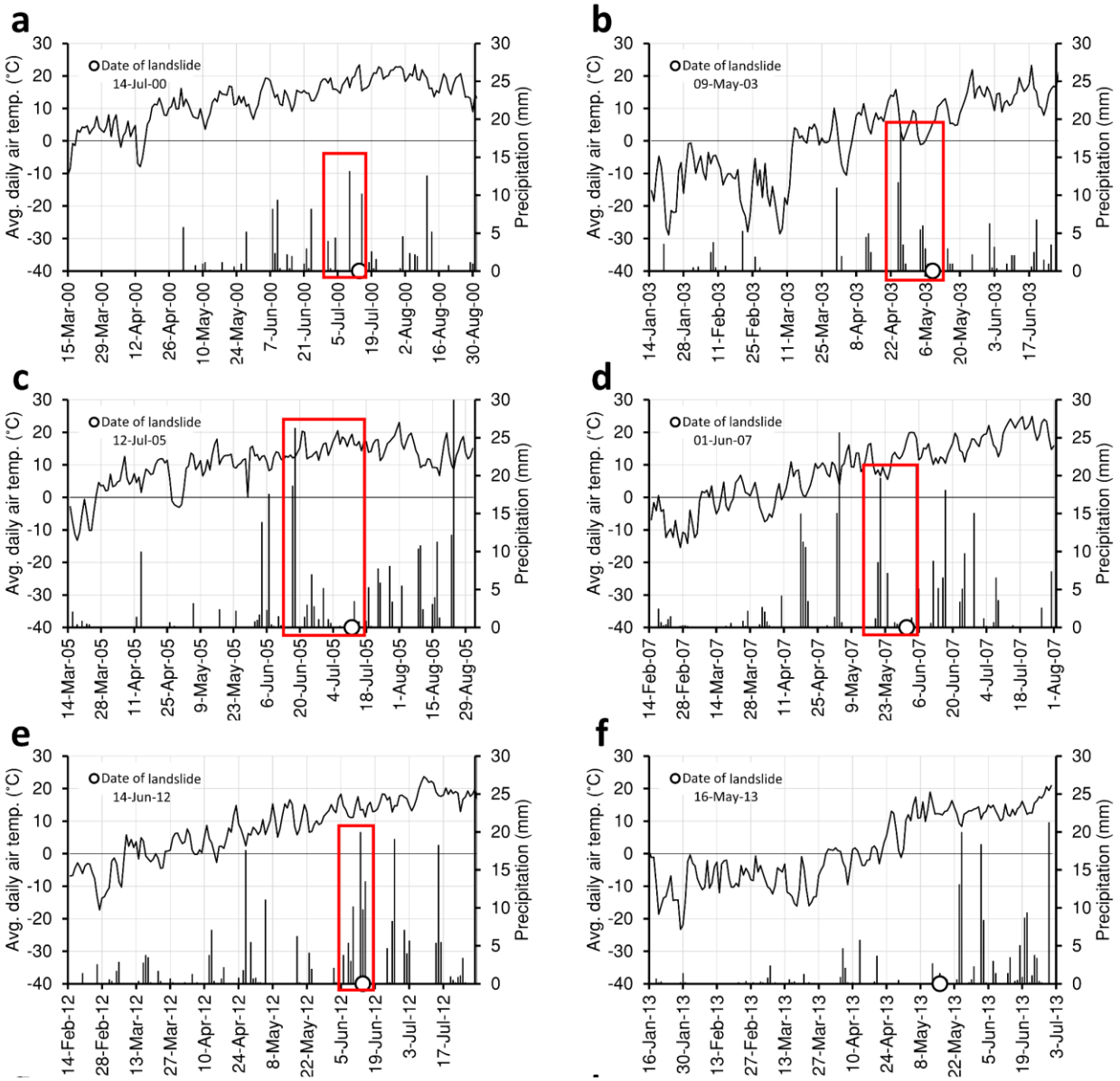

Figure 3-7: Antecedent precipitation and temperature for the recorded landslides on 14-Jul-2000 (a), 9-May-2003 (b), 12-Jul-2005 (c), 1-Jun-2007 (d), 14-Jun-2012 (e), 16-May-2013 (f), 9-Jun-2017 (g), 13-Dec-2017 (h), 22-May-2018 and 10-Jun-2018 (i), and 4-Jan-2021 (j). Red boxes show the precipitation events for landslides with a significant amount of antecedent rainfall.

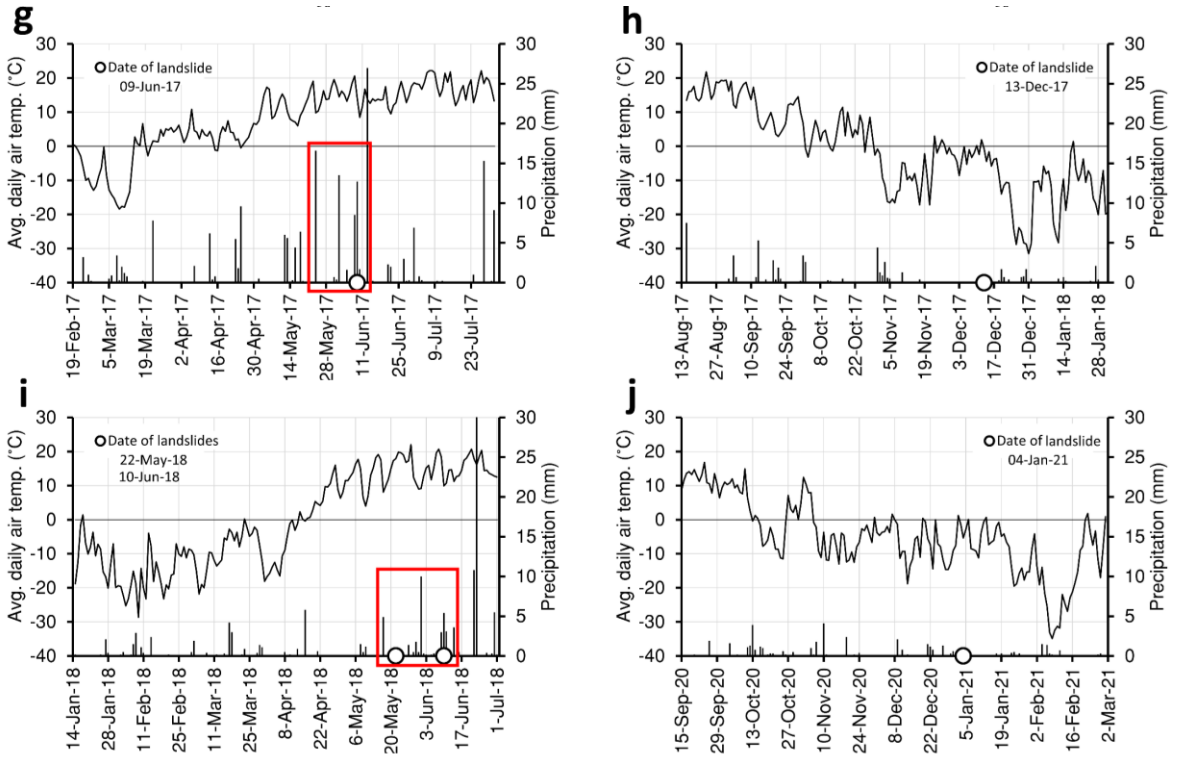

Figure 3-7 (continued).

This suggests that the mechanisms that led to these landslides are different. The cumulative precipitation and freeze-thaw cycles calculated for different time periods before each landslide are shown in Figure 3-8.

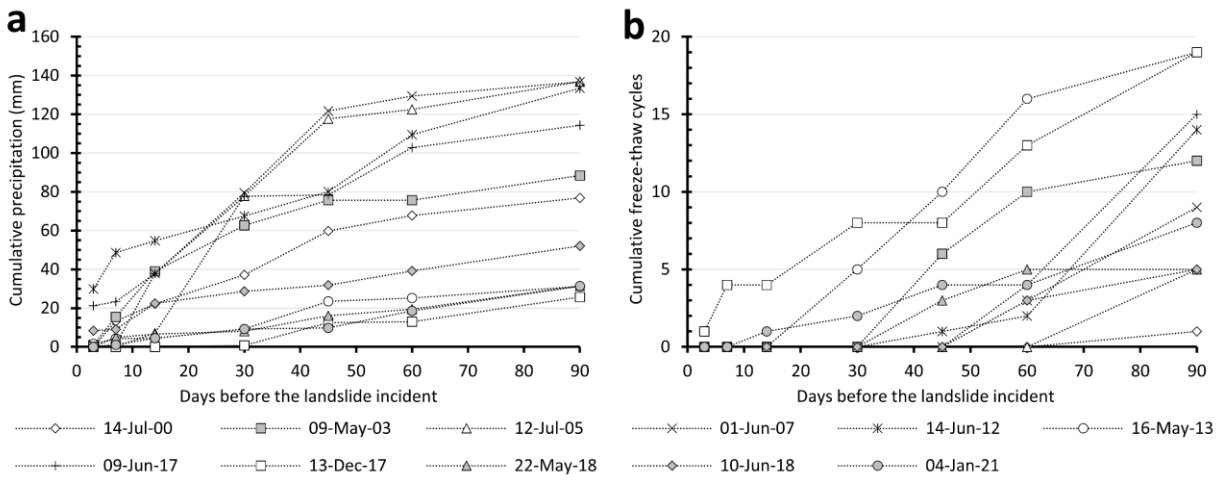

Figure 3-8: Cumulative precipitation (a), and cumulative freeze-thaw cycles (b) preceding the 11 landslide events

Spring and summer landslides

Table 3-4 shows the antecedent average and minimum rainfall values for spring and summer documented landslide events, during each antecedent time period (3, 7, 14, 30, 45, 60, and 90 days). This table shows that, on average, 6.9 mm of rain had fallen in the three days preceding the landslides. It also shows that at least 4.4 mm of rainfall had occurred during the 14 days prior to the occurrence of the landslides.

Table 3-4: Antecedent average and minimum precipitation of all landslides reported in spring and summer, and for each antecedent time period

Precipitation (mm)	Days before the landslide						
	3	7	14	30	45	60	90
Average	6.9	13.4	25.8	49.8	67.2	76.8	89.0
Minimum	0	0.2	4.4	8.1	16.1	19.4	31.2

The rock materials at the site are susceptible to moisture degradation, as previously described. Rain, thawing snowfall, and potentially thawing snowpack will cause moisture to penetrate the weathered material and allow the weathering front to progress into the substrata. As the weathering front progresses over time, wetting-drying cycles leading to swelling-shrinking cycles will increase the depth of weathering penetration. Therefore, after periods of rainfall, there is a greater chance for moisture to reach the deeper layers via seepage through weathered materials, providing a suitable environment for further weathering. This repetitive process reduces the strength of the materials until driving forces due to gravity overcome the reduced strength, aided by increased material weight and decreasing effective stresses (as moisture increases during precipitation periods). The correlation between the timing of rainfall events and the occurrence of landslides suggests that precipitation is a key factor in the landslide activity at the C018 site.

Winter landslides

The cumulative number of freeze-thaw cycles for all landslides is presented in Figure 3-8b, which shows that a total of eight and two cycles had occurred during the 30 days prior to the occurrence of the December 2017 and January 2021 landslides, respectively.

The December 2017 landslide was described as a fall of frozen clumps of soil, that detached from the face of the slope approximately 5 m to 30 m above the highway (Klohn Crippen Berger 2018). The weather data (Figure 3-9) shows that on October 31 (43 days before the incident), with the onset of rainfall, the temperature dropped 26 °C and remained below 0°C for the next 23 days. After that, the average air temperature fluctuated with peaks around 0°C and above for 20 days before the occurrence of the landslide. Figure 3-9 also indicates that a total of 12.5 mm of rainfall and a total of eight freeze-thaw cycles had occurred during the previous 45 days.

It is postulated that the simultaneity of the rainfall and sudden drop in temperature would have caused the rain to freeze shortly after reaching the ground, and before the water had the chance to evaporate or penetrate deeper into the formation. The water would have remained frozen for at least two weeks before the temperature rose to the thawing point. The moisture content that remains frozen provides some apparent cohesion to the weaker material; thawing eliminates this apparent cohesion until the moment in which the loss of cohesion and the presence of excess moisture leads to a landslide.

The temperature fluctuations during the seven days before the landslide caused four freeze-thaw cycles which could decrease the soil cohesion significantly according to the experimental study done by Guo et al. (2014). The landslide occurred 20 days after the average air temperature reached approximately 0˚C (i.e., on December 13, 2017).

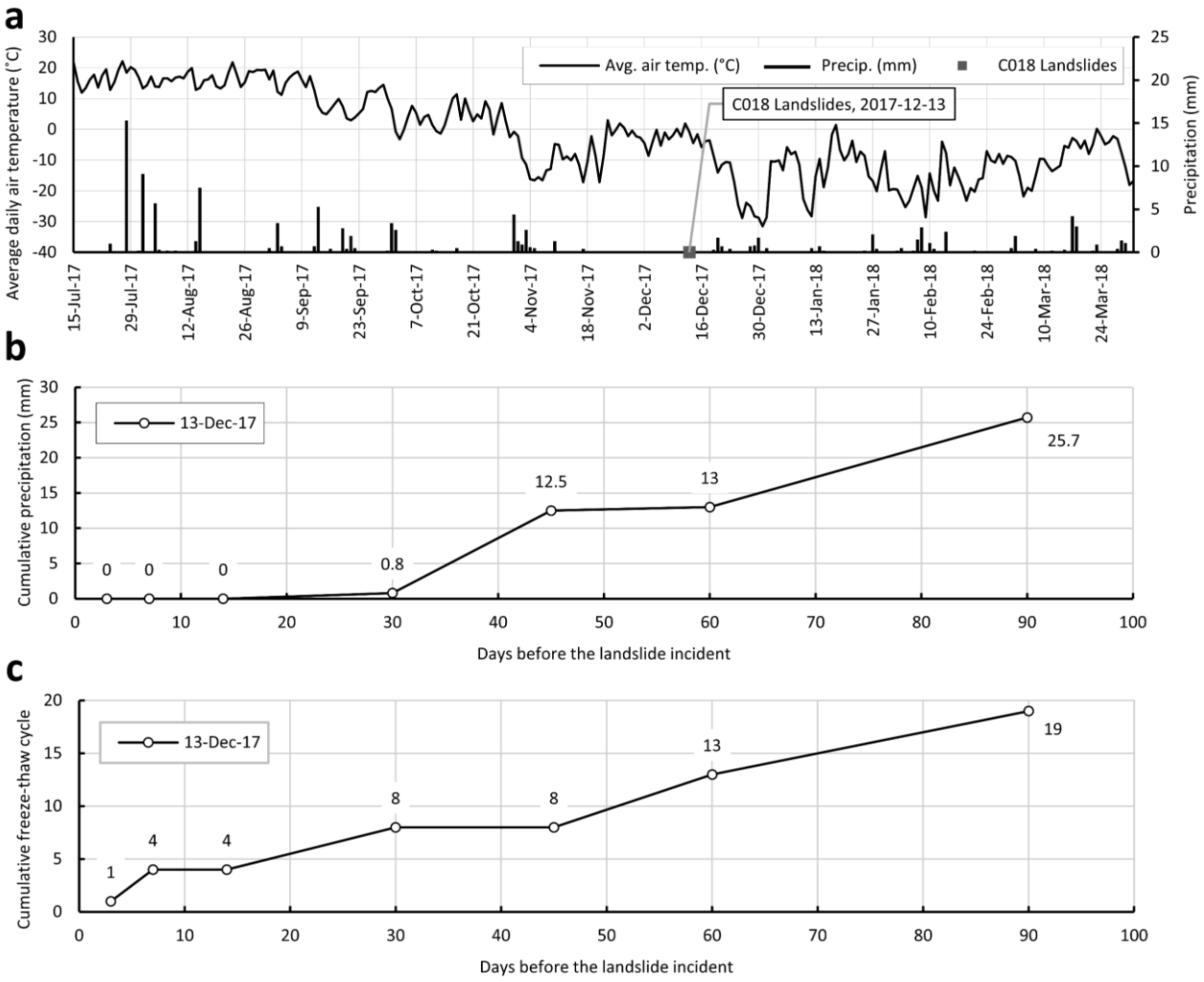

Figure 3-9: December 2017 landslide weather data. Average daily air temperature (a), cumulative precipitation (b), and cumulative freeze-thaw cycle (c)

On January 4, 2021, another landslide classified as an earthflow occurred at the site. Figure 3-10 shows weather data for a period of 4 months before the occurrence of the landslide. By comparing the cumulative precipitation between this event and the December 13, 2017 landslide, which is shown in Figure 3-11, it is observed that during the 45 days before the landslides, at least 9.8 mm of rain had fallen.

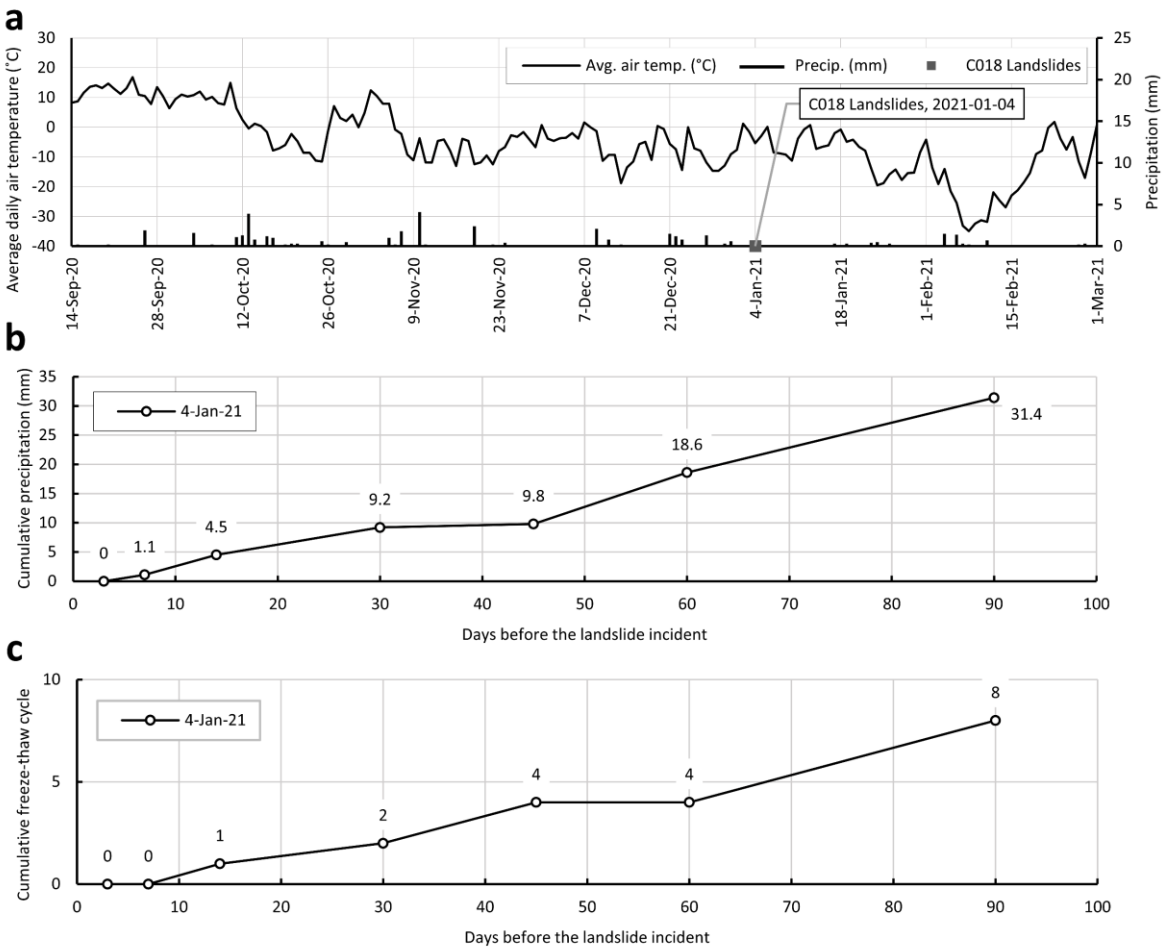

Figure 3-10: January 2021 landslide weather data. Average daily air temperature (a), cumulative precipitation (b), and cumulative freeze-thaw cycle (c)

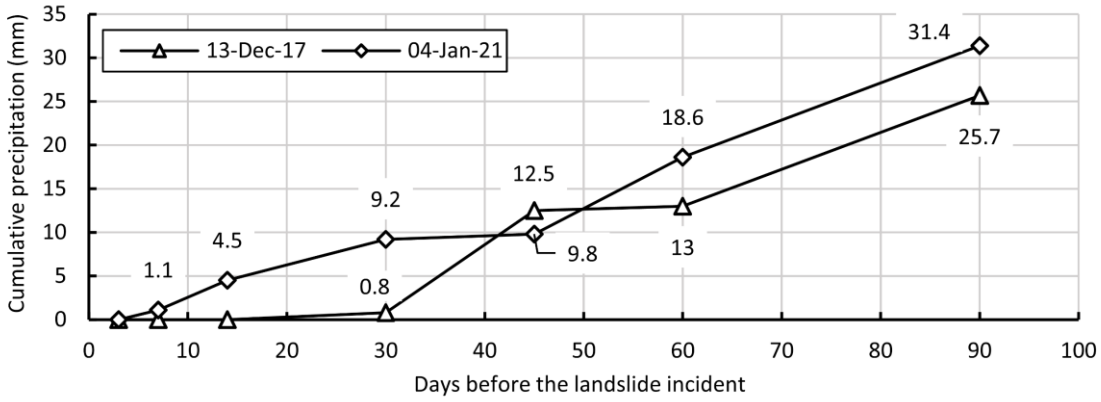

Figure 3-11: Cumulative precipitation preceding January 2021 and December 2017 landslides

Similar to the December 2017 landslide, rainfall and a sudden decrease in temperature occurred approximately at the same time, 55 days before the January 2021 landslide. The landslide took place after four freeze-thaw cycles when the average air temperature increased and fluctuated with peaks around and above 0˚C for several weeks.

For the January 2021 landslide, similar to the December 2017 landslide, the simultaneity of rainfall and drop in temperature would have caused the moisture in the soil to freeze and expand, which subsequently weakened and destroyed the material cohesion. Consecutive freeze and thaw cycles, which are shown in Figure 3-9 and Figure 3-10, exacerbate the conditions, expanding existing cracks in the material and generating new ones. This process continues until the driving loads exceed the resisting loads, and a landslide occurs. Although the sudden decrease in temperature and rainfall are both common phenomena in winter, it is hypothesized that the simultaneity of their occurrences, the subsequent thawing, and the fluctuation of temperatures around the freezing point after the deep freeze are what led to these landslides.

3.4.3 Landslide probability as a function of weather and climate

In attempting to quantify the relationship between the landslides and antecedent precipitation, I calculated the number of time periods in spring and summer, between January 2000 and December 2021, in which the 7- and 14-day cumulative precipitation is higher than a set threshold value. This number was then used to calculate the three defined probabilities as a function of the selected threshold. Results are shown in Figure 3-12 and Figure 3-13. As an example, Figure 3-12a shows that if there is more than 10 mm of rainfall in a 7-day time period, considering all of the recorded landslides in spring and summer, there is an approximately 3% conditional probability of a landslide in the same time period (spring and summer), with around 0.1% conditional probability that a landslide occurs if there is less than 10 mm of rainfall in 7 days (Figure 3-12b). In this case, the difference in landslide conditional probabilities between both periods defined by the threshold selected is a factor of 30 (Figure 3-14).

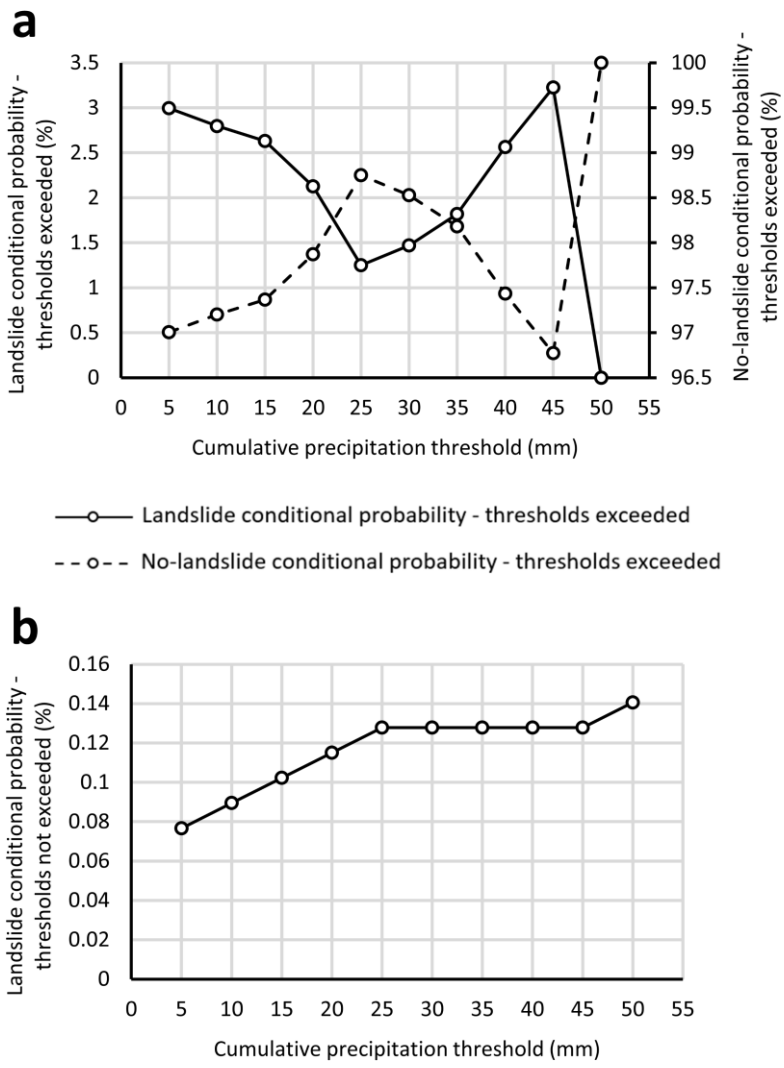

Figure 3-12: Results of the 7-day statistical analysis. "Landslide conditional probability - thresholds exceeded" (a), and "landslide conditional probability - thresholds not exceeded" (b)

The analysis shows that when the antecedent 14-day precipitation exceeds 20 mm, the probability of a landslide is 6%, while it decreases to around 0.1% if this threshold is not exceeded, providing a difference of 60 times in landslide hazard probability based on weather monitoring (numbers are rounded). Given this high number of false negatives, it would not be advisable that risk mitigation strategies during the predicted more hazardous periods become too stringent (e.g., full road

closure), however active warning for drivers to be aware of potential debris on the road, partial lane closures, or monitoring for fallen debris during these periods, could be considered.

Figure 3-14 shows the ratio of the landslide conditional probability when the precipitation threshold is exceeded over the conditional probability when the threshold is not exceeded, considering a range of different cumulative precipitation thresholds.

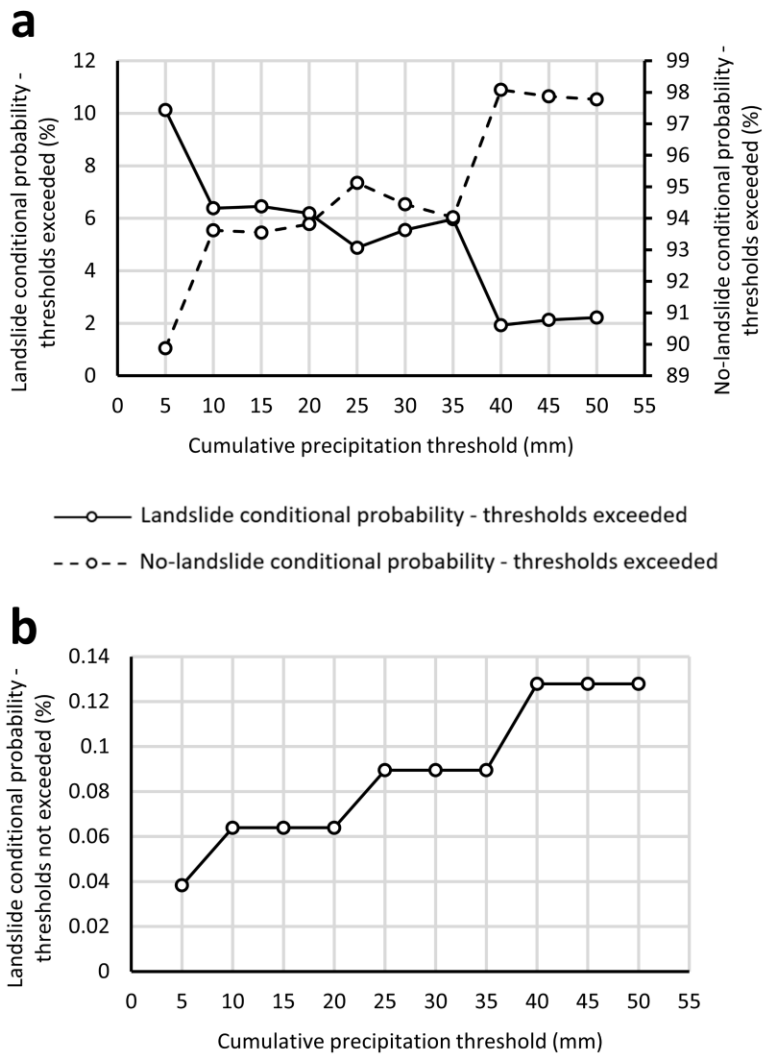

Figure 3-13: Results of the 14-day statistical analysis. “Landslide conditional probability - thresholds exceeded” (a), and “landslide conditional probability - thresholds not exceeded” (b)

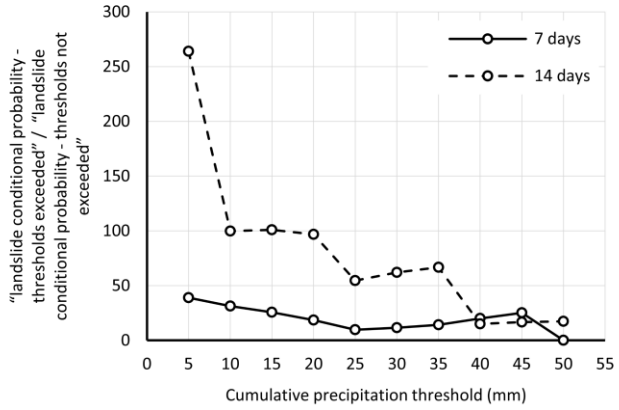

Figure 3-14: Ratio of "landslide conditional probability - thresholds exceeded" over "landslide conditional probability - thresholds not exceeded" for 7- and 14-day statistical analysis

The better threshold is the one that has a higher landslide conditional probability when the conditions are exceeded and a lower landslide conditional probability when not exceeded (higher ratio). Based on Figure 3-14, a 10 mm rainfall in 7 days and a 20 mm rainfall in 14 days can be considered as reasonable threshold values for the C018 site, considering the low number of landslides in the record. The 5 mm threshold, which provides the highest ratios, was discarded as it occurs regularly in the database and the probability of no-landslide (false alarm) when exceeding the 5 mm threshold becomes very large.

3.4.4 Histograms and binomial approximation of the landslide and weather databases

Histograms of the annual number of landslides and periods when the selected precipitation thresholds are exceeded can be built from the event records, as summarized in Table 3-5. Table 3-5 also shows the values of daily probabilities (p). As seen in Table 3-5, some years exhibit higher precipitation, but fewer landslides are recorded. This discrepancy arises from biases in landslide recording. There could be large landslides that went unrecorded, possibly because they were entirely contained by the highway ditch or concrete barriers. On the other hand, smaller failures may be documented by the maintenance crew due to a few rock blocks reaching the highway. This phenomenon may be attributed to the erosional process of slope material at the site. In case of a

major rainfall event, a substantial amount of eroded material washes out and slides down the slope, leaving less material available for subsequent major rainfall events.

Table 3-5: Annual distribution of recorded landslides and occurrences in which the defined precipitation thresholds are exceeded

Year	Recorded landslides	Number of occurrences with over 10 mm total rainfall in 7 days	Number of occurrences with over 20 mm total rainfall in 14 days
2000	1	7	6
2001	0	3	1
2002	0	6	3
2003	1	8	5
2004	0	8	5
2005	1	8	4
2006	0	12	8
2007	1	9	7
2008	0	9	6
2009	0	8	3
2010	0	7	7
2011	0	5	4
2012	1	10	6
2013	1	7	3
2014	0	10	8
2015	0	8	3
2016	0	7	5
2017	2	7	4
2018	2	10	5
2019	0	6	4
2020	0	7	3
2021	1	7	6
p	0.00137	0.02103	0.013191

The corresponding histograms (Figure 3-15, Figure 3-16, and Figure 3-17) show the cumulative relative frequency of landslides and instances when the precipitation threshold is exceeded, together with the fitted binomial distributions. The binomial distributions are calculated considering n equals 365 days for both regular and leap years, and x as the annual number of landslides (Figure 3-15) or occurrences where the precipitation threshold is exceeded (Figure 3-16 and Figure 3-17).

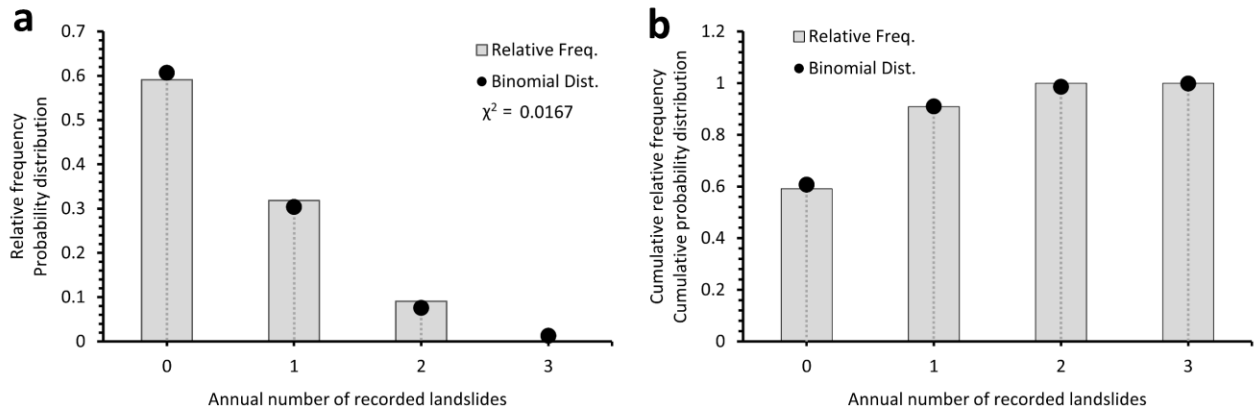

Figure 3-15: Relative frequency (a) and cumulative relative frequency (b) of records and fitted binomial distributions of recorded landslides

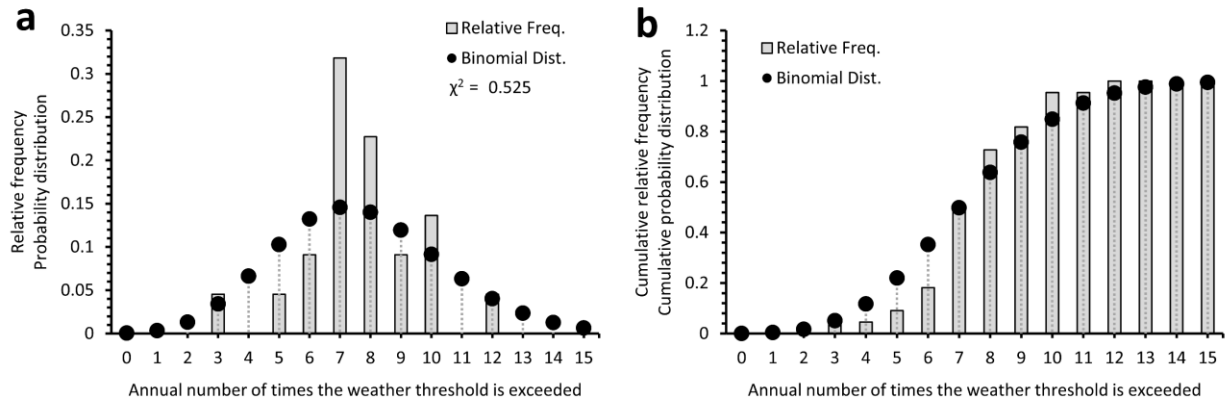

Figure 3-16: Relative frequency (a) and cumulative relative frequency (b) of records and fitted binomial distributions of occurrences when the total rainfall is more than 10 mm in 7 days

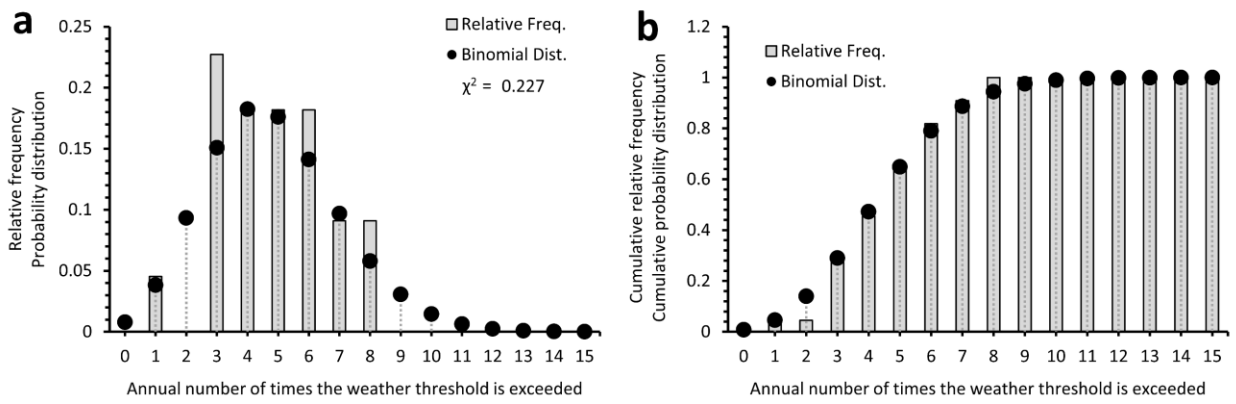

Figure 3-17: Relative frequency (a) and cumulative relative frequency (b) of records and fitted binomial distributions of occurrences when the total rainfall is more than 20 mm in 14 days

Pearson's χ^2 test results are also shown for each binomial distribution. These results suggest good fits between the observed and expected distributions with χ^2 less than critical values at the significance level of 0.05. The critical values are 5.99 and 23.68 for 2 and 14 degrees of freedom, respectively.

The landslide probabilities for periods when precipitation thresholds are exceeded provide a basis for landslide mitigation strategies that aim at warning drivers of possible debris on the highway, trigger increased inspection frequency, or possible speed reductions. The added value of the Binomial distribution fits is the quantification of the expected annual number of landslides, and expected times during the year when landslide probabilities are high, for risk assessment and mitigation purposes.

3.4.5 Expected change in landslide probability with climate change

The historical seasonal precipitation and temperature for the C018 site, as well as forecasts to the year 2085, are shown in Figure 3-18. These forecasts follow the ACCESS1.0-RCP4.5 GCM and are presented for different seasons. Seasonal temperatures at the site are expected to increase by an average of 3 ˚C over the next 65 years. It is predicted that mean spring precipitation could rise by 12%, while mean summer and fall precipitation decrease by 7%, and mean winter precipitation would remain almost unchanged.

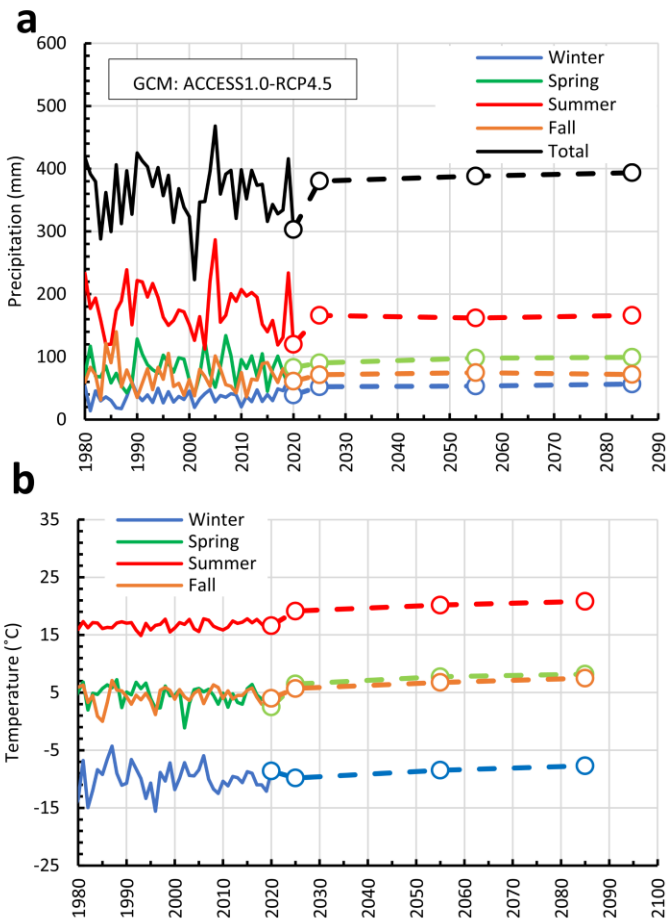

Figure 3-18: Predicted precipitation (a), and temperature (b) at the C018 site

According to the results from the given climate model, over the next decades, higher rainfall is anticipated in spring. Increasing average winter temperature could also be reflected in increased time with temperatures near the freezing point. This could lead to an increased number of freeze-thaw cycles, which could potentially increase the weathering rate of the slope materials. It is understood that landslide events depend on the occurrence of triggers and the availability of unstable volumes on the rock slope. However, the evidence presented in this paper and the climate change forecasts suggest the possibility of an increase in the frequency of episodes of landslides at the C018 site, as a result of climate change.

Figure 3-19 compares the number of times the specified precipitation thresholds (10 mm in 7 days, and 20 mm in 14 days) are exceeded. The figure shows an increase in the annual number

of times the precipitation thresholds are exceeded in spring and fall and a slight decrease in summer compared to the 2000-2021 weather data.

The cumulative probabilities $f(x \geq a)$, where a is the annual number of times the precipitation threshold is exceeded, are calculated for the current, 2050s, and 2080s weather databases. Results are presented in Figure 3-20 and show that the probability of exceeding the defined precipitation thresholds a given number of times per year increases for the climate change predictions.

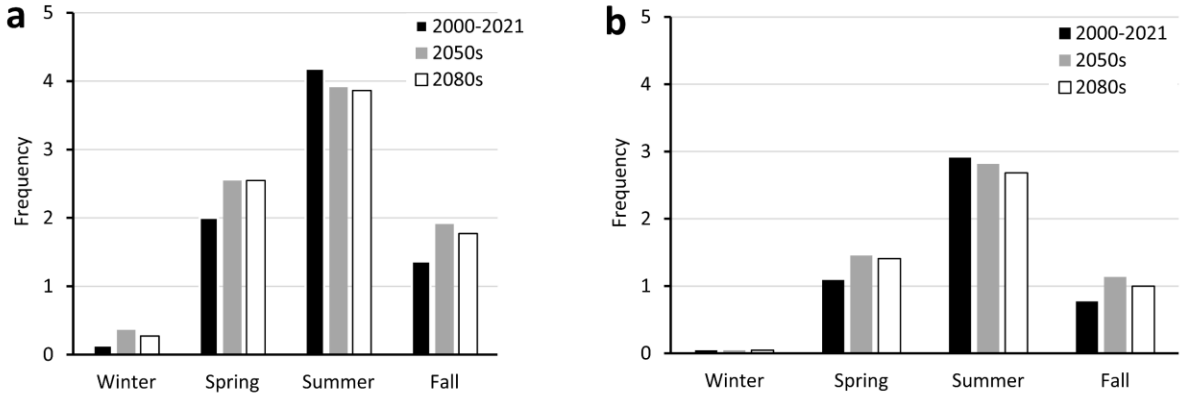

Figure 3-19: Number of times the precipitation thresholds are exceeded for when the total precipitation is more than 10 mm during 7 days (a), and when the total precipitation is more than 20 mm during 14 days (b)

The rate of increase in probability is greatest between the present time and the 2050s, with a reduced rate of increase between the 2050s and the 2080s, so that the probability of exceeding the thresholds a given number of times per year is lower in the 2080s compared to 2050s. This is consistent with the results plotted in Figure 3-18 and Figure 3-19, which show that the seasonal precipitation and the frequency of times the precipitation thresholds are exceeded are expected to decrease after 2050s. Both scenarios present higher probabilities of exceeding the precipitation thresholds a given number of times per year, compared to the present day.

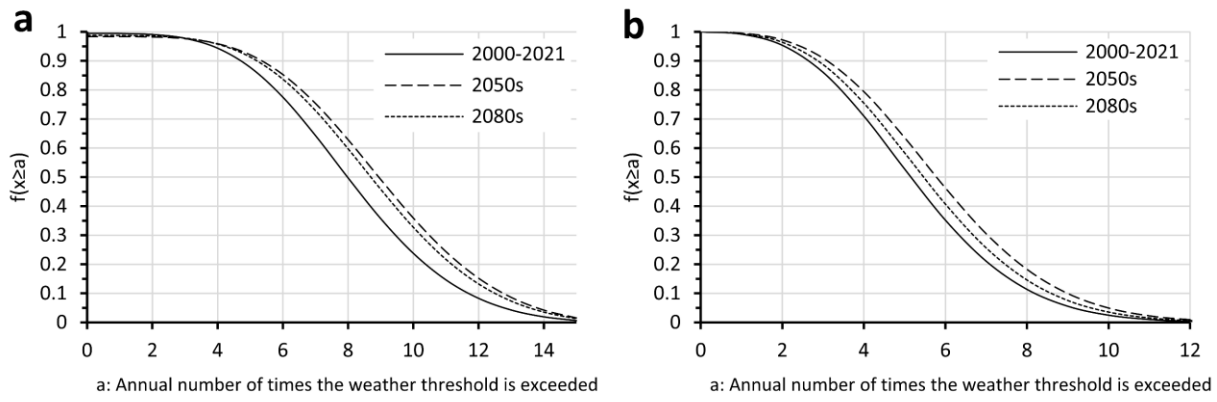

Figure 3-20: Probability f(x ≥ a) for when the total precipitation is more than 10 mm during 7 days (a), and when the total precipitation is more than 20 mm during 14 days (b)

The probability distributions are shown in Figure 3-21 to better compare the results. Annual mean values for incidences in the 2050s and 2080s when the total precipitation is more than 10 mm in 7 days, are expected to be 8.7 and 8.4 respectively which show an increase of 13% and 9% compared to the 2000-2021 weather database. The corresponding increases for when the total precipitation is more than 20 mm in 14 days, are 15% and 6% for 2050s and 2080s, respectively.

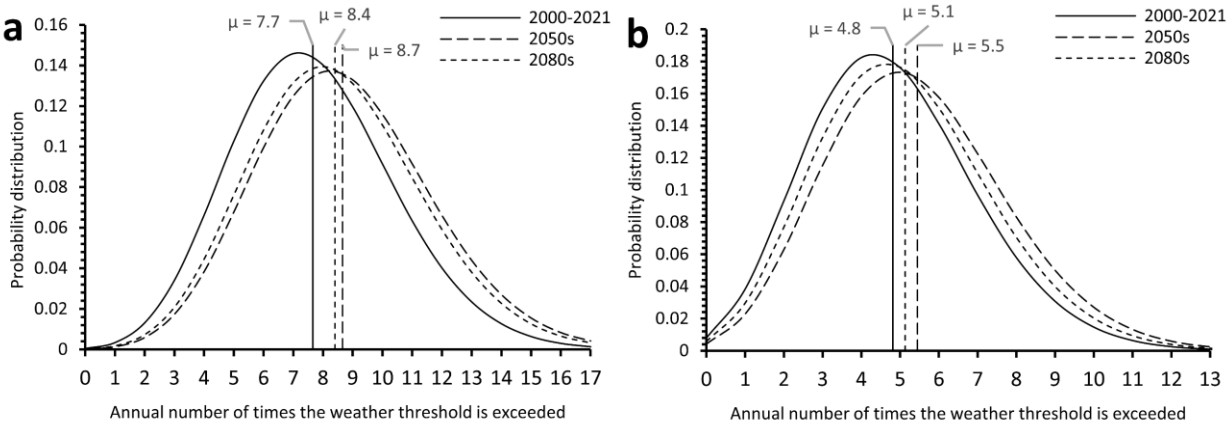

Figure 3-21: Landslide probability distribution for when the total precipitation is more than 10 mm during 7 days (a), and when the total precipitation is more than 20 mm during 14 days (b)

The increase in the number of times that the precipitation thresholds are exceeded will result in an increase in the landslide probability. The landslide probabilities for the expected annual mean (μ), and mean plus one standard deviation ($\mu + \sigma$) values of the distributions shown in Figure 3-21 are calculated and compared for all weather databases in Table 3-6 and Table 3-7. According to Table 3-6, the corresponding probability of a landslide (for mean values) expected for the 2050s and 2080s when the total precipitation is more than 10 mm in 7 days, are estimated to increase by 13% and 10% compared to the 2000-2021 weather database. The corresponding increases for when the total precipitation is more than 20 mm in 14 days, are 13% and 7% for the 2050s and 2080s, respectively (Table 3-7).

Table 3-6: Landslide probabilities for when the total precipitation is more than 10 mm during 7 days

		2000-2021	2050s	2080s		
Mean number of times precipitation is exceeded per year	μ	7.66	8.66	8.40		
Standard deviation	σ	2.72	2.86	2.83		
					Increase compared to the current weather conditions (%)	
Daily landslide probability	θ		1.37×10^{-3}		2050s	2080s
Corresponding mean landslide probability	μ x θ	1.05×10^{-2}	1.18×10^{-2}	1.15×10^{-2}	13	10
Corresponding mean plus 1 SD landslide probability	(μ + σ) x θ	1.42×10^{-2}	1.58×10^{-2}	1.54×10^{-2}	11	8

Table 3-7: Landslide probabilities for when the total precipitation is more than 20 mm during 14 days

		2000-2021	2050s	2080s		
Mean number of times precipitation is exceeded per year	μ	4.81	5.45	5.13		
Standard deviation	σ	2.18	2.32	2.25		
					Increase compared to the current weather conditions (%)	
Daily landslide probability	θ		1.37×10^{-3}		2050s	2080s
Corresponding mean landslide probability	$\mu \times \theta$	6.59×10^{-3}	7.46×10^{-3}	7.03×10^{-3}	13	7
Corresponding mean plus 1 SD landslide probability	$(\mu + \sigma) \times \theta$	9.57×10^{-3}	1.06×10^{-2}	1.01×10^{-2}	11	6

These results indicate a moderate increase in landslide hazard at the C018 site with future climate change and may inform AT's decision-making for allocating resources for landslide mitigation and climate resilience. Importantly, these results illustrate a method to quantify changes in landslide hazard for climate change scenarios.

It is worth noting that climate models make predictions based on complex mathematical equations and assumptions. Therefore, there is an uncertainty in their predictions which should be considered when this methodology is used. One limitation is climate models' inability to accurately predict the time and intensity of extreme precipitation events. Given that many landslides occur following such extreme events, estimating future landslide severity due to extreme weather conditions becomes a challenging task. However, it is undeniable that the projected increase in future precipitation will lead to a higher number of landslides.

3.5 Conclusion

This study showed the applicability of the proposed methodology to correlate antecedent weather conditions with landslide activity and to forecast future changes in landslide activity due to climate change. The methodology presented in this study was developed based on the available landslide records and needs to be validated and updated as more data become accessible.

The effect of antecedent weather conditions on landslide occurrences at the C018 site adjacent to Highway 837 in Alberta, Canada, was investigated for recorded events between 2000 and 2021. The study of the landslides showed that there is a relationship between the occurrence of the landslides and the antecedent weather at this site. According to the highway maintenance reports, nine landslides occurred during spring and summer, and two landslides were recorded during winter. Evaluating the 4-month antecedent weather conditions preceding each landslide showed that except for the May 2013 landslide, all other eight landslides that occurred in spring and summer occurred shortly after a period of rainfall. Results show that an average of 6.9 mm of rain had fallen in the previous three days. Precipitation data also show that at least 4.4 mm of rainfall had occurred during the 14 days before the landslide.

Landslide probabilities were calculated assuming an antecedent rainfall threshold for two time-windows: 7-day and 14-day. Results showed that if there is more than 10 mm of rainfall in a 7-day period, there will be an approximately 3% probability of a landslide, with around 0.1% probability that a landslide occurs if there is less than 10 mm of rainfall in 7 days. The values for a 20 mm rainfall in a 14-day period are a 6% probability of a landslide if the threshold is exceeded, and approximately 0.1% probability that a landslide occurs if there is less than 20 mm of rainfall in 14 days. Based on these findings, 10 mm rainfall in 7 days and 20 mm rainfall in 14 days can be considered useful thresholds for landslide hazard monitoring and risk reduction strategies at this site.

The ACCESS1.0-RCP4.5 global climate model forecasts an increase in the mean spring precipitation at the C018 site of 12% over the next 65 years. Moreover, mean seasonal temperatures are also expected to increase in the future, which means that more freeze-thaw cycles could be anticipated in winter. The two winter landslide events (December 2017 and January 2021) occurred when the air temperature fluctuated around 0°C, and freeze-thaw cycles were more likely to occur.

These findings also suggest that the probability of landslides at the C018 site during winter months could increase as a result of climate change.

Synthetic weather databases were created based on the recorded weather data from 2000 to 2021 and the predictions made in the ACCESS1.0-RCP4.5 model. The expected landslide probabilities in the 2050s and 2080s were calculated for the specified precipitation thresholds. The results show increases in landslide probabilities in the future. Landslide probability is expected to rise about 13% in the 2050s compared to 2000-2021. Results also reveal that the landslide probability increases by 13% and 7% in the 2050s and 2080s, respectively, when the total precipitation is more than 20 mm in 14 days.

The landslide probabilities for periods when precipitation thresholds are exceeded, provide a basis for landslide mitigation strategies that aim at warning drivers of possible debris on the highway and trigger increased inspection frequency or possible speed reductions. The added value of the Binomial distribution fits is the quantification of the expected annual number of landslide occurrences (or highway service disruptions) and the expected times when landslide probabilities are high, for risk mitigation purposes. The work presented also provides a probabilistic approach for quantifying the effect of climate change on the landslide hazard, which may assist the highway agency in prioritizing sites for climate resiliency interventions.

3.6 Acknowledgement

This research was made possible through the collaboration between Klohn Crippen Berger, Alberta Transportation, and the University of Alberta. Funding was provided by Klohn Crippen Berger and the Natural Sciences and Engineering Research Council of Canada (NSERC) and through a Collaborative Research and Development Grant.

3.7 References

Aditian A, Kubota T, Shinohara Y (2018) Comparison of GIS-based landslide susceptibility models using frequency ratio, logistic regression, and artificial neural network in a tertiary region of Ambon, Indonesia. Geomorphology 318:101–111. https://doi.org/10.1016/j.geomorph.2018.06.006

Alberta Climate Information Service (2020) Current and Historical Alberta Weather Station Data Viewer. http://agriculture.alberta.ca/acis/weather-data-viewer.jsp. Accessed 11 August 2021

Alberta Transportation (2021) Annual Landslides Assessments for Central Region (CMA511-516). https://www.transportation.alberta.ca/PlanningTools/GMS/Annual Landslides Assessments/Reg-Central Region (CMA511-516)/Inspection Sites/837_02 (C18) - Red Deer River Scour 1.9km from SH575/Reports/. Accessed 23 August 2021

Arabameri A, Pradhan B, Rezaei K et al (2019) GIS-based landslide susceptibility mapping using numerical risk factor bivariate model and its ensemble with linear multivariate regression and boosted regression tree algorithms. J Mt Sci 16:595–618. https://doi.org/10.1007/s11629-018-5168-y

Arosio D, Longoni L, Mazza F et al (2013) Freeze-Thaw Cycle and Rockfall Monitoring. In: Margottini C, Canuti P, Sassa K (eds) Landslide Science and Practice. Springer, Berlin, Heidelberg. https://doi.org/10.1007/978-3-642-31445-2_50

Barredo JI, Benavides A, Hervás J, Van Westen CJ (2000) Comparing heuristic landslide hazard assessment techniques using GIS in the Tirajana basin, Gran Canaria Island, Spain. Int J Appl Earth Obs Geoinf 2000:9–23. https://doi.org/10.1016/s0303-2434(00)85022-9

Bhardwaj A, Wasson RJ, Ziegler AD et al (2019) Characteristics of rain-induced landslides in the Indian Himalaya: A case study of the Mandakini Catchment during the 2013 flood. Geomorphology 330:100–115. https://doi.org/10.1016/j.geomorph.2019.01.010

Bi D, Dix M, Marsland S et al (2013) The ACCESS coupled model: description, control climate and evaluation. Aust Meteorol Oceanogr J 63:41–64. https://doi.org/10.22499/2.6301.004

Brooks SM, Crozier MJ, Glade TW, Anderson MG (2004) Towards Establishing Climatic Thresholds for Slope Instability: Use of a Physically-based Combined Soil Hydrology-slope Stability Model. Pure Appl Geophys 161:881–905. https://doi.org/10.1007/s00024-003-2477-y

Brunetti MT, Melillo M, Peruccacci S et al (2018) How far are we from the use of satellite rainfall products in landslide forecasting? Remote Sens Environ 210:65–75. https://doi.org/10.1016/j.rse.2018.03.016

Bush E, Lemmen DS (2019) Canada's Changing Climate Report. Government of Canada, Ottawa, ON.

Chen W, Panahi M, Tsangaratos P et al (2019) Applying population-based evolutionary algorithms and a neuro-fuzzy system for modeling landslide susceptibility. Catena 172:212–231. https://doi.org/10.1016/j.catena.2018.08.025

Chen W, Pourghasemi HR, Panahi M et al (2017) Spatial prediction of landslide susceptibility using an adaptive neuro-fuzzy inference system combined with frequency ratio, generalized additive model, and support vector machine techniques. Geomorphology 297:69–85. https://doi.org/10.1016/j.geomorph.2017.09.007

Coe JA, Godt JW (2012) Review of approaches for assessing the impact of climate change on landslide hazards. In: Eberhardt E, Froese C, Turner AK, and Leroueil S (eds) Landslides and Engineered Slopes, Protecting Society Through Improved Understanding: Proceedings of the 11th International and 2nd North American Symposium on Landslides and Engineered Slopes, Banff, Canada, 3-8 June, Taylor & Francis Group, London, pp 371-377

Collins M, Knutti R, Arblaster J et al (2013) Long-term Climate Change: Projections, Commitments and Irreversibility. In: Climate Change 2013: The Physical Science Basis. Contribution of Working Group I to the Fifth Assessment Report of the Intergovernmental Panel on Climate Change. Cambridge University Press, Cambridge, United Kingdom and New York, NY, USA, pp 1029–1136

Crozier MJ (2010) Deciphering the effect of climate change on landslide activity: A review. Geomorphology 124:260–267. https://doi.org/10.1016/j.geomorph.2010.04.009

Cruden DM, Varnes DJ (1996) Landslide types and processes. In: Turner AK. and Shuster RL (eds) Landslides: Investigation and Mitigation. Transportation Research Board Special Report 247, Washington, DC, pp 36-75

Curtis Engineering Associates (2009) Geotechnical investigation - proposed residential subdivision SE 27-29-21W4M - MD of Kneehill, Alberta

Dehnavi A, Nasiri Aghdam I, Pradhan B, Morshed Varzandeh MH (2015) A new hybrid model using step-wise weight assessment ratio analysis (SWARA) technique and adaptive neuro-fuzzy inference system (ANFIS) for regional landslide hazard assessment in Iran. Catena 135:122–148. https://doi.org/10.1016/j.catena.2015.07.020

Fahey BD, Lefebure TH (1988) The freeze-thaw weathering regime at a section of the Niagara escarpment on the Bruce Peninsula, Southern Ontario, Canada. Earth Surf Process Landforms 13:293–304. https://doi.org/10.1002/esp.3290130403

Godt JW, Baum RL, Chleborad AF (2006) Rainfall characteristics for shallow landsliding in Seattle, Washington, USA. Earth Surf Process Landforms 31:97–110. https://doi.org/10.1002/esp.1237

Government of Canada (2020) Historical weather data. https://climate.weather.gc.ca/historical_data/search_historic_data_e.html. Accessed 10 August 2021

Guo Y, Shan W, Jiang H et al (2014) The Impact of Freeze–thaw on the Stability of Soil Cut Slope in High-latitude Frozen Regions. In: Shan W, Guo Y, Wang F, Marui H, Strom A (eds) Landslides in Cold Regions in the Context of Climate Change. Environ Sci Eng, pp 85–98. https://doi.org/10.1007/978-3-319-00867-7_7

Guzzetti F, Peruccacci S, Rossi M, Stark CP (2008) The rainfall intensity-duration control of shallow landslides and debris flows: An update. Landslides 5:3–17. https://doi.org/10.1007/s10346-007-0112-1

Hamblin AP (2004) The Horseshoe Canyon Formation in southern Alberta: surface and subsurface stratigraphic architecture, sedimentology, and resource potential. Geological Survey of Canada, No. 578, pp 1–180.

Hong H, Pourghasemi HR, Pourtaghi ZS (2016) Landslide susceptibility assessment in Lianhua County (China): A comparison between a random forest data mining technique and bivariate and multivariate statistical models. Geomorphology 259:105–118. https://doi.org/10.1016/j.geomorph.2016.02.012

Huang AB, Lee JT, Ho YT et al (2012) Stability monitoring of rainfall-induced deep landslides through pore pressure profile measurements. Soils Found 52:737–747. https://doi.org/10.1016/j.sandf.2012.07.013

Huang F, Yao C, Liu W et al (2018) Landslide susceptibility assessment in the Nantian area of China: A comparison of frequency ratio model and support vector machine. Geomatics, Nat Hazards Risk 9:919–938. https://doi.org/10.1080/19475705.2018.1482963

Huang F, Zhang J, Zhou C et al (2020) A deep learning algorithm using a fully connected sparse autoencoder neural network for landslide susceptibility prediction. Landslides 17:217–229. https://doi.org/10.1007/s10346-019-01274-9

IPCC (2021) Climate Change 2021: The Physical Science Basis. Contribution of Working Group I to the Sixth Assessment Report of the Intergovernmental Panel on Climate Change. Cambridge University Press. In Press.

IPCC (2014) Climate Change 2014: Synthesis Report. Contribution of Working Groups I, II and III to the Fifth Assessment Report of the Intergovernmental Panel on Climate Change. Gian-Kasper Plattner, Geneva, Switzerland

Iverson RM (2000) Landslide triggering by rain infiltration. Water Resour Res 36:1897–1910. https://doi.org/10.1029/2000WR900090

Iverson RM, Major JJ (1987) Rainfall, ground-water flow, and seasonal movement at Minor Creek landslide, northwestern California: physical interpretation of empirical relations. Geol Soc Am Bull 99:579–594. https://doi.org/10.1130/0016-7606(1987)99<579:RGFASM>2.0.CO;2

Jolliffe IT, Cadima J (2016) Principal component analysis: a review and recent developments. Philosophical Transactions of the Royal Society A 374:20150202. https://doi.org/10.1098/rsta.2015.0202

Kavzoglu T, Sahin EK, Colkesen I (2014) Landslide susceptibility mapping using GIS-based multi-criteria decision analysis, support vector machines, and logistic regression. Landslides 11:425–439. https://doi.org/10.1007/s10346-013-0391-7

Klohn Crippen Berger (2000) Central Region Landslide Assessment SH837:02 River Scour @ km 1.9 Emergency Geotechnical Inspection Report, July 25, 2000

Klohn Crippen Berger (2018) CON0017608 Central Region GRMP – Call-Out Report C018 Hwy 837:02 Call-Out Report January 19, 2018. Red Deer

Krautblatter M, Moser M (2009) A nonlinear model coupling rockfall and rainfall intensity based on a four year measurement in a high Alpine rock wall (Reintal, German Alps). Nat Hazards Earth Syst Sci 9:1425–1432. https://doi.org/10.5194/nhess-9-1425-2009

Laherrère J (2019) Are there enough fossil fuels to generate the IPCC CO2 baseline scenario? https://aspofrance.files.wordpress.com/2019/08/ipccco2rcp.pdf. Accessed 18 March 2021

Leyva S, Cruz-Pérez N, Rodríguez-Martín J et al (2022) Rockfall and Rainfall Correlation in the Anaga Nature Reserve in Tenerife (Canary Islands, Spain). Rock Mech Rock Eng. https://doi.org/10.1007/s00603-021-02762-y

Macciotta R (2019) Review and latest insights into rock fall temporal variability associated with weather. Proc Inst Civ Eng Geotech Eng 172(6):556–568. https://doi.org/10.1680/jgeen.18.00207

Macciotta R, Hendry M, Cruden DM et al (2017a) Quantifying rock fall probabilities and their temporal distribution associated with weather seasonality. Landslides 14:2025–2039. https://doi.org/10.1007/s10346-017-0834-7

Macciotta R, Martin CD, Cruden DM et al (2017b) Rock fall hazard control along a section of railway based on quantified risk. Georisk 11(3):272–284. https://doi.org/10.1080/17499518.2017.1293273

Macciotta R, Martin CD, Edwards T et al (2015a) Quantifying weather conditions for rock fall hazard management. Georisk 9(3):171–186. https://doi.org/10.1080/17499518.2015.1061673

Martinović K, Gavin K, Reale C, Mangan C (2018) Rainfall thresholds as a landslide indicator for engineered slopes on the Irish Rail network. Geomorphology 306:40–50. https://doi.org/10.1016/j.geomorph.2018.01.006

Mateos RM, García-Moreno I, Azañón JM (2012) Freeze-thaw cycles and rainfall as triggering factors of mass movements in a warm Mediterranean region: The case of the Tramuntana Range (Majorca, Spain). Landslides 9:417–432. https://doi.org/10.1007/s10346-011-0290-8

Mbogga M, Wang T, Hansen C, Hamann A (2010) A comprehensive set of interpolated climate data for Alberta. Government of Alberta, Publication Number: Ref. T/235.

McGreevy JP, Whalley WB (1982) The geomorphic significance of rock temperature variations in cold environments: A discussion. Arct Alp Res 14(2):157–162. https://doi.org/10.2307/1551114

Meinshausen M, Smith SJ, Calvin K et al (2011) The RCP greenhouse gas concentrations and their extensions from 1765 to 2300. Clim Change 109:213–241. https://doi.org/10.1007/S10584-011-0156-Z

Pratt C, Macciotta R, Hendry M (2019) Quantitative relationship between weather seasonality and rock fall occurrences north of Hope, BC, Canada. Bull Eng Geol Environ 78:3239–3251. https://doi.org/10.1007/s10064-018-1358-7

Rahardjo H, Li XW, Toll DG, Leong EC (2001) The effect of antecedent rainfall on slope stability. Geotech Geol Eng 19:371–399. https://doi.org/10.1023/A:1013129725263

Rhinehart RR, Bethea RM (2021) Applied Engineering Statistics. (2nd ed.). CRC Press. https://doi.org/10.1201/9781003222330

Rosi A, Peternel T, Jemec-Auflič M et al (2016) Rainfall thresholds for rainfall-induced landslides in Slovenia. Landslides 13:1571–1577. https://doi.org/10.1007/S10346-016-0733-3

Roustaei M, Macciotta R, Hendry M et al (2020) Characterisation of a rock slope showing three weather-dominated failure modes. In: Proceedings of the 2020 International Symposium on Slope Stability in Open Pit Mining and Civil Engineering. Australian Centre for Geomechanics, Perth, pp 427–438

Shu H, Hürlimann M, Molowny-Horas R et al (2019) Relation between land cover and landslide susceptibility in Val d'Aran, Pyrenees (Spain): Historical aspects, present situation and forward prediction. Sci Total Environ 693:1–14. https://doi.org/10.1016/j.scitotenv.2019.07.363

Song Y, Gong J, Gao S et al (2012) Susceptibility assessment of earthquake-induced landslides using Bayesian network: A case study in Beichuan, China. Comput Geosci 42:189–199. https://doi.org/10.1016/j.cageo.2011.09.011

Stalker AM (1973) Surficial geology of the Drumheller area, Alberta. Geological Survey of Canada, Memoir 370. https://doi.org/10.4095/103298

Tappenden KM, Skirrow RK (2020) Vision for Geotechnical Asset Management at Alberta Transportation. In: GeoVirtual 2020, Resilience and Innovation, 14-16 September

Wang T, Hamann A, Mbogga M (2008) ClimateAB v3.21 software package. available at http://tinyurl.com/ClimateAB

Weidner L, DePrekel K, Oommen T, Vitton S (2019) Investigating large landslides along a river valley using combined physical, statistical, and hydrologic modeling. Eng Geol 259:105169. https://doi.org/10.1016/j.enggeo.2019.105169

Witte, R. S. and Witte, J. S. (2016) Statistics (11th ed.). John Wiley & Sons.

Yuan G, Che A, Tang H (2021) Evaluation of soil damage degree under freeze–thaw cycles through electrical measurements. Eng Geol 293:106297. https://doi.org/10.1016/j.enggeo.2021.106297

CHAPTER 4

Influence of Precipitation on Landslide Volume

Contribution of this chapter to the overall study

This chapter presents a study that investigates the relationship between cumulative precipitation and the volume of the landslides recorded at the C018 site between 2018 and 2022. This study aims to contribute to the first and second objectives of this thesis which involve developing a methodology to quantify the change in landslide hazard as a response to changes in weather conditions and forecasting changes in landslide hazard as a response to climate change at a local scale. The methodology developed in this chapter includes the following steps in general:

- This analysis needs several consecutive point clouds from the study site which are generated over a long period of time. The point clouds can be created by any means including a photogrammetry technic which is employed in this study.
- Perform change detection analysis on consecutive point clouds using cloud computing software.
- Calculate annual landslide volumes based on the normal distance between each two consecutive point clouds.
- Calculate annual cumulative precipitation for the selected time period from the available weather station network.
- Investigate the relationship between the annual landside volumes and annual precipitation. The relationship can then be used to estimate the annual landside volumes in the future due to climate change.

- Estimate annual precipitation for the selected time periods in the future using available climate change models.
- Estimate landslide volumes in the future using the relationship developed in the earlier stages and the predicted annual precipitation.

A modified version of the research presented in this chapter was submitted to the Natural Hazards journal in November 2023 with the following citation:

Mirhadi N, Macciotta R, Gräpel C, Assessing the Influence of Precipitation on Landslide Volume in Alberta, Canada: Implications for Climate Change-Driven Landslide Hazards. Submitted to "Natural Hazards" on November 24, 2023

Abstract

Precipitation, physical weathering, and human activities create conditions that can lead to landslides. Precipitation in particular increases the potential for landslides by adding weight to the soil, increasing the internal water pressures, and weakening the bonds holding the slope material together (e.g., rock breakage). Depending on the susceptibility of the slope material to moisture, permeability, and rate of the weathering of the slope material, landslides may occur immediately or within a few hours to several weeks after the precipitation event. This suggests that the accumulated effects of precipitation play an important role in landslides occurrences. The relationship between the annual precipitation and landslide volume is demonstrated for a weathered sedimentary rock slope in Alberta, Canada. The study looked at the correlation between precipitation and landslides between 2018 and 2022. The results show that a linear relationship can be approximated between the annual amount of precipitation and the annual volume of landslides. This relationship is utilized, together with knowledge about slope dimensions, geology, and failure mechanisms, to estimate the annual volume of landslides by considering the projected annual precipitation based on the climate change models for the region. This approach and results enhance our understanding of landslide processes, and importantly, provide a means for predicting landslide volumes in the next decades as a consequence of climate change. This can prove to be

very important information for agency resource allocation towards increasing resiliency in the built environment in the coming decades and promoting sustainable development.

4.1 Introduction

A slope may become unstable in the presence of an external factor. An external factor such as a rainfall event, erosion at the toe of a slope, weathering, fatigue, and prolonged wet period reduces the factor of safety of a stable slope through time (Popescu 1994). Ultimately, these factors may bring the slope to a marginally stable state, where the factor of safety is one and the slope is sensitive to any triggering factor. This triggering factor could be another precipitation event, an external load, or a factor that reduces the shear stress such as soil shear or rock breakage. When a triggering factor is applied, slope failure or the full development of a landslide will occur. After the displacement of the slope material, the slope may return to a more stable state where the factor of safety is well above one, or the slope may stay in a marginally stable state, hovering about equilibrium (McColl 2022). In the latter case, the slope remains sensitive to all of the factors affecting the factor of safety and can be reactivated from time to time. This suggests that time and the accumulated effects of the involved factors play an important role in landslides occurrences. Generally, landslides are triggered by the following factors (Cruden and Varnes 1996):

- Climatic conditions such as precipitation, snowmelt, and freeze-thaw cycles.
- Physical weathering and expansion of joints and cracks.
- Seismic events.
- Changes in the external loads acting on the slope due to human activity.

The aforementioned factors do not impact the stability of a slope to the same extent, and each may have different effects depending on the geographical location and associated geological conditions. For example, freeze-thaw cycles are known rock fall triggers in areas where there is enough moisture in the slope and the air temperature periodically falls below zero degrees Celsius (Macciotta et al. 2015a; Wyllie 2017; Yang et al. 2021), whereas landslides of various types are known to have been triggered by earthquakes in highly seismic regions.

Some landslide triggers are related to climatic conditions. These triggers include intense and prolonged precipitation, rapid snowmelt, freeze-and-thaw cycles, and shrink-and-swell weathering (Cruden and Varnes 1996). Many researchers have studied the impact of weather as a cause of landslides and established rainfall thresholds linked to a specific duration of time for landslide prediction (Iverson and Major 1987; Iverson 2000; Rahardjo et al. 2001; Godt et al. 2006; Guzzetti et al. 2008; Huang et al. 2012; Macciotta et al. 2017a, 2015a; Rosi et al. 2016; Martinović et al. 2018; Brunetti et al. 2018; Bhardwaj et al. 2019; Weidner et al. 2019; Macciotta 2019; Pratt et al. 2019; Leyva et al. 2022). For example, Leyva et al. (2022) examined the rock falls and the weather data from 2010 to 2016 in Anaga, Canary Islands. They set precipitation thresholds to determine the probability of rock fall and found that the likelihood of an event increases to 70% if the accumulated rainfall over 12 hours surpasses 60 mm. In another study, Macciotta et al. (2015a) looked into the connection between weather conditions and the occurrence of rock falls on hard rock slopes along a railway section in the Canadian Cordillera and found that 90% of rock falls could be predicted by the 3-day antecedent precipitation and number of freeze-thaw cycles.

Uchiogi (1971) was one of the first researchers who studied the relationship between cumulative rainfall and landslide volume and presented an empirical equation based on the area of the watershed, the cumulative rainfall, a critical rainfall threshold, and two other parameters that are calibrated from the long-term data available for the study area. Since then, many studies have been conducted to find a relationship between precipitation and landslide volume (Dai and Lee 2001; Chi and Lee 2013; Liu et al. 2013; Fan et al. 2020; Wu and Chou 2021). In a study on 4744 landslides associated with rainfall events throughout Japan, Saito et al. (2014) found that rainfall totals are a suitable predictor of landslide volumes mobilized during typhoons and frontal storms.

Precipitation leads to physical weathering, and therefore, the creation or expansion of internal cracks (micro and macro scales), and relative movement of slope particles (shearing). These mechanisms are associated with the displacements within the slope. Therefore, more precipitation results in more displacement in the form of slope damage and internal deformation. Ultimately, the displacements lead to the formation of a failure surface and the occurrence of a landslide. Precipitation also increases the weight of the slope materials which in turn increases the driving force acting on the slope. Surface water runoff enters opened cracks increasing their internal pressure, and changes the pore water pressure in the soil through infiltration. These factors,

in turn, change the state of the slope through displacements done by weathering and expansion of existing soil/rock fissures, which subsequently move the slope towards a state of failure, resulting in the occurrence of a landslide.

Maintaining the equilibrium state implies that there should be a relationship between landslides and their affecting factors. This relationship depends on the current state of the slope (i.e., how far the slope is from the state where the factor of safety reaches below one) and can be unique for each location, although similar geologic contexts and climatic conditions would likely show similar behaviour.

In this study, I investigate the relationship between the annual precipitation and the annual volume of the landslides at a study site in southern Alberta and argue that this relationship can be formulated in a simple manner as follows:

$$V_{Landslide} = F(Precipitation) \quad (4\text{-}1)$$

where, $V_{Landslide}$ is the landslide volume, and $F(Precipitation)$ is a function of the amount of precipitation (snow and rain combined).

This approach implies that the volume of landslides depends on the current sate of the slope and does not necessarily occur immediately or after a short period of a precipitation event. In many cases, landslides do not necessarily occur immediately after a rainfall period but require some background cumulative precipitation (Macciotta et al. 2015a; Leyva et al. 2022).

The case study presented in this paper illustrates this relationship for a slope where precipitation is known to be a dominant triggering factor for landslides. The cumulative effects of other factors in this case study are assumed to be low based on the observations at the site. For application at other locations, this assumption would need to be validated or other dominating factors be included in the analysis.

4.2 Methods and materials

4.2.1 Study area

The study area is known as C018, following the geohazard nomenclature used by Transportation and Economic Corridors (TEC) as part of their Geohazard Risk Management Program (GRMP) (Tappenden and Skirrow 2020). The C018 site is a 500 m long, 60 m high rock slope located 12 km northwest of Drumheller in central Alberta, Canada, parallel to the Red Deer River valley and along Highway 837 (Figure 4-1). Local weather stations report monthly temperatures ranging from an average low of -15.9°C in February to an average high of 25.0°C in July, with annual extreme temperatures outside of this range. The annual average precipitation is 370 mm of combined snow and rainfall.

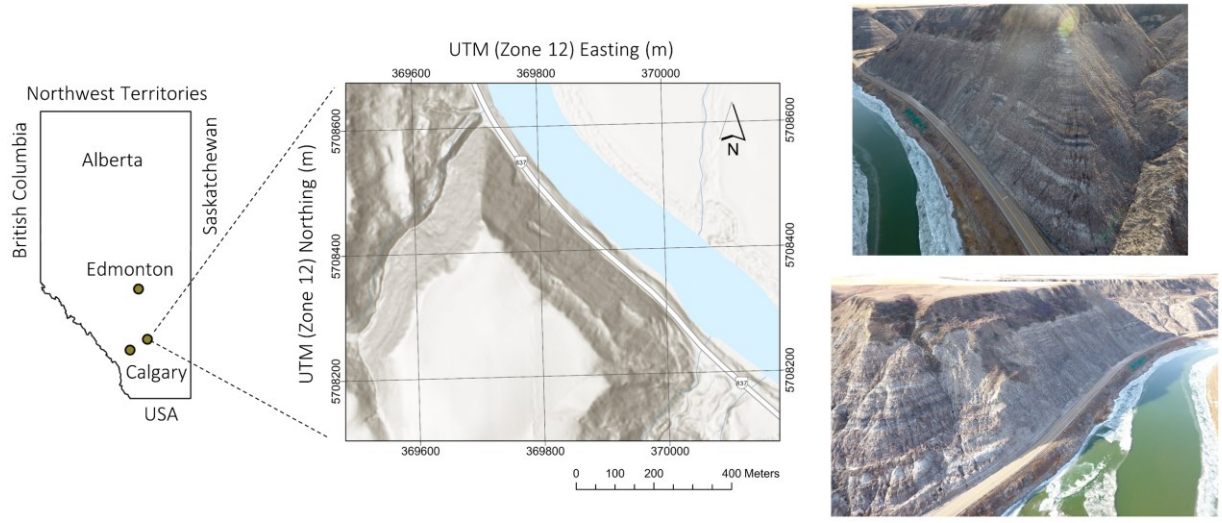

Figure 4-1: Location of the study area

Roustaei et al. (2020) found that the continuous weathering of surficial rock materials at the C018 site results in a surficial layer of soil-like materials that undergo a continuous loss of cohesion. Since July 2000, AT has recorded 11 landslides at this site, including earthflows, rock falls, and slides of frozen slabs (Alberta Transportation 2021). The monthly frequency of the recorded

landslides shows that nine of the failures occurred in spring and summer, and two occurred in winter (December 2017 and January 2021).

Figure 4-2 shows the weather conditions and the time of the recorded landslides from 2018 to 2022. Since December 2017, three landslides have been recorded at the site. It should be noted that the recorded events were landslides that were large enough to reach the highway or to be noticed by the highway maintenance crew, meaning that several smaller events are likely undocumented. Therefore, the recorded landslides are not necessarily representative of the total volume of landslides at the site.

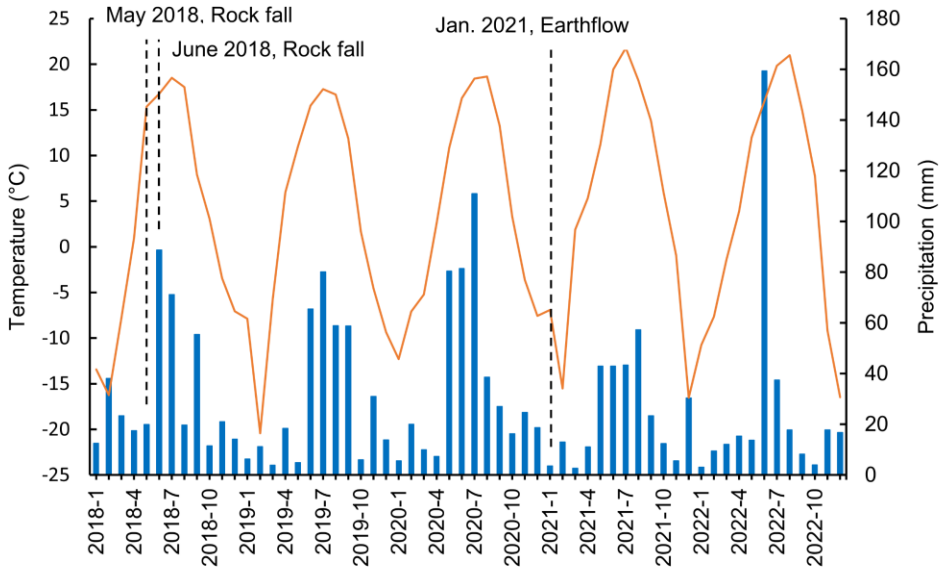

Figure 4-2: Precipitation, temperature, and the failures occurred at the C018 site since January 2018

4.2.2 Climate model and precipitation prediction

Daily weather data from 16 climate models were collected from ClimateData.ca, which provides historical and predicted future high-resolution weather data for Canada (ClimateData.ca 2023). The BCC-CSM1.1m climate model, which is a 110 km horizontal-resolution model developed by the Beijing Climate Center, was selected to predict annual precipitation until 2100 (Wu et al. 2019). The BCC-CSM1.1m climate model was selected because it had the lowest average differences

between the modelled precipitation and the observed data at the C018 site between 2018 and 2022. Representative greenhouse gas Concentration Pathway (RCP) 4.5 was selected to calculate the predicted weather data as it is a moderate scenario and Laherrère (2019) showed that RCP 4.5 is in line with future fossil fuel production and emission expectations.

4.2.3 Photogrammetry, change detection analysis, and landslide volume

Unmanned Aerial Vehicles (UAVs) and digital photogrammetry techniques have become a common practice to develop three-dimensional surface models of landsides that allow for detailed characterization of landslide features, and rock mass structure, amongst others. Subsequent surveys and the developed surfaces can be used to generate high-density point clouds that allow for change detection between surveys and monitor slope deformations (Niethammer et al. 2012; Lucieer et al. 2014; Turner et al. 2015; Rosi et al. 2016; Rodriguez et al. 2020; Rodriguez-Caballero et al. 2021). In this study, UAV was used twice a year between 2018 and 2022 to collect high-resolution images for photogrammetry and develop surface point clouds. To minimize the errors in change detection, surveys were done once before the first snowfall occurred and once after the snow cover had melted, before the vegetation started to cover the slope. The DJI Phantom 4 and the default FC330 camera were used in the surveys. The 12-megapixel camera had a 1/2.3" CMOS sensor and was attached to a three-axis gimbal to reduce the vibrations. The UAV uses an internal GPS/GLONASS to fly on the desired path in automatic mode and to record the photo locations (DJI 2021). To create a high-resolution point cloud, a minimum overlap of 60% between the photos is required (Rodriguez et al. 2020). This is achieved by capturing photos every 3 m horizontally and every 5 m vertically from a distance of approximately 100 m from the slope. To capture the details of steep slopes, photos were taken with the camera pointing at an oblique angle to the slope. The UAV was flown both manually and automatically to increase the availability of adequate imaging.

After each survey, a visual inspection was done to remove low-quality photos (overexposed, blurry, etc.) to reduce errors in constructing the point cloud. Then, point clouds were generated with the software 3DM Analyst (ADAM Technology 2021). After constructing the point clouds, CloudCompare v2.10.2 (a 3D point cloud processing software) was used to calculate the difference between subsequent point clouds (CloudCompare 2022). For this purpose, first, the

closest point method (C2C) was used as an efficient (fast) tool to estimate the difference between surfaces and to calibrate the alignment of the point clouds (Girardeau-Montaut et al. 2005; Rodriguez et al. 2020). Once the calculated difference between point clouds on areas assumed to have had no deformation was minimized (C2C provides a check for this), the Multiscale Model to Model Cloud Comparison (M3C2) was used to calculate the change between point clouds from previous and subsequent surveys. M3C2 is a statistically robust method for change detection that computes the local distance between two point clouds along the normal direction to the surfaces (Lague et al. 2013). Change detection analyses were performed on the point clouds taken at the C018 site between May 2018 and July 2022.

CloudCompare computes the negative and positive volumes between two point clouds using a user-specified grid and the normal distance (M3C2 distance) between each set of points (CloudCompare 2022). A sensitivity analysis was done on the grid size to find the finest possible grid with the highest accuracy. The accuracy depends on the density of the point clouds. The volume of the landslides at the C018 site was calculated after each photogrammetry survey and relative to the first survey taken in December 2017. It should be noted that due to the removal of fallen materials by the maintenance crew from the highway ditch regularly, only the negative volumes which represent the volume of the landslides were calculated.

4.2.4 General approach to quantify the relationship between the volume of landslides and current and predicted weather

A direct comparison between the annual cumulative precipitation and the annual calculated landslide volume was made on the available data between 2018 and 2022. The annual precipitation and landslide volume were plotted, and the best-fit curve was fitted and tested through the R-squared method. Once the best-fit curve was found, it was used to estimate the future landslide volume according to the predicted weather data. It should be noted that an 85% confidence level was considered for the best-fitted curve to make sure that most of the available data fit well inside an acceptable range. Therefore, the future annual landslide volumes were estimated with 85% confidence for some of the years with extreme precipitation conditions and for the given climate model. The uncertainty associated with the climate model was not included in the confidence assessment.

4.3 Results and discussion

4.3.1 Change detection analysis

Results of the M3C2 analyses with the mean and standard deviation of the distances between the selected point cloud and the December 2017 point cloud are shown in Figure 4-3, in which, material gain is represented by cooler colours ranging from green to blue (Positive values), while material loss is depicted by warmer colours ranging from yellow to red (Negative values). The mean distance values are all below 3 cm, indicating that the subsequent point clouds are properly aligned, and the highlighted parts show the actual changes on the slope. All slope changes were calculated relative to December 2017. Change detection analyses reveal the erosion process at six major locations on the slope as shown in Figure 4-4. These active zones, especially Zone 5 which is the largest zone, have constantly been moving since December 2017 and are the main cause for the materials falling and blocking the road. Change detection results show that the highest material loss has occurred at Zone 5 with a maximum depth of approximately three meters normal to the slope surface. The area containing Zones 3 to 6, which covers almost half of the slope length, can be considered the most active area with a higher possibility of erosion and falling materials. The erosion process makes the slope unstable and causes several failures to occur in the same area, as can be seen in Figure 4-3. As a result of multiple smaller landslides, since November 2019 the flanks of the landslide in Zone 5 have enlarged on both sides in particular towards the northwest, while the crown moved higher up the slope.

It is worth noting that there may be some small failures between photogrammetry surveys and that the types of these failures are impossible to identify since no recorded data are available from the highway maintenance team. However, the volumes of these failures are captured in subsequent surveys and are considered in this analysis.

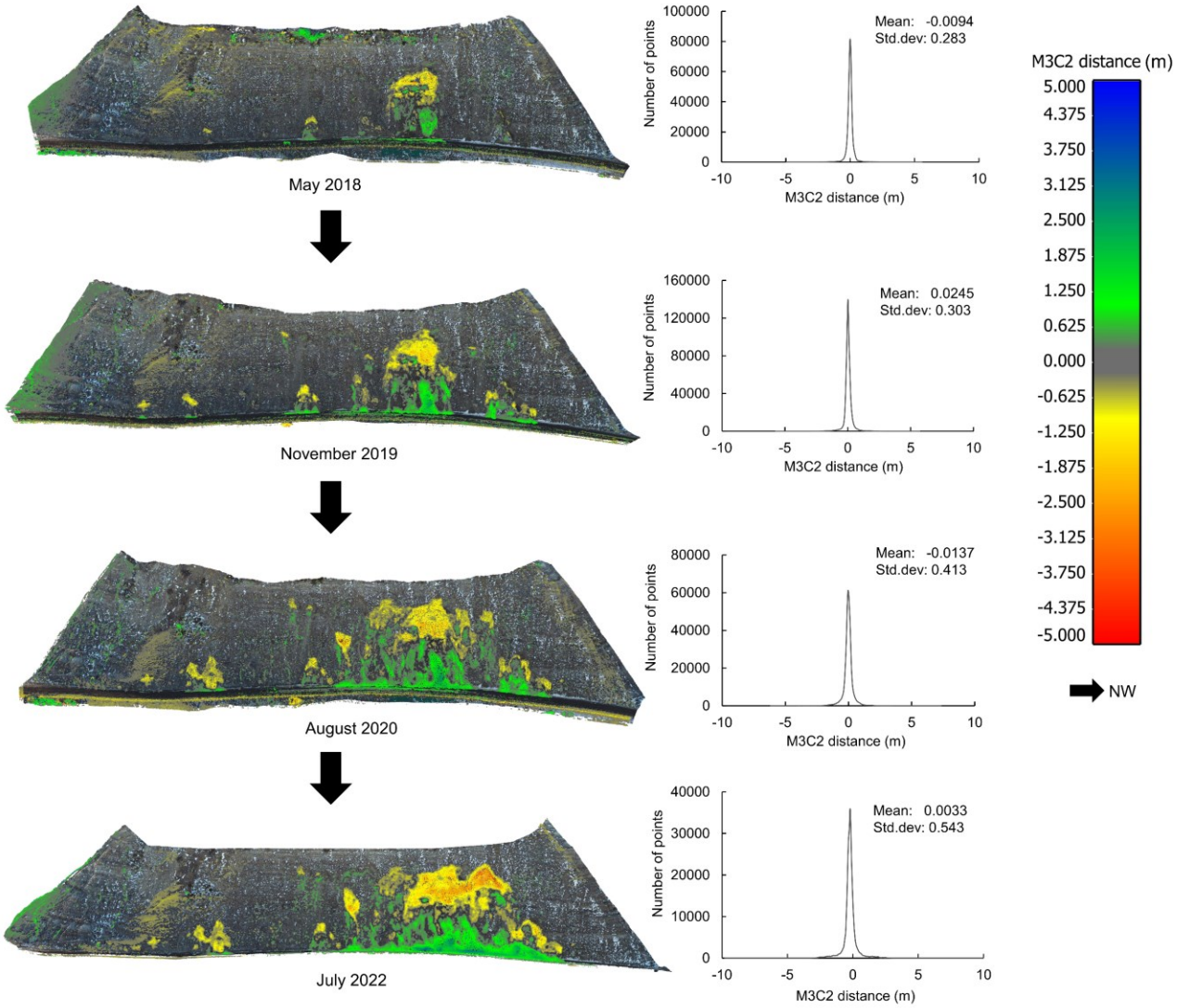

Figure 4-3: Results of change detection analyses. M3C2 distances are calculated relative to the December 2017 photogrammetry survey and are normal to the slope surface.

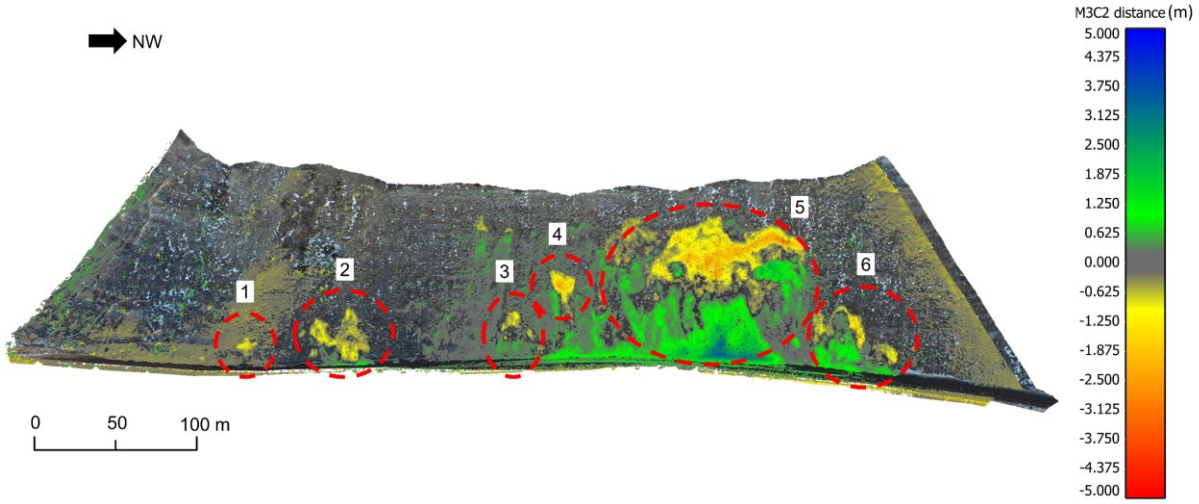

Figure 4-4: Active zones shown on July 2022 point cloud

4.3.2 The correlation between precipitation and landslide volume and predicted failure volumes with climate change

The total landslide volume for the entire slope relative to December 2017 and after each photogrammetry survey is shown in Table 4-1. The number of significant digits was selected based on the accuracy of the change detection analysis. It was difficult to capture any movement less than 20 cm because of the presence of vegetation on the slope and the difficulty in the alignment process. It should be noted that due to missing the photogrammetry survey in November 2020, the total volume calculated for 2020 is not completely representative of the total landslide volume in that year. The November 2020 survey could not be completed due to snow cover at the time of surveying. However, according to Mirhadi et al. (2022), more than 80% of the recorded landslides at the C018 site occurred in spring and summer (May, June, and July) which suggests that the volume of landslide calculated for the year 2020 can be used as an acceptable value in this analysis.

The annual accumulated precipitation was calculated using the daily weather data from the Drumheller East weather station 16 km away from the site. Figure 4-5 shows the relationship between the annual landslide volume and the annual cumulative precipitation at the C018 site between 2018 and 2022.

Table 4-1: Volume of the landslides relative to the December 2017 point cloud

Date of the photogrammetry survey	Volume of the fallen material relative to December 2017 (m^3)
May-18	858.47
Nov-18	903.23
Aug-19	1233.68
Nov-19	1355.20
Aug-20	2110.45
May-21	2484.14
Nov-21	2544.57
Apr-22	2580.69
Jul-22	2902.16

This figure suggests that the relationship between the volume of landslides and precipitation can be approximated well with a linear correlation ($R^2 = 0.67$). The equation of the correlation is given below:

$$V = 3.26 \times P - 591.81 \quad (4\text{-}2)$$

Where V is the annual landslide volume (m^3) and P is the annual accumulated precipitation (mm). In order to see how well the linear correlation represents the recorded data, the 85% confidence lines were also plotted in Figure 4-5. These confidence lines show that four out of five (80%) of the recorded data points fall within the confidence band. It should be noted that the confidence lines were plotted based on the available data for the site and should be revised as more data becomes available in the future.

Equation (4-2) implies that the intercept of the linear correlation with the horizontal axis is 182 mm. This suggests that at least 182 mm of precipitation is needed annually to activate the

failures on the slope. The intercept value could be a characteristic of the slope materials, geology, slope geometry, and environmental conditions such as evapotranspiration provided by humidity, annual temperatures and direct exposure to the sunlight.

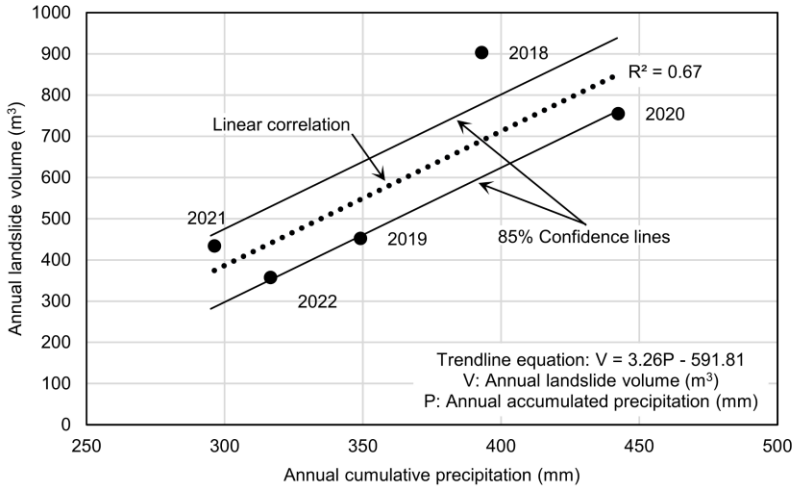

Figure 4-5: The relationship between annual landslide volume and the annual accumulated precipitation at the C018 site

On the other hand, the slope of the linear correlation could be a sign of how sensitive the slope is to the amount of precipitation. In this case, once the annual precipitation exceeds 182 mm, the annual volume of landslides increases by a factor of 3.26 with increasing annual cumulative precipitation. The slope of the linear correlation could be indicative of the susceptibility of material disaggregation and damage as the factor of safety drops below one. This factor is possibly influenced by the geology and material characteristics such as intact rock strength and weathering susceptibility. These two numbers (i.e., intercept and slope) could be considered as characteristic values and can be used as indicators for comparing landslide activities in different regions.

Predicted precipitation in the coming decades as a consequence of climate change can be input into equation (4-2) to estimate the expected annual volume of landslides. For this study, the annual cumulative precipitation until 2100 was estimated using the BCC-CSM1.1m climate model. Figure 4-6a compares the predicted annual precipitation with the observed values at the C018 site between 2018 and 2022, showing the maximum recorded annual precipitation in that

period (i.e., 441 mm). This figure also presents a line showing precipitation levels that are 20% higher than the maximum observed. According to these predictions, it is anticipated that the site will receive more than 441 mm of precipitation in 17 years and more than 529 mm in 6 years by the year 2100. These predictions are based on a single climate model; thus, using different RCP scenarios or climate models might yield different outcomes. However, there is no doubt that there will be an increase in the annual precipitation.

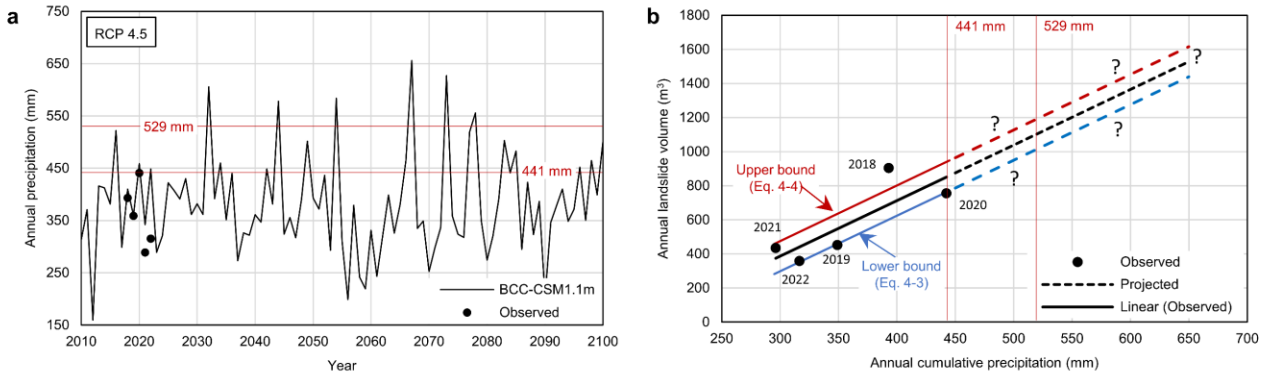

Figure 4-6: The comparison between the observed annual precipitation and the predicted values for the C018 site including lines representing the maximum recorded annual precipitation as well as a line indicating precipitation levels 20% above the maximum (a), predicted annual landslide volume using the weather data collected from the BCC-CSM1.1m climate model (b) Question marks indicate the uncertainty in extrapolating the correlations found.

Equations (4-3) and (4-4), which are given below, are used to estimate the lower and upper bounds of volumes with 85% confidence, according to the relationship developed using data currently available for the site. It is acknowledged that there is significant uncertainty in extrapolating the correlation found for estimating changes in the future. To refine the estimates, additional photogrammetry surveys and more data gathering would be necessary.

$$V_{Lower\ bound} = 3.26 \times P - 680.58 \quad (4\text{-}3)$$

$$V_{Upper\ bound} = 3.26 \times P - 503.04 \quad (4\text{-}4)$$

Equations (4-3) and (4-4) were used to estimate the possible range in landslide volumes in the future, based on the predicted annual precipitation. Results show that with 20% more precipitation than the maximum observed precipitation between 2018 and 2022, the annual landslide volume can increase up to 1044-1222 m^3 with 85% confidence, which is 16-35% more than the highest observed volume (903 m^3) in 2018. Landslide volumes can also be estimated for the years with the most unfavourable weather conditions when annual precipitation is predicted to be significantly higher than average. In the years with extreme precipitation levels, the predicted volumes may even surpass and reach up to 1636 m^3. It is worth noting that climate models predict weather data using sophisticated mathematical equations and consider many assumptions in their calculations. Therefore, there is an uncertainty in their predictions which should be considered when the equations (4-3) and (4-4) are used. Moreover, despite the presence of various failure types at the C018 site, the process involved in all failures is the same—an erosional process, specifically a slope mass wasting process. Therefore, as long as the failure process remains unchanged, the methodology used in this analysis remains applicable for future landslides at the site.

As of the end of 2022, a total of approximately 6000 m^2 of active zones had been identified at the C018 site, using change detection from photogrammetric point clouds. Assuming an extraordinarily wet year, a total of 1450-1650 m^3 landslide volume is plausible from a kinematic and geometric perspective (for example, such volume is equivalent to the reactivation of half of the active zones with a thickness of 0.5 m). It should be noted that equations (4-3) and (4-4) are based on only five years of data and therefore there is an uncertainty in the estimates provided in this paper. However, this study demonstrates that there is a correlation between the annual cumulative precipitation and the corresponding volume of landslides at the study site. The correlations found in this study and the estimated landslide volumes can be updated regularly in light of new information. Importantly, the methodology presented in this study can be applied in other areas to compare the intercepts and slopes of the linear correlations discovered.

4.4 Conclusion

This paper showed that there is a direct relationship between the amount of precipitation and the landslide volume. This paper provided a methodology to investigate this relationship, which can be expanded to other sites with different geological contexts and for other triggering factors that could have more impact on slope stability. I applied the proposed methodology to a study site in Alberta, Canada and found a linear relationship between the annual volume of landslides and the annual cumulative precipitation.

It should be noted that the equations presented in this paper are obtained based on the limited data available for the site and as more data become available, the relationship between precipitation and landslide volume can be updated.

Climate change models show that annual precipitation is expected to increase in the study area. To assess how climate change affects landslide volume at the site, the proposed equations were used to estimate the lower and upper bounds of annual landslide volume in future years using the predicted weather data from the BCC-CSM1.1m climate model. Predictions reveal that up to 81% more annual landslide volume could be expected in future years of above-average precipitation. Larger landslide volumes due to climate change would be associated with higher landslide hazards for the area and increased maintenance costs; a greater number of people exposed to landslide risk may also occur at this site with future population growth and increasing frequency of landslides.

Moreover, the methodology presented in this paper has the potential to be utilized in other study areas as a means of measuring the impact of climate change on landslide volumes. Based on these findings, authorities could prioritize resource allocation and focus their monitoring efforts on the most critical sites.

4.5 Acknowledgement

This research was made possible by a collaboration between Klohn Crippen Berger, Alberta Transportation, and the University of Alberta. This study was supported financially by Klohn

Crippen Berger and the Natural Sciences and Engineering Research Council of Canada (NSERC) and through a Collaborative Research and Development Grant. Special acknowledgement to Kristen Tappenden (AT) and Roger Skirrow (AT) for reading the manuscript and providing valuable feedback.

4.6 References

ADAM Technology (2021) 3DM Analyst. Available at: https://www.adamtech.com.au

Alberta Transportation (2021) Annual Landslides Assessments for Central Region (CMA511-516). https://www.transportation.alberta.ca/PlanningTools/GMS/Annual Landslides Assessments/Reg-Central Region (CMA511-516)/Inspection Sites/837_02 (C18) - Red Deer River Scour 1.9km from SH575/Reports/. Accessed 23 August 2021

Bhardwaj A, Wasson RJ, Ziegler AD, et al (2019) Characteristics of rain-induced landslides in the Indian Himalaya: A case study of the Mandakini Catchment during the 2013 flood. Geomorphology 330:100–115. https://doi.org/10.1016/j.geomorph.2019.01.010

Brunetti MT, Melillo M, Peruccacci S et al (2018) How far are we from the use of satellite rainfall products in landslide forecasting? Remote Sens Environ 210:65–75. https://doi.org/10.1016/j.rse.2018.03.016

Chi Y, Lee Y (2013) Assessment of landslide volume for Alishan Highway based on database of rainfall-induced slope failure. Int J Environ Chem Ecol Geol Geophys Eng 7:693–698

ClimateData.ca (2023) Climate data for a resilient Canada. https://climatedata.ca/. Accessed 18 Oct 2022

CloudCompare (version 2.10.2) [GPL software] (2022) Retrieved from: http://www.cloudcompare.org/

Cruden DM, Varnes DJ (1996) Landslide types and processes. In: Turner AK. and Shuster RL (eds) Landslides: Investigation and Mitigation. Transportation Research Board Special Report 247, Wasington, DC, pp 36-75

Dai F, Lee C (2001) Frequency–volume relation and prediction of rainfall-induced landslides. Eng Geol 59:253–266. https://doi.org/10.1016/S0013-7952(00)00077-6

DJI (2021) Phantom 4 - Product Information - DJI. https://www.dji.com/ca/phantom-4/info. Accessed 26 Dec 2021

Fan L, Lehmann P, Zheng C, Or D (2020) Rainfall intensity temporal patterns affect shallow landslide triggering and hazard evolution. Geophys Res Lett 47:1–9. https://doi.org/10.1029/2019GL085994

Girardeau-Montaut D, Roux M, Marc R, Thibault G (2005) Change detection on points cloud data acquired with a ground laser scanner. Int Arch Photogramm Remote Sens Spat Inf Sci 36:30–35

Godt JW, Baum RL, Chleborad AF (2006) Rainfall characteristics for shallow landsliding in Seattle, Washington, USA. Earth Surf Process Landforms 31:97–110. https://doi.org/10.1002/esp.1237

Guzzetti F, Peruccacci S, Rossi M, Stark CP (2008) The rainfall intensity-duration control of shallow landslides and debris flows: An update. Landslides 5:3–17. https://doi.org/10.1007/s10346-007-0112-1

Huang A, Lee JT, Ho Y Te, et al (2012) Stability monitoring of rainfall-induced deep landslides through pore pressure profile measurements. Soils Found 52:737–747. https://doi.org/10.1016/j.sandf.2012.07.013

Iverson RM (2000) Landslide triggering by rain infiltration. Water Resour Res 36:1897–1910. https://doi.org/10.1029/2000WR900090

Iverson RM, Major JJ (1987) Rainfall, ground-water flow, and seasonal movement at Minor Creek landslide, northwestern California: physical interpretation of empirical relations. Geol Soc Am Bull 99:579–594. https://doi.org/10.1130/0016-7606(1987)99<579:RGFASM>2.0.CO;2

Lague D, Brodu N, Leroux J (2013) Accurate 3D comparison of complex topography with terrestrial laser scanner: Application to the Rangitikei canyon (N-Z). ISPRS J Photogramm Remote Sens 82:10–26. https://doi.org/10.1016/j.isprsjprs.2013.04.009

Laherrère J (2019) Are there enough fossil fuels to generate the IPCC CO2 baseline scenario? https://aspofrance.files.wordpress.com/2019/08/ipccco2rcp.pdf. Accessed 18 Mar 2021

Leyva S, Cruz-Pérez N, Rodríguez-Martín J et al (2022) Rockfall and rainfall correlation in the Anaga Nature Reserve in Tenerife (Canary Islands, Spain). Rock Mech Rock Eng. https://doi.org/10.1007/s00603-021-02762-y

Liu KF, Wu YH, Chen YC et al (2013) Large-scale simulation of watershed mass transport: A case study of Tsengwen reservoir watershed, southwest Taiwan. Nat Hazards 67:855–867. https://doi.org/10.1007/S11069-013-0611-4

Lucieer A, Jong SM, Turner D (2014) Mapping landslide displacements using Structure from Motion (SfM) and image correlation of multi-temporal UAV photography. Prog Phys Geogr 38:97–116. https://doi.org/10.1177/0309133313515293

Macciotta R (2019) Review and latest insights into rock fall temporal variability associated with weather. Proc Inst Civ Eng Geotech Eng 172:556–568. https://doi.org/10.1680/jgeen.18.00207

Macciotta R, Hendry M, Cruden DM et al (2017a) Quantifying rock fall probabilities and their temporal distribution associated with weather seasonality. Landslides 14:2025–2039. https://doi.org/10.1007/s10346-017-0834-7

Macciotta R, Martin CD, Edwards T et al (2015a) Quantifying weather conditions for rock fall hazard management. Georisk Assess Manag Risk Eng Syst Geohazards 9:171–186. https://doi.org/10.1080/17499518.2015.1061673

Martinović K, Gavin K, Reale C, Mangan C (2018) Rainfall thresholds as a landslide indicator for engineered slopes on the Irish Rail network. Geomorphology 306:40–50. https://doi.org/10.1016/j.geomorph.2018.01.006

McColl ST (2022) Landslide causes and triggers. In: Shroder JF, Davies T, Rosser N (eds) Landslide Hazards, Risks, and Disasters. Elsevier, pp 13–41. https://doi.org/10.1016/B978-0-12-818464-6.00011-1

Mirhadi N, Macciotta R, Gräpel C et al (2022) Antecedent weather signatures for various landslide failure modes at a 60-m-high rock slope near Drumheller, AB. In: Geohazards8, 8th Canadian Conference on Geotechnique and Natural Hazards: Innovative geoscience for tomorrow. Québec City, pp 447–455

Niethammer U, James MR, Rothmund S et al (2012) UAV-based remote sensing of the Super-Sauze landslide: Evaluation and results. Eng Geol 128:2–11. https://doi.org/10.1016/J.ENGGEO.2011.03.012

Popescu ME (1994) A suggested method for reporting landslide causes. Bull Int Assoc Eng Geol 50:71–74. https://doi.org/10.1007/BF02594958

Pratt C, Macciotta R, Hendry M (2019) Quantitative relationship between weather seasonality and rock fall occurrences north of Hope, BC, Canada. Bull Eng Geol Environ 78:3239–3251. https://doi.org/10.1007/s10064-018-1358-7

Rahardjo H, Li XW, Toll DG, Leong EC (2001) The effect of antecedent rainfall on slope stability. Geotech Geol Eng 19:371–399. https://doi.org/10.1023/A:1013129725263

Rodriguez-Caballero E, Rodriguez-Lozano B, Segura-Tejada R et al (2021) Landslides on dry badlands: UAV images to identify the drivers controlling their unexpected occurrence on vegetated hillslopes. J Arid Environ 187:104434. https://doi.org/10.1016/j.jaridenv.2020.104434

Rodriguez J, Macciotta R, Hendry MT et al (2020) UAVs for monitoring, investigation, and mitigation design of a rock slope with multiple failure mechanisms—a case study. Landslides 17:2027–2040. https://doi.org/10.1007/s10346-020-01416-4

Rosi A, Peternel T, Jemec-Auflič M et al (2016) Rainfall thresholds for rainfall-induced landslides in Slovenia. Landslides 13:1571–1577. https://doi.org/10.1007/s10346-016-0733-3

Roustaei M, Macciotta R, Hendry M et al (2020) Characterisation of a rock slope showing three weather-dominated failure modes. In: Proceedings of the 2020 International Symposium on Slope Stability in Open Pit Mining and Civil Engineering. Australian Centre for Geomechanics, Perth, pp 427–438

Saito H, Korup O, Uchida T et al (2014) Rainfall conditions, typhoon frequency, and contemporary landslide erosion in Japan. Geology 42:999–1002. https://doi.org/10.1130/G35680.1

Tappenden KM, Skirrow RK (2020) Vision for geotechnical asset management at Alberta Transportation. In: GeoVirtual 2020, Resilience and Innovation. p 10

Turner D, Lucieer A, Jong SM (2015) Time series analysis of landslide dynamics using an Unmanned Aerial Vehicle (UAV). Remote Sens 2015, Vol 7, Pages 1736-1757 7:1736–1757. https://doi.org/10.3390/RS70201736

Uchiogi T (1971) Landslides due to one continual rainfall. Japan Soc Eros Control Eng 23:21–34. https://doi.org/https://doi.org/10.11475/sabo1948.23.4_21

Weidner L, DePrekel K, Oommen T, Vitton S (2019) Investigating large landslides along a river valley using combined physical, statistical, and hydrologic modeling. Eng Geol 259:105169. https://doi.org/10.1016/j.enggeo.2019.105169

Wu C-Y, Chou P-K (2021) Prediction of total landslide volume in watershed scale under rainfall events using a probability model. Open Geosci 13:944–962. https://doi.org/10.1515/geo-2020-0284

Wu T, Lu Y, Fang Y et al (2019) The Beijing Climate Center Climate System Model (BCC-CSM): the main progress from CMIP5 to CMIP6. Geosci Model Dev 12:1573–1600. https://doi.org/10.5194/gmd-12-1573-2019

Wyllie DC (2017) Rock slope engineering. CRC Press, fifth edition. Taylor & Francis, CRC Press

Yang Z, Lv J, Shi W et al (2021) Experimental study of the freeze thaw characteristics of expansive soil slope models with different initial moisture contents. Sci Rep 11:23177. https://doi.org/10.1038/s41598-021-02662-9

CHAPTER 5

Quantitative Correlation Between Rock Fall and Weather Seasonality to Predict Changes in Rock Fall Hazard with Climate Change

Contribution of this chapter to the overall study

Following the investigation into the influence of weather conditions on landslides at the local scale, the impact of precipitation and freeze-thaw cycle on the rock falls recorded at CN's Yale subdivision was studied through a statistical approach. Moreover, the relationships found in this study were used to explore potential shifts in the timing and frequency of future rock falls resulting from climate change. Similar to Chapters 3 and 4, this study was conducted to meet the first and second objectives of this thesis which aim to develop a methodology to quantify the change in landslide hazard as a response to changes in weather conditions and to forecast changes in landslide hazard as a response to climate change at a local scale. The methodology developed in this chapter includes the following steps in general:

- Create a 30-year weather database using modelled historical data provided by different climate change models. The weather database used in this study is an ensemble of 24 climate models.
- Calculate average monthly rockfalls and related weather factors such as precipitation and freeze-thaw cycles.
- Adjust the average values to 30 days and normalize the resulting values to the average annual totals.
- Define von Mises distributions that are representative of the monthly adjusted normalized weather conditions.

- Combine von Mises distributions with relative weights to find the best-fitted model to the adjusted normalized monthly rock fall data.
- Create weather databases for the selected time periods in the future using available climate change models.
- Define proper von Mises distributions on the predicted adjusted normalized monthly weather factors.
- Combine the newly defined von Mises distributions with the relative weights found in earlier stages to create predicted rockfall distributions for the selected time periods in the future.
- Compare the rock fall distributions to investigate the effects of climate change on the future of rockfall activity in the study area.

The research presented in this chapter has been published in the Landslides journal in June 2023 with the following citation:

Mirhadi N, Macciotta R (2023) Quantitative correlation between rock fall and weather seasonality to predict changes in rock fall hazard with climate change. Landslides. https://doi.org/10.1007/s10346-023-02105-8

Abstract

The Canadian Cordillera in the province of British Columbia witnesses numerous rock falls every year. Studies on the recorded rock fall data in this area show that rock fall hazard follows weather conditions, especially precipitation and freeze-thaw cycles. This relationship indicates that a weather-based approach can be implemented to estimate possible changes in the rock fall hazard due to climate change. In this paper, I used a statistical approach to quantify the relationship between monthly weather averages and rock fall frequencies for a section of a transportation corridor along the Fraser River in British Columbia, Canada. In this regard, von Mises distributions are used to find the best-fitted models to the monthly precipitation and freeze-thaw cycles, and proper relative weights are applied to the models in order to calibrate them to the rock fall monthly

frequency. The calibrated model is used with input data from climatic predictions for 2041-2070 and 2071-2100 to see how rock fall distribution will be affected due to climate change in the future decades. Results show that between 9% and 19% more rock fall is anticipated in future winters. Rock falls are expected to decrease in other months, especially in October, November, March, and April. This paper presents a method for predicting changes in rock fall hazard seasonality due to climate change and illustrates the method with a case study along a section of the Canadian Cordillera.

5.1 Introduction

The Canadian Cordillera in the province of British Columbia witnesses numerous rock falls every year (Hungr et al. 1999). This natural hazard causes financial losses to infrastructure facilities, including Canadian National Railway (CN) lines and inter-provincial highways connecting Alberta to British Columbia (Hungr et al. 1999). According to Porter et al. (2019), the annual financial impact of landslides in some parts of the western Canadian sedimentary basin, which includes parts of Manitoba, Saskatchewan, Alberta, British Columbia, and Northwest Territories, is approximately CA$100 to CA$148 million, of which CA$9 to CA$17 million is estimated direct damage to the railways, and CA$16 to CA$22 million is the estimated damage to the provincial transportation network.

CN has been recording information about rock falls since 1995, including the time, location, and approximate size of the fallen rocks along its railway network in British Columbia. This information has been used by several researchers to better understand the relationship between rock falls and the triggering factors, such as weather, geology, and geometry of slopes (Macciotta et al. 2011; Macciotta et al. 2013; Macciotta et al. 2015a; Macciotta et al. 2015b; Macciotta et al. 2017a; Macciotta et al. 2017b; Macciotta 2019; Pratt et al. 2019).

Assessing the effects of weather or climatic conditions on the occurrence of rock falls leads to a better understanding of the failure mechanism, and when combined with the weather and climate predictions, the results may be used toward improving risk mitigation strategies for the study area.

According to Bjerrum and Jørstad (1968), weather-related factors have the highest role in occurring rock falls. They showed that 90% of rock fall events in their study were triggered by climate-induced processes. In another study, Leyva et al. (2022) analyzed the weather data from 2010 to 2016 and the rainfall-induced rock falls in Anaga, Canary Islands. They defined three precipitation thresholds (60/100/180 mm in 12 hours) to calculate rock fall probability. They showed that the probability of occurrence of an event increases to 70% if the 12-hour accumulated rainfall exceeds 60 mm.

A study conducted by Macciotta et al. (2015a) examined the relationship between weather conditions and the occurrence of rock falls on the hard rock slopes along a railway section in the Canadian Cordillera. According to their findings, 90% of rock falls could be predicted by the 3-day antecedent precipitation and freeze-thaw cycles. They also observed that some rock falls which could not be predicted by the 3-day antecedent approach, occurred during the first two weeks of the spring thaw.

Global climate change has had measurable effects, and it is predicted to intensify in the years to come (Bush and Lemmen 2019; IPCC 2021). According to Crozier (2010), changing climate can lead to increased precipitation, temperature, wind speed and duration, and rain-bearing weather systems.

Changes in climatic conditions are expected to lead to changes in the erosional processes and therefore change the frequency of rock falls. Hungr et al. (1999) provide a study where they show the cumulative frequency of different rock fall volumes along a section of the Fraser River Valley in British Columbia. It is plausible that the changes in erosional processes will also lead to changes in the volume distribution of rock falls. Therefore, rock fall inventories will be very valuable in future studies into rock fall hazards, as these will allow evaluating changes in the rock fall volume-frequency relationships.

According to White et al. (2023), a large number of post-wildfire landslides occurred after the unprecedented heat wave of June 2021 in the summer and fall of 2021 in British Columbia, Canada, which left extensive damages to Lytton and Lytton First Nation reserves and affected railway and highway infrastructures. Gariano and Guzzetti (2016) predict an increase in the number of people exposed to landslide risk, where global warming is expected to increase the frequency and intensity of severe rainfall events. However, the current knowledge is limited about

the effects of climate and its variation on slope stability, landslides (including rock falls), landslide hazards, and related risks (Gariano and Guzzetti 2016). This suggests that quantifying the relationships between climate and rock fall activity provides an opportunity to understand the potential changes in the frequency of events because of climate change.

A number of research projects have been conducted in Canada to investigate the impact of climate change on future landslide activities. Bovis and Jones (1992) used aerial photos, dendrochronological (tree-ring dating) data, and stratigraphic data to show that many earth flows in British Columbia were reactivated during the relatively wet period of 1950-1985, responding to Holocene climatic variations.

Jakob and Lambert (2009) studied the effect of global warming on the relative frequency of landslides along the British Columbia coast by examining the monthly mean simulations of precipitation from 19 climate models using three IPCC climate change scenarios. Their calculations show that, on average, a 10% increase in 4-week antecedent rainfall and a 6% increase in 24-hour precipitation can be expected by the end of the 21st century. Comparing this amount of rainfall increase with the thresholds calibrated on landslide and storm data in the period 1963-2007, they suggested that the total number of debris flows in the studied area increases by 28% by the year 2100.

In another research, Jakob and Owen (2021) studied the changes in the frequency and magnitude of shallow landslides and resulting debris flows because of the impacts of climate change in the North Shore Mountains of Vancouver, BC. They calculated the changes in precipitation for two emission scenarios for the 2050s and 2080s. Based on the weather projections, they concluded there will be an increase of approximately 140% to 280% in the number of landslides by the 2050s, whereas, for the 2080s, it ranges approximately between 130% and 380%.

This paper focuses on rock fall phenomena and the expected changes in rock fall hazard as a consequence of climate change. The paper presents a framework to estimate changes in rock fall monthly distribution due to climate change, illustrated along a section of railway exposed to rock fall occurrences in the Canadian Cordillera. The results and framework provide a tool to inform decision-makers to develop risk mitigation plans and resilience strategies associated with climate change along transportation corridors exposed to rock fall hazards.

5.2 Study area

5.2.1 Location and geology

The study area is a 32 km section of railway operated by the Canadian National Railway (CN), which is part of CN's Yale subdivision in the Canadian Cordillera in British Columbia, Canada. The study area begins at Milepost 5 west of China Bar, continues south along the Fraser River and ends near Yale (Figure 5-1). The study area is located adjacent to steep valley walls and cuts.

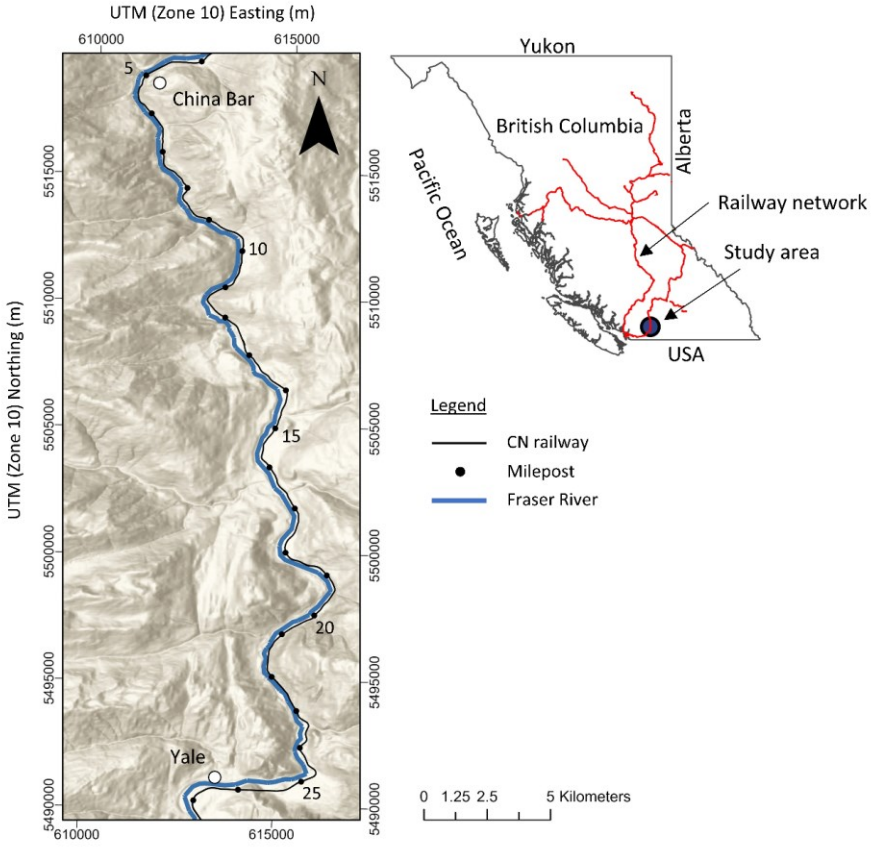

Figure 5-1: Location of the study area

Figure 5-2 shows the lithologic units and the location of the major faults within the study area as mapped by the British Columbia Geological Survey (Cui et al. 2017). The study area comprises sedimentary, metamorphic, intrusive, and volcanic rocks which are well-exposed throughout the Fraser River valley (Macciotta et al. 2011; Cui et al. 2017).

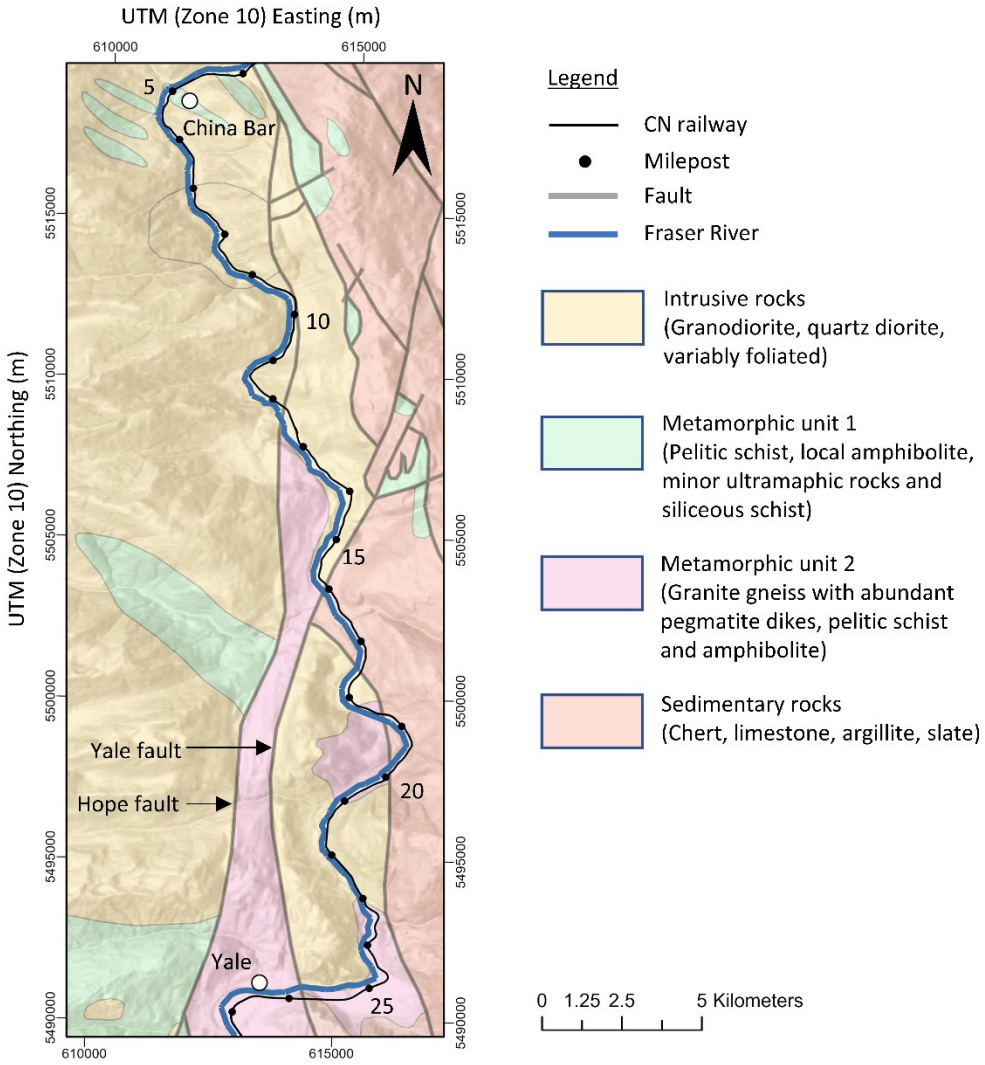

Figure 5-2: Bedrock geology and the location of the major faults in the study area (after Macciotta et al. 2011)

According to Monger (1970), the area has been intensely glaciated such that the highest peaks and ridges stood above the level of Pleistocene ice and now bear evidence of alpine glaciation. Due to this glaciation, the Fraser River valley is characterized by a U-shaped section with truncated spurs and hanging side valleys. Macciotta et al. (2011) noted that the Fraser River stream action carved a V-shaped cut at the bottom of the valley with a depth of about 30 meters which has led to a succession of constrictions within a larger canyon where the river velocity increases significantly. They also stated that the high river velocity, together with alluvial fans, have caused significant

lateral erosion, resulting in toe unloading and steepening of the valley slopes. These conditions have led to the emergence of an area with high rock fall activity in the vicinity of the CN rail track between Milepost 5 and 25.

5.2.2 Weather

According to the modelled historical weather data for the period of 1990-2019, the temperatures range from a monthly average low of -3.9˚C in January to a monthly average high of 16.8˚C in July. The average monthly temperature and precipitation for this data period are shown in Figure 5-3. An average of approximately 550 mm of precipitation falls from November to the following January, and the average temperature is below 0˚C from December to the following February of the next year. The method of collecting and analyzing the weather data is described in the Methods and materials section.

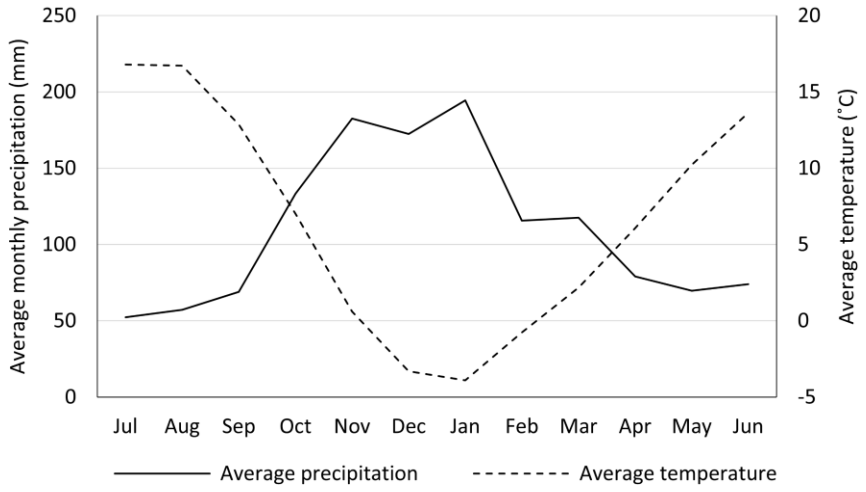

Figure 5-3: Monthly average precipitation and temperature from 1990 to 2019

One limitation of this study is that the available weather databases do not distinguish rainfall from snowfall in the precipitation data. Therefore, the precipitation data in this study represents total precipitation without specifying whether it is snow or rain. However, according to Pratt et al.

(2019), nearby weather stations recorded approximately 93% of total precipitation as rainfall, therefore limiting the impact of this simplification.

5.2.3 Recorded rock fall activity

CN continuously records the rock falls that occur along its railway network. The Yale subdivision's rock fall database includes the time, location, and approximate size of the rock blocks, with data extending back to 1996. The spatial distribution of the recorded rock falls, which is shown in Figure 5-4, reveals that 81% of total rock falls occurred between Mileposts 5 and 25.

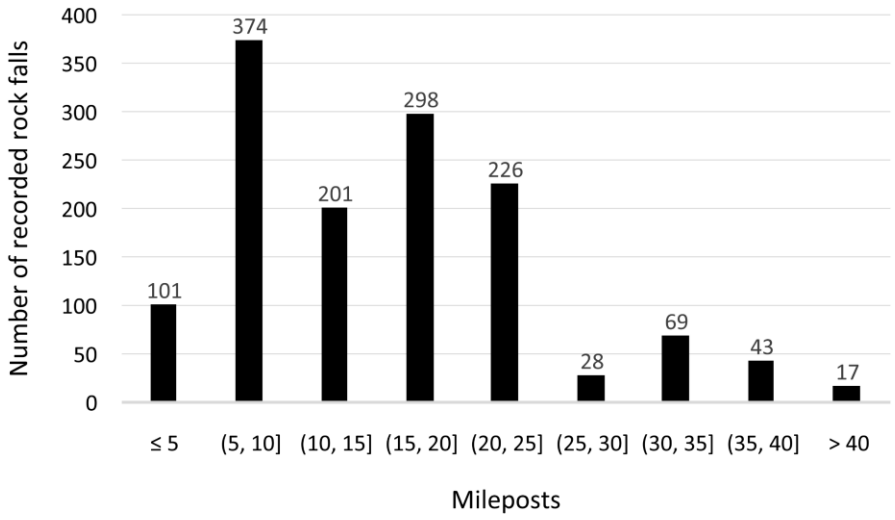

Figure 5-4: Number of recorded rock falls per five mileposts between 1996 and 2021 at CN's Yale subdivision

The time distribution of the rock falls, which is shown in Figure 5-5, reveals two inconsistencies in the frequency of records. The first change in the frequency is observed after the first two years of records (i.e., after 1997). The second discrepancy is observed after 2011 when the average annual rock falls decreased drastically from 37 per year to about four events per year. According to Pratt et al. (2019), these discrepancies are because of the changes made in the recording

standards in 1998 and 2012. To minimize the bias in my analyses, I used the records between 1998 and 2011.

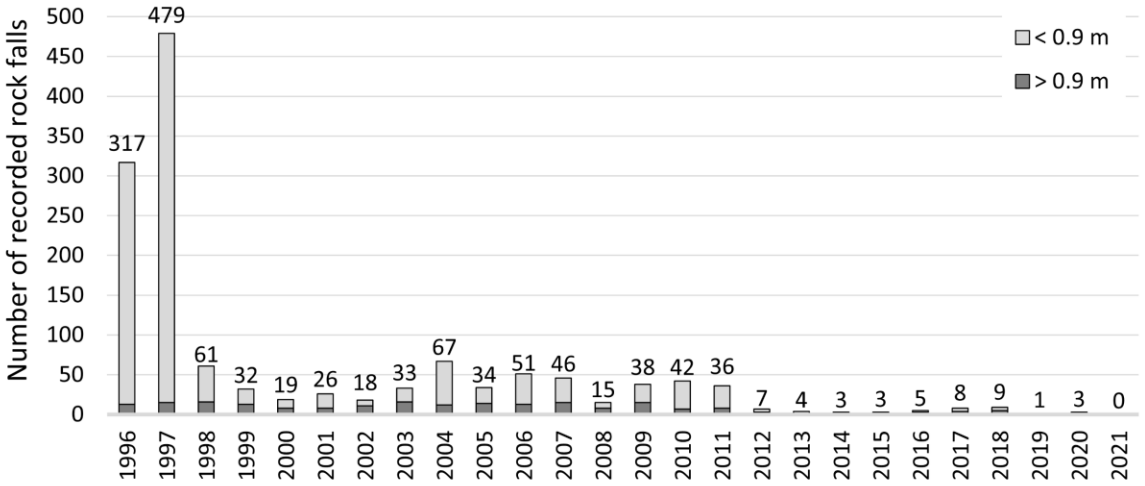

Figure 5-5: Number of recorded rock falls per year between 1996 and 2021 at CN's Yale subdivision. CN records events based on the approximate block diameter and uses a threshold of 0.9 m to differentiate events that can cause derailment (over 0.9 m) from those with a lower risk of derailment (less than 0.9 m).

The resulting rock fall database used in this study consists of 401 rock falls between Mileposts 5 and 25, which were recorded between 1998 and 2011. Figure 5-6 shows a summary of weather data and annual rock fall frequency. The annual average precipitation is 1317 mm, with an average of 194 mm in January. This figure also shows that on average 88 freeze-thaw cycles, and 29 rock falls occur every year.

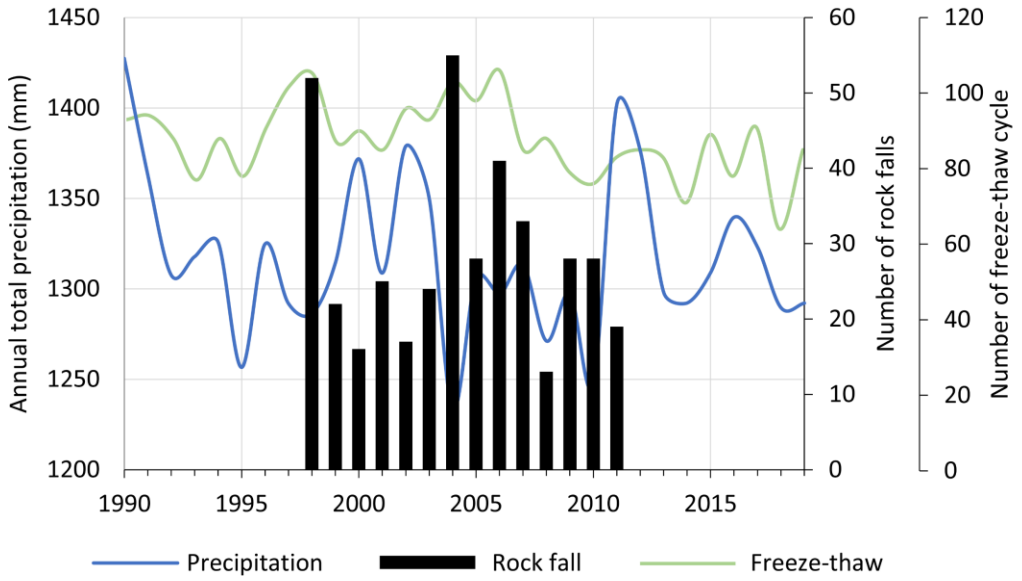

Figure 5-6: Summary of weather data and landslide annual frequency between Mileposts 5 and 25 of CN's Yale subdivision

5.3 Methods and materials

5.3.1 von Mises circular distribution

The von Mises circular distribution method is a way of representing data that is circular in nature. Many natural phenomena, including meteorological events, follow cyclic time series. From the point of view of statistical inference, one of the most useful distributions on the circle is the von Mises distribution (Mardia 1972). Therefore, I adopted this technique in my study as a powerful tool to find a relationship between climate data and rock fall occurrences. The von Mises probability density function is defined as follows (Mardia 1972):

$$M(\mu_0, \kappa) = \frac{1}{2\pi I_0(\kappa)} e^{\kappa \cos(\omega - \mu_0)},\ 0 < \omega \leq 2\pi, \quad \kappa > 0,\ 0 < \mu_0 \leq 2\pi \tag{5-1}$$

where $M(\mu_0, \kappa)$ is the von Mises probability density function, ω is the variable (transformed to equivalent angle), μ_0 is the mean direction (angle), κ is a parameter known as the concentration parameter (the larger the value of κ, the greater the clustering around the μ_0). $I_0(\kappa)$ is the modified Bessel function of the first kind and order zero which can be defined by:

$$I_0(\kappa) = \sum_{r=0}^{\infty} \frac{1}{r!^2} \left(\frac{\kappa}{2}\right)^{2r} \quad (5\text{-}2)$$

According to the historical and predicted weather data of the study area, both precipitation and freeze-thaw cycle are bi-modal which suggests that more than one von Mises distribution is required to represent the weather data. Therefore, the bi-modal distribution can be determined as a sum of weighted uni-modal von Mises distributions as follows:

$$F_M = \sum_{i=1}^{n} W_i F_i(\omega), \ where \ W_1 + W_2 + \cdots + W_n = 1 \quad (5\text{-}3)$$

where F_M is the mixture distribution, $F_i(\omega)$ is the ith von Mises distribution, W_i is the relative weight for the ith distribution, and n is the number of von Mises distributions defined for that parameter.

Weather data and rock fall records must be transformed into angular form prior to fitting the von Mises distributions. In the case of a monthly analysis, each month is represented as 1/12 of a circle ($\pi/6$) or 30 days of a year. However, because the length of the months (number of days) is not equal, some adjustments are required:

- The recorded frequency of the months with 31 days must be multiplied by the ratio 30/31.
- The recorded frequency for the month of February must be multiplied by the ratio 30/28.

- To maintain the total number of records as per the original, the previously adjusted frequencies must be multiplied by the ratio S/S', where S is the original total number of records, and S' is the sum of records obtained after the first two steps.

5.3.2 Weather database

The available weather station network does not cover the entire study area, and its data is not extensive enough to create a 30-year weather database for the area. Therefore, I used modelled historical data that has been calibrated to existing stations in the region to complete a 30-year weather database from 1990 to 2019 along the study area. It is noted that climate models do not generally represent information at the same spatial scale as meteorological observations. However, I consider this approach overcomes weather data limitations and provides consistency between the weather models used for the rock fall hazard projections and the historic rock fall-weather relationships. Furthermore, the importance of testing this approach lies in being able to apply the methodology in the paper to other locations with limited weather station data.

It should be noted that because modelled historical data is simulated data, the weather events will not be exactly the same as observed historical data but will represent the events in the region, and the monthly and annual averages will be representative (ClimateData.ca 2022).

The modelled historical weather data is produced by using climate models in order to compare the model simulations with historical observations (Cannon et al. 2015; ClimateData.ca 2022). Daily weather data, including minimum and maximum temperatures, and total precipitation for the periods of 1990-2019, 2041-2070, and 2071-2100, were collected from ClimateData.ca, which provides historical and future data for the entire of Canada based on 24 climate models.

Since the rock fall database includes records from 1998 to 2011 (14 years), I created a 30-year weather database from 1990 to 2019 such that the rock fall records fall exactly in the middle.

Freeze-thaw cycles

Daily minimum and maximum temperatures were used to determine the occurrence of freeze-thaw cycles. Freezing and thawing points were set to -1°C and +1°C, respectively, and one freeze-thaw cycle is counted when the daily minimum temperature is below -1°C (freezing) and the maximum daily temperature is above +1°C (thawing). Because the weather database was limited to daily values, it was not possible to consider multiple freeze-thaw cycles per day. It should also be noted that the number of freeze-thaw cycles and the associated effects of weathering could be different on slopes with different aspects. For example, a south-facing slope receives more sunlight than a north-facing slope which could result in different rates of weathering.

The -1°C was chosen to ensure that the freezing front could penetrate the rock joints, and +1°C was selected to ensure that the frozen material had enough time to thaw. This approach is consistent with previous studies on rock fall mechanisms (McGreevy and Whalley 1982; Macciotta et al. 2015a; Pratt et al. 2019).

5.3.3 Climate-change models

ClimateData.ca provides climate simulations from 24 different climate models for the period of 2005 to 2100, considering three Representative greenhouse gas Concentration Pathways (RCP): RCP 2.6, 4.5, and 8.5.

The Intergovernmental Panel on Climate Change (IPCC) defines four different RCPs as emission pathways for the 21st century (IPCC 2014). IPCC describes RCP 4.5 as an intermediate scenario that needs intermediate efforts to constrain emissions. This scenario was selected for this study as it is within the probable future CO_2 emissions and is in line with future fossil fuel productions (Laherrère 2019). In RCP 4.5, emissions peak around 2040 and then decline (Meinshausen et al. 2011). The mean surface temperature is anticipated to increase by 1.4 °C in 2046-2065 and 1.8 °C in 2081-2100 globally relative to the reference period of 1986-2005 (Collins et al. 2013). It is noted that the framework presented in this paper can be used for other concentration paths.

Each climate model uses sophisticated mathematical approaches to predict climatic conditions, and because each model is unique and uses different model parameters, inter-model differences would be expected (ClimateData.ca 2022). Therefore, it is recommended to use an ensemble of climate models to get a better understanding of how the climate may be in the future. To create the weather database, I identified the 10^{th} and 90^{th} percentiles of the daily values from all 24 available climate models, and after removing the outliers, the median (50^{th} percentile) values were calculated. The daily median values form the ensemble database and are used in calculating the cumulative precipitation and freeze-thaw cycles. This approach was applied to the predicted values considering the RCP 4.5 emission scenario. It is noted that this approach provides better estimates of monthly weather trends but should not be adopted if the objective is to evaluate differences in the results between models, or if the evaluation aims at identifying the effects of 24-hour extreme events.

Figure 5-7, Figure 5-8, and Figure 5-9 illustrate climate change between 2020 and 2100 for different RCPs. These figures reveal the fact that precipitation and average temperatures are expected to increase in the study area in all RCP scenarios. Because precipitation and freeze-thaw cycles have the greatest influence on rock fall occurrences, any changes in these triggering factors affect the rock fall probability.

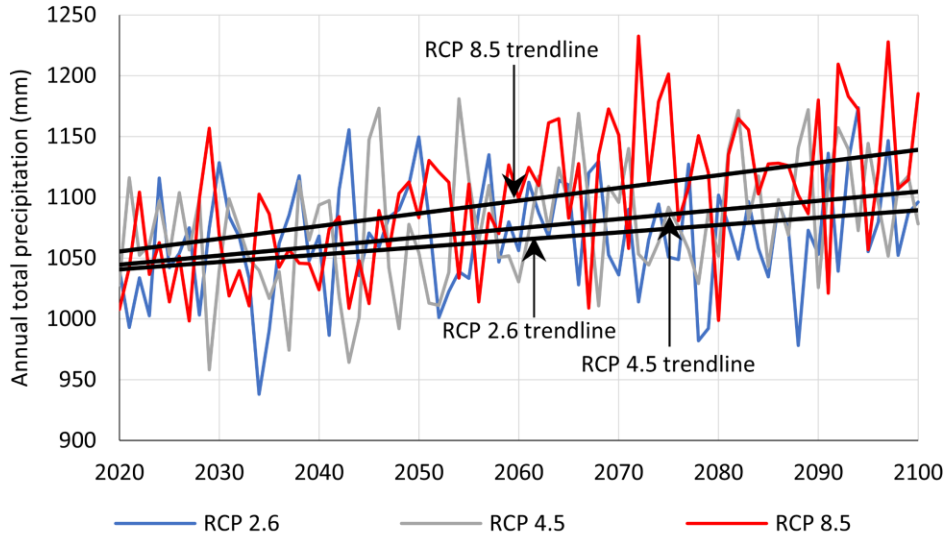

Figure 5-7: Annual precipitation prediction for RCP 2.6, 4.5 and 8.5

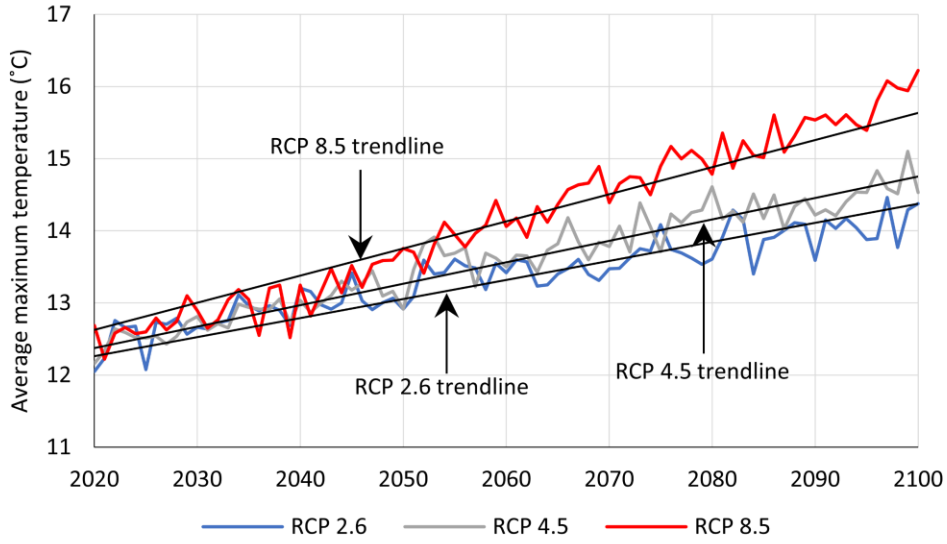

Figure 5-8: Average maximum temperature prediction for RCP 2.6, 4.5 and 8.5

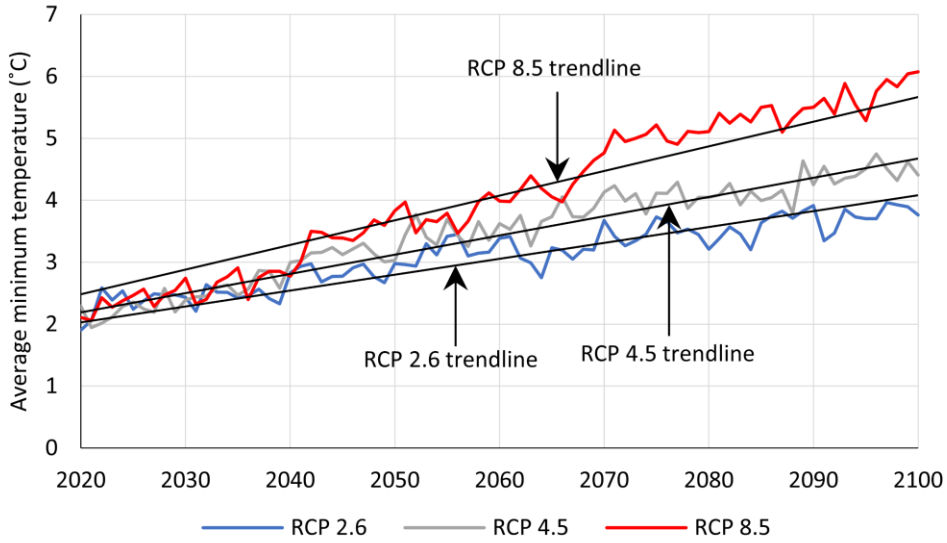

Figure 5-9: Average minimum temperature prediction for RCP 2.6, 4.5 and 8.5

5.3.4 Methodology used in this study

The methodology applied in this paper is adopted from that proposed by Macciotta et al. (2017a). This methodology works well in the areas where there is a direct monthly relationship between

weather and rock fall occurrences. The following are the general steps required to apply the method.

1. Calculate average monthly rock falls, precipitation, freeze-thaw cycles, or other weather-related triggering factors identified in the area. In this paper, monthly average rock fall occurrences are calculated from the 14-year recorded data between 1998 and 2011. Thirty-year daily weather data for the periods of 1990-2019, 2041-2071, and 2071-2100 were analyzed, and the corresponding monthly averages were calculated for each time period. My goal is to study how rock fall distribution at the study site reacts to the current and predicted climate. According to the World Meteorological Organization (WMO), a minimum of 30 years of consecutive weather data is required to calculate climate normals (WMO 2019). It is important to use no less than 30 years of simulated data when considering future climate conditions, as using less than this may show a trend that differs from a longer-term climate change trend (ClimateData.ca 2022).
2. Adoption of a statistical model to represent the seasonality and magnitude of weather characteristics identified as triggers at the site. I recommend the use of circular distributions to represent cyclic information.
3. Because the number of days is not equal in different months, monthly averages must be adjusted to 30 days in order to be used in a circular distribution. Therefore, each month can be assigned a range of $\pi/6$ in a circular distribution, like von Mises (Macciotta et al. 2017a; Mardia 1972).
4. The adjusted average values must be normalized to the average annual totals to provide monthly relative frequencies.
5. Separate von Mises distributions must be defined and combined for each weather trigger that is believed to have an impact on the rock fall occurrences in the study area, such that

the resulting probability density function is as close as possible to the adjusted normalized values.

6. The defined von Mises distributions must be combined with proper relative weights to find the best-fitted model to the adjusted normalized rock fall data. This provides a simple, evidence-based quantitative relationship between weather and rock fall seasonality; supported by the morphological understanding of rock fall mechanisms and triggers at the site.
7. Finally, in order to see how climate change affects rock fall distribution, new von Mises distributions should be defined on predicted climate data. The predicted rock fall distribution can then be found by applying the same relative weights found in Step 6. This approach assumes that at a particular site, the relative importance of weather rock fall triggers would be consistent in time as the lithology and structure of the rock mass will remain.

Figure 5-10 illustrates the general methodology used in this study.

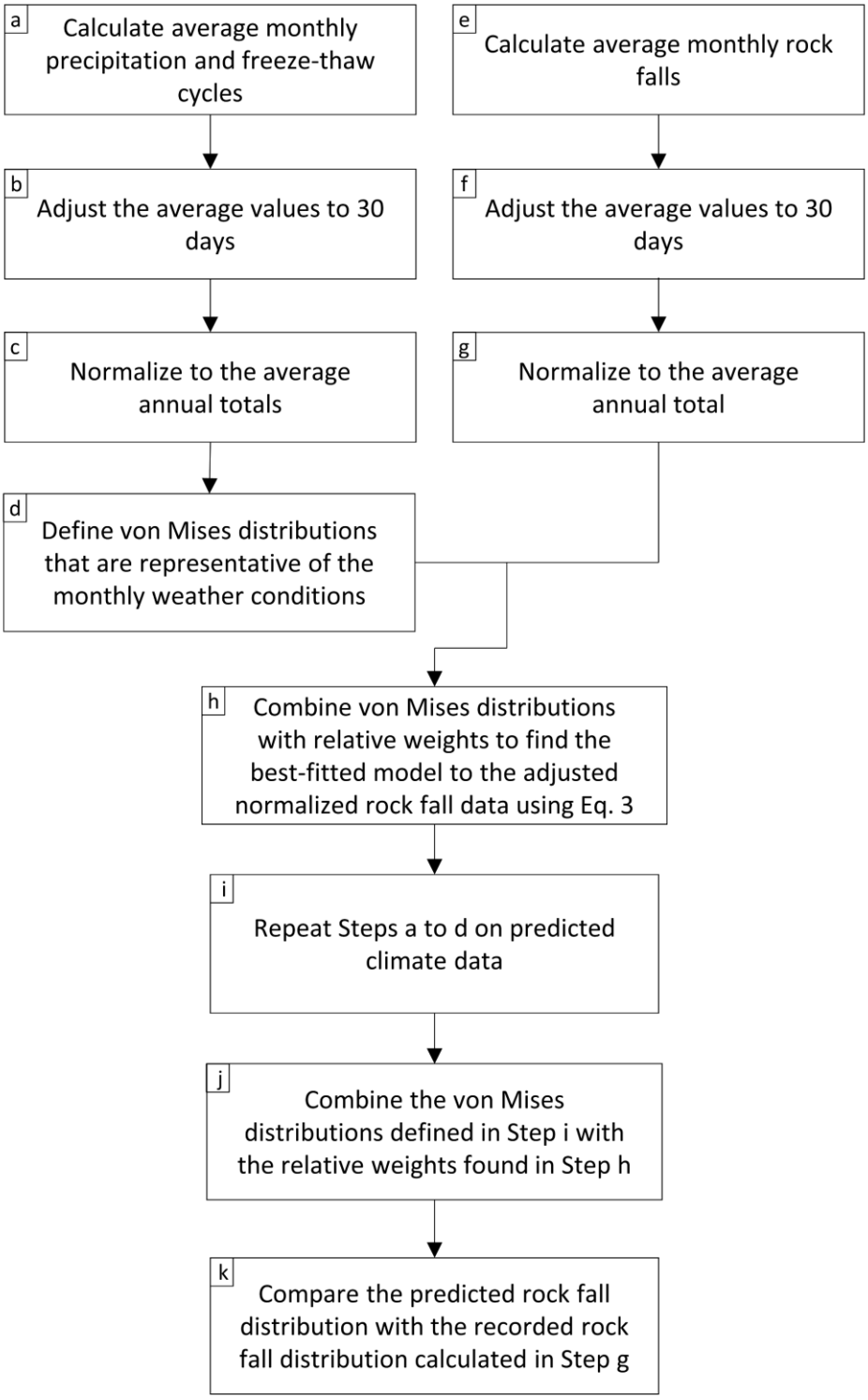

Figure 5-10: Flowchart of the methodology used in this study

5.4 Results and discussion

5.4.1 Distribution fits to the current climatic conditions

Monthly distributions of precipitation and freeze-thaw cycles, which are shown in Figure 5-11 and Figure 5-12, show that the weather data in the study area follows uni- or bi-modal continuous cyclic patterns every year. This suggests that circular distributions such as von Mises can be used to represent weather data.

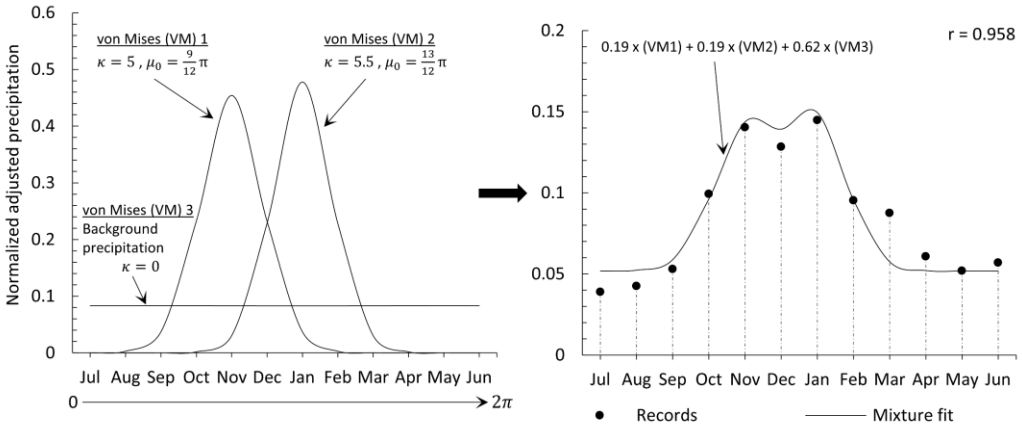

Figure 5-11: Defined von Mises distributions and the mixture fit to normalized monthly precipitation for the period of 1998 to 2019

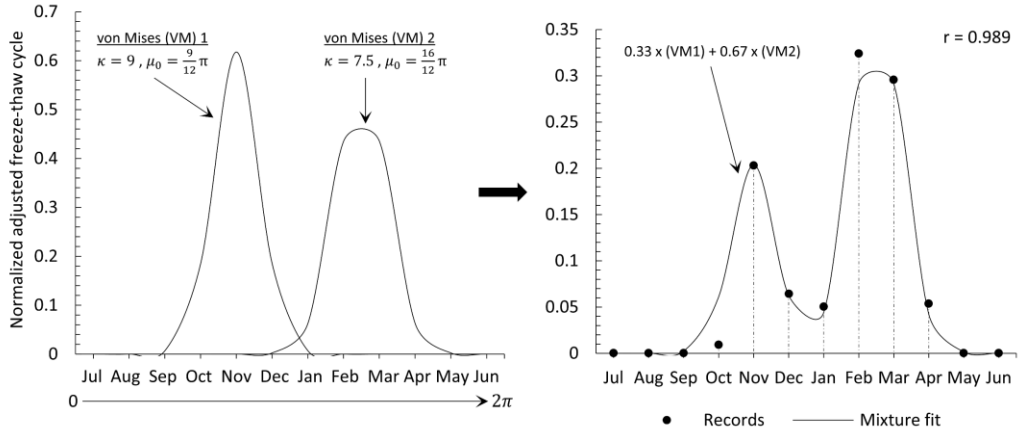

Figure 5-12: Defined von Mises distributions and the mixture fit to normalized monthly freeze-thaw cycle for the period of 1998 to 2019

Precipitation

Three von Mises distributions, as shown in Figure 5-11, were defined and mixed to find the best fit to the monthly normalized precipitation. The parameters of these distributions are as follows:

- von Mises 1: represents the last peak of precipitation that occurs at the end of fall around November of each year. $\mu_0 = \frac{9}{12}\pi$, and $\kappa = 5$.
- von Mises 2: represents the first peak of precipitation that occurs in the middle of winter around January of each year. $\mu_0 = \frac{13}{12}\pi$, and $\kappa = 5.5$.
- von Mises 3: a uniform distribution which represents background precipitation (minimum average monthly precipitation expected) of 65 mm per month. $\kappa = 0$.

To ensure that the defined distributions are representative of the corresponding weather data, they were combined by applying relative weights, and the correlation coefficient between the recorded weather data and the mixture fit was calculated. Figure 5-11 shows the monthly adjusted normalized precipitation and the fitted mixture distribution with a correlation coefficient of 0.958. The relative weights used for fitting the distributions to precipitation are presented in Table 5-1.

Table 5-1: Relative weights used to fit the von Mises distributions to the normalized precipitation data

	von Mises 1, W_1	von Mises 2, W_2	von Mises 3, W_3
W_j	0.19	0.19	0.62

Freeze-thaw cycles

As shown in Figure 5-12, freeze-thaw cycles peak two times every year; once at the end of fall in November and once in late winter/early spring in February/March. Therefore, two von Mises

distributions were defined and combined to find the best fit to the monthly normalized freeze-thaw cycles. The parameters of these von Mises distributions are as follows:

- von Mises 1: represents the last peak of the freeze-thaw cycle that occurs around November of each year. $\mu_0 = \frac{9}{12}\pi$, and $\kappa = 9$.
- von Mises 2: represents the first peak of the freeze-thaw cycle that occurs around February and March of each year. $\mu_0 = \frac{16}{12}\pi$, and $\kappa = 7.5$.

Figure 5-12 also shows the monthly adjusted normalized freeze-thaw cycle and the fitted mixture distribution with a correlation coefficient of 0.989. The relative weights used for fitting the von Mises distributions to freeze-thaw cycle are given in Table 5-2.

Table 5-2: Relative weights used to fit the defined distributions to the normalized freeze-thaw cycle data

	von Mises 1, W_1	von Mises 2, W_2
W_j	0.33	0.67

5.4.2 Rock fall events and their relationship to climate

The mixture fits shown in Figure 5-11 and Figure 5-12 demonstrate that the defined von Mises distributions represent weather conditions well and, therefore, can be used to find a relationship between climate data and rock fall events. For this purpose, the relative weights summarized in Table 5-3 were used to create a multi-modal fit for the rock fall records. This mixture fit, which is shown in Figure 5-13 with a correlation coefficient of 0.975, shows that precipitation and freeze-thaw cycle are adequate parameters for finding the relationship between climate and rock fall events. The relative weights reveal that precipitation has the highest role in rock fall occurrences in the study area, with 78% of the total weight. This is consistent with the general observation that rock fall occurrences are mainly triggered by precipitation events (Coe and Godt 2012). This also

shows that any changes in the precipitation patterns may change the rock fall distribution significantly.

Table 5-3: Relative weights to fit climatic data to rock fall events

	Precipitation			Freeze-thaw cycle	
Description	von Mises 1	von Mises 2	von Mises 3	von Mises 1	von Mises 2
Symbol	W_{p_1}	W_{p_2}	W_{p_3}	W_{FT_1}	W_{FT_2}
Value	0.07	0.41	0.3	0.07	0.15

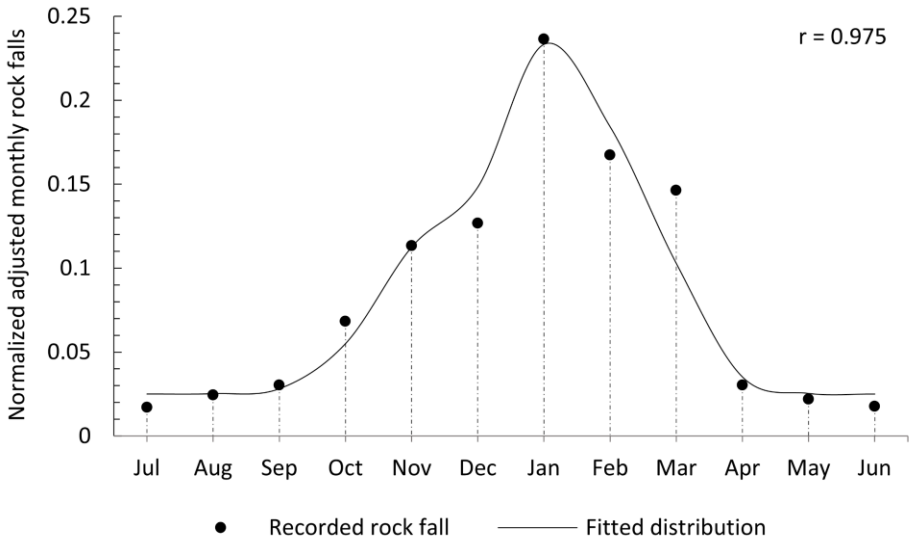

Figure 5-13: Normalized recorded rock falls and the weighted distribution fit

5.4.3 Expected change in rock fall distribution with climate change

Weather databases

Figure 5-14 and Figure 5-15 show the normalized monthly precipitation and freeze-thaw cycles for 2041-2070 and 2071-2100 compared to the 1990-2019 data. Climate predictions show that

higher precipitation is anticipated in November through the following January, which according to the recorded rock fall activity, it is the time period in which most rock falls occur (Figure 5-13). Moreover, Figure 5-15 reveals that freeze-thaw cycles change substantially over the next decades, with increases in December and January, and decreases in November and March, suggesting that the overall duration of the freeze-thaw cycles will be shorter relative to the reference period of 1990-2019.

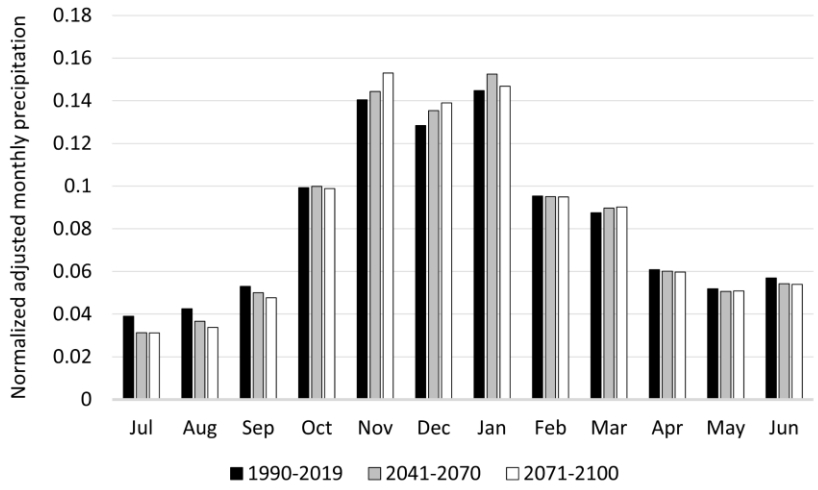

Figure 5-14: Normalized monthly precipitation for different time periods used in this study

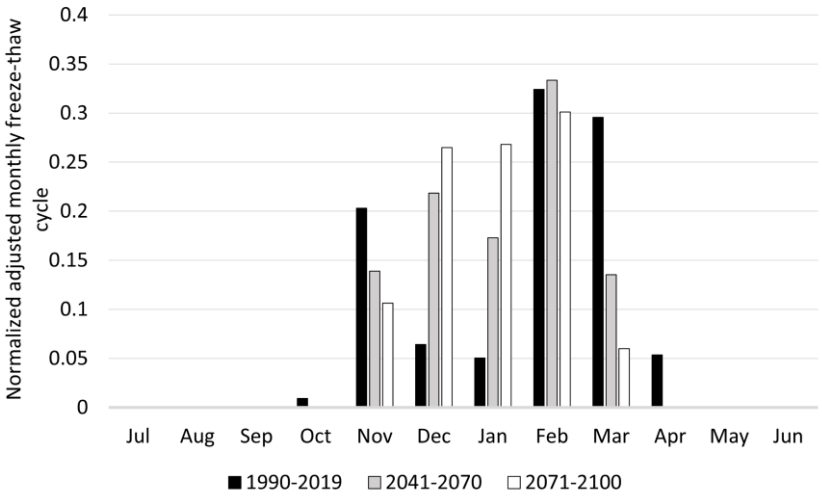

Figure 5-15: Normalized monthly freeze-thaw cycle for different time periods used in this study

According to the predicted climate data, three von Mises distributions are needed to model monthly precipitation (Figure 5-14). These von Mises distributions will represent the background precipitation, and the two peaks visible in the data; one in late fall and the other one in the middle of winter. It should be noted that these new von Mises distributions are independent of the ones that were considered earlier for the current climatic conditions and are defined in a way that the mixture fit has the highest correlation coefficient with the predicted values. The mixture fits for the predicted monthly precipitation for 2041-2070, and 2071-2100 are shown in Figure 5-16.

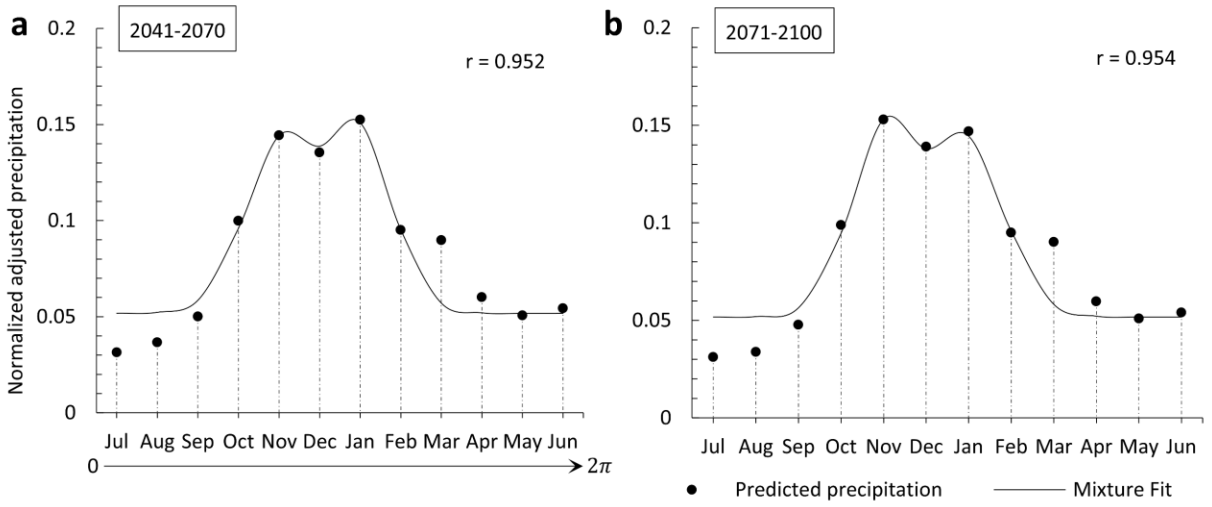

Figure 5-16: Mixture fits to predicted normalized precipitation for periods of 2041-2070 (a), and 2071-2100 (b)

As described earlier, freeze-thaw cycle is anticipated to change considerably in the next decades. However, predictions suggest that there will be two distinguished periods in the monthly data (one in early winter and one in early spring) in which freeze-thaw cycles reach a local peak. Therefore, two von Mises distributions are sufficient for finding the best fit for the predicted values. These mixture fits are shown in Figure 5-17.

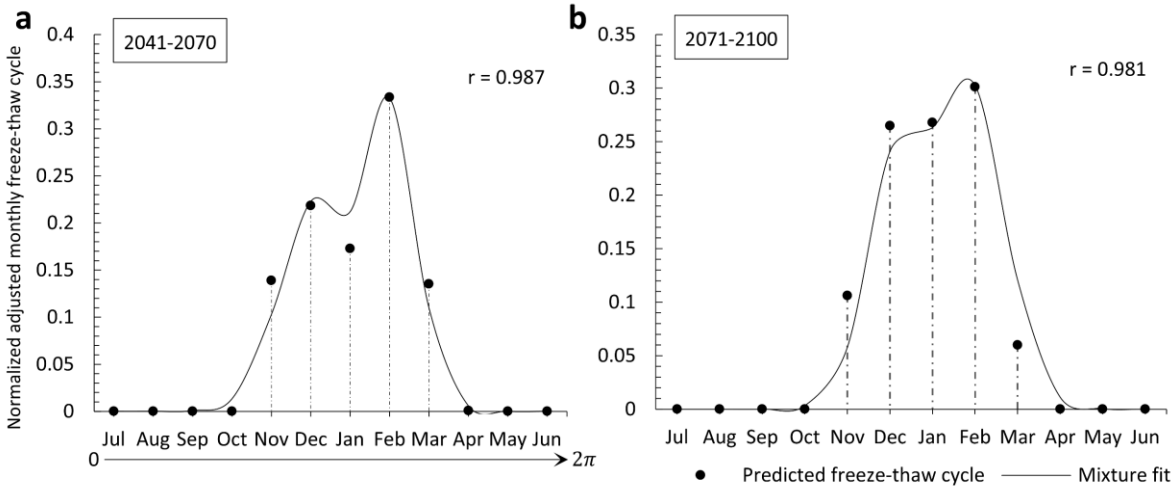

Figure 5-17: Mixture fits to predicted normalized freeze-thaw cycle for periods of 2041-2070 (a), and 2071-2100 (b)

The properties of the distributions defined for precipitation and freeze-thaw cycle for the periods of 2041-2070 and 2071-2100 are summarized in Table 5-4.

Table 5-4: Properties of von Mises distributions for predicted climate data

	Precipitation			Freeze-thaw cycle	
	von Mises 1	von Mises 2	von Mises 3	von Mises 1	von Mises 2
Description	Peaks at the end of fall	Peaks in the middle of winter	Background precipitation	Peaks at the beginning of winter	Peaks at the end of winter
2041-2070	$\mu_0 = \frac{9}{12}\pi, \kappa = 5.1$	$\mu_0 = \frac{13}{12}\pi, \kappa = 5.7$	$\kappa = 0$	$\mu_0 = \frac{11}{12}\pi, \kappa = 5.6$	$\mu_0 = \frac{15}{12}\pi, \kappa = 8$
2071-2100	$\mu_0 = \frac{9}{12}\pi, \kappa = 6$	$\mu_0 = \frac{13}{12}\pi, \kappa = 5.2$	$\kappa = 0$	$\mu_0 = \frac{11}{12}\pi, \kappa = 7$	$\mu_0 = \frac{15}{12}\pi, \kappa = 6.5$

The relationship between climatic data and rock fall events at the study site was found earlier by applying relative weights to five von Mises distributions defined for precipitation and freeze-thaw cycles. Finally, to predict the rock fall changes for the next decades, the same relative weights,

given in Table 5-3, were used on the corresponding von Mises distributions which were defined for the predicted climatic data. The predicted rock fall monthly distributions for 2041-2070 and 2071-2100 are shown in Figure 5-18.

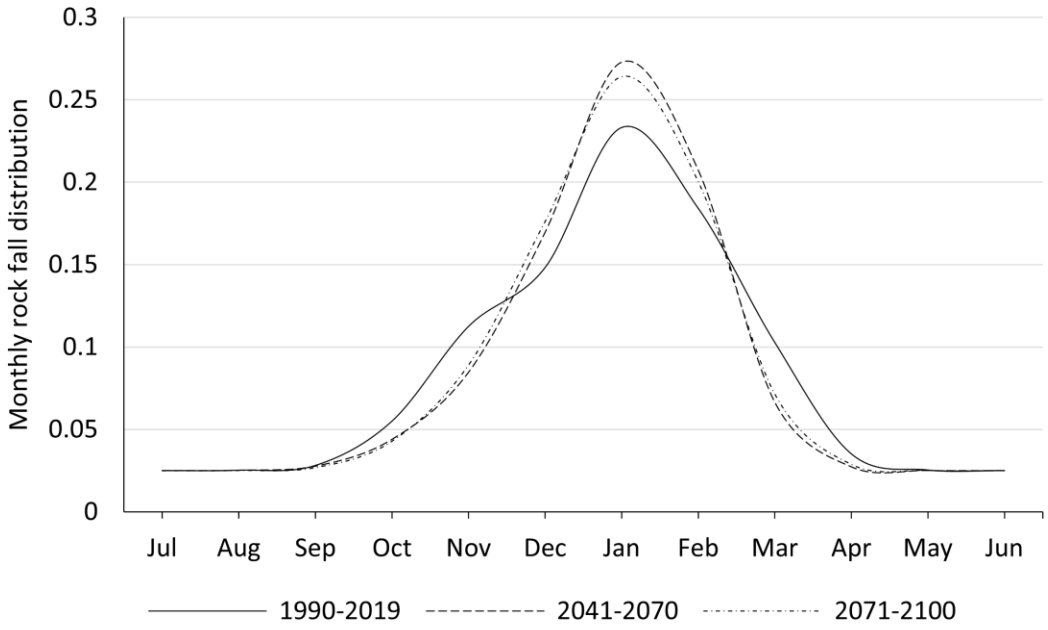

Figure 5-18: Comparison of rock fall distributions

Figure 5-18 shows how rock fall distribution may change in the next decades due to climate change. The relative percentage change for each period is shown in Figure 5-19. According to the results, for the period of 2041-2070, at least 13% more rock fall activity is expected in winter (December to February). The maximum increase in the rock fall events in the period of 2041-2070 is predicted to occur in January. Results also show that the increase in the rock fall activity in the period of 2071-2100 is greatest in December and reaches 19% relative to the reference period of 1990-2019.

On the other hand, rock fall predictions indicate fewer events in the fall and spring, which could be caused by the expected shorter period in which freeze-thaw cycles occur. Based on the results, it is anticipated that the number of rock fall events will decrease by 24% on average in

October, November, March, and April. Based on these findings, the average annual number of rock falls is expected to decrease by 2.31% in 2041-2070 (i.e., from 28.64 events per year to 27.98), and by 2.15% in 2071-2100 (i.e., from 28.64 events per year to 28.03).

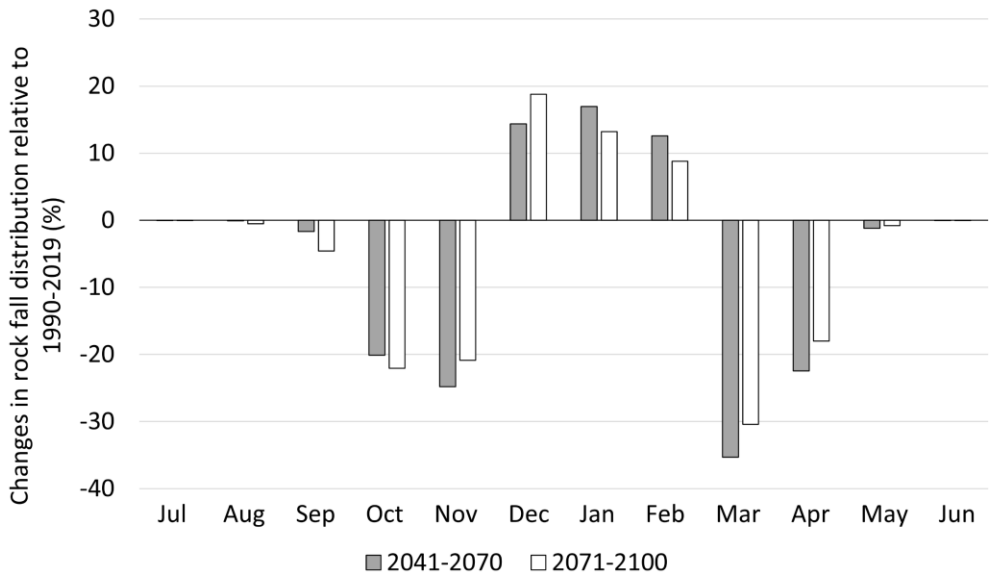

Figure 5-19: Predicted changes in rock fall distribution relative to the period of 1990-2019

These results indicate a relative increase in rock fall hazard between late November and February and a relative decrease in rock fall hazard in October, November, March, and April. Importantly, the results provide a quantified estimate of rock fall risk variation throughout the year as a consequence of climate change. Such results will inform the need for rock fall risk mitigation strategies and required investment for increased resiliency in railway operations as a consequence of projected rock fall hazards due to climate change, in particular along the section of the railway presented in this paper.

The rate of increase in rock fall events is greatest between the present time and 2041-2070, with a reduced rate of increase between 2041-2070 and 2071-2100.

It is worth noting that rock fall events depend on the occurrence of triggers and the availability of unstable rock volumes on the slope. However, changes in climatic data suggest the

possibility for an increase in the frequency of rock fall events in the future decades where rock fall is kinematically feasible.

5.5 Conclusion

This study provided a methodology to correlate a relationship between monthly recorded rockfalls and monthly precipitation and freeze-thaw cycles. The methodology was then used to forecast future changes in the rockfall distribution due to climate change.

Predicted rock fall distributions show that 9% to 19% more rock fall is anticipated in the future winter months of December through February. Rock falls are expected to decrease in other months, especially in October, November, March, and April. Moreover, it is expected that the rate of change in rock fall events decreases sometime between the two time periods considered in this study.

Based on these findings, more accurate rock fall hazard monitoring and risk reduction strategies can be developed in this area. Importantly, this study presents a method to quantify changes in rock fall hazard for climate change scenarios, which can be employed by infrastructure authorities to prioritize their monitoring resources for risk mitigation and to enhance resiliency along transportation corridors for those periods of time when rock fall hazards are the highest. This method and the case study also highlight the importance of robust and available weather databases, and importantly, the value of comprehensive rock fall records.

The rock fall recording standards vary after 2011. Therefore, it is not possible to extend the study to the present. In this regard, it is recommended that robust rock fall records be developed and maintained to allow for enhanced hazard assessments and forecasting for evaluating infrastructure and operational resilience needs in the future.

5.6 Acknowledgement

This research was made possible by the (Canadian) Railway Ground Hazard Research Program. I wish to thank the Canadian National Railway Company (CN) for providing the rock fall data that made this study possible. Special acknowledgement to Trevor Evans (CN) for his insights about the rock fall activity in the area, inferred kinematics and triggers, and suggestions on the project.

5.7 References

Bjerrum L, Jørstad F (1968) Stability of rock slopes in Norway. Nor Geotech Inst Publ 79:1–11

Bovis MJ, Jones P (1992) Holocene history of earthflow mass movements in south-central British Columbia: the influence of hydroclimatic changes. Can J Earth Sci 29:1746–1755. https://doi.org/10.1139/e92-137

Bush E, Lemmen DS (2019) Canada's changing climate report. Environment and Climate Change Canada, Government of Canada, Ottawa, ON.

Cannon AJ, Sobie SR, Murdock TQ (2015) Bias correction of GCM precipitation by quantile mapping: How well do methods preserve changes in quantiles and extremes? J Clim 28:6938–6959. https://doi.org/10.1175/JCLI-D-14-00754.1

ClimateData.ca (2022) Climate data for a resilient Canada. https://climatedata.ca/. Accessed 18 Oct 2022

Coe JA, Godt JW (2012) Review of approaches for assessing the impact of climate change on landslide hazards. In: Eberhardt E, Froese C, Turner AK, and Leroueil S (eds) Landslides and Engineered Slopes, Protecting Society Through Improved Understanding: Proceedings of the 11th International and 2nd North American Symposium on Landslides and Engineered Slopes, Banff, Canada, 3-8 June, Taylor & Francis Group, London, pp 371-377

Collins M, Knutti R, Arblaster J et al (2013) Long-term Climate Change: Projections, Commitments and Irreversibility. In: Climate Change 2013: The Physical Science Basis. Contribution of Working Group I to the Fifth Assessment Report of the Intergovernmental Panel on Climate Change. Cambridge University Press, Cambridge, United Kingdom and New York, NY, USA, pp 1029–1136

Crozier MJ (2010) Deciphering the effect of climate change on landslide activity: A review. Geomorphology 124:260-267. https://doi.org/10.1016/j.geomorph.2010.04.009

Cui Y, Miller D, Schiarizza P, Diakow LJ (2017) British Columbia digital geology. British Columbia Ministry of Energy, Mines and Petroleum Resources, British Columbia Geological Survey Open File 2017-8, p 9

Gariano SL, Guzzetti F (2016) Landslides in a changing climate. Earth-Science Rev 162:227–252. https://doi.org/10.1016/j.earscirev.2016.08.011

Hungr O, Evans SG, Hazzard J (1999) Magnitude and frequency of rock falls and rock slides along the main transportation corridors of southwestern British Columbia. Can Geotech J 36:224–238. https://doi.org/10.1139/t98-106

IPCC (2021) Climate Change 2021: The physical science basis. Contribution of working group I to the sixth assessment report of the intergovernmental panel on climate change. Cambridge University Press. In Press.

IPCC (2014) Climate Change 2014: Synthesis Report. Contribution of Working Groups I, II and III to the Fifth Assessment Report of the Intergovernmental Panel on Climate Change. Gian-Kasper Plattner, Geneva, Switzerland

Jakob M, Lambert S (2009) Climate change effects on landslides along the southwest coast of British Columbia. Geomorphology 107:275–284. https://doi.org/10.1016/j.geomorph.2008.12.009

Jakob M, Owen T (2021) Projected effects of climate change on shallow landslides, North Shore Mountains, Vancouver, Canada. Geomorphology 393. https://doi.org/10.1016/j.geomorph.2021.107921

Laherrère J (2019) Are there enough fossil fuels to generate the IPCC CO2 baseline scenario? https://aspofrance.files.wordpress.com/2019/08/ipccco2rcp.pdf. Accessed 18 March 2021

Leyva S, Cruz-Pérez N, Rodríguez-Martín J et al (2022) Rockfall and rainfall correlation in the Anaga Nature Reserve in Tenerife (Canary Islands, Spain). Rock Mech Rock Eng. https://doi.org/10.1007/s00603-021-02762-y

Macciotta R (2019) Review and latest insights into rock fall temporal variability associated with weather. Proc Inst Civ Eng Geotech Eng 172(6):556–568. https://doi.org/10.1680/jgeen.18.00207

Macciotta R, Cruden D, Martin D et al (2013) Spatial and temporal aspects of slope hazards along a railroad corridor in the Canadian Cordillera. In: Proceedings of the 2013 international symposium on slope stability in open pit mining and civil engineering. Australian Centre for Geomechanics, Perth, pp 1171–1185

Macciotta R, Cruden DM, Martin CD, Morgenstern NR (2011) Combining geology , morphology and 3D modelling to understand the rock fall distribution along the railways in the Fraser River valley, between Hope and Boston Bar, B.C. In: Slope Stability 2011: International symposium on rock slope stability in open pit mining and civil engineering. Vancouver, Canada

Macciotta R, Hendry M, Cruden DM et al (2017a) Quantifying rock fall probabilities and their temporal distribution associated with weather seasonality. Landslides 14:2025–2039. https://doi.org/10.1007/s10346-017-0834-7

Macciotta R, Martin CD, Cruden DM (2015b) Probabilistic estimation of rockfall height and kinetic energy based on a three-dimensional trajectory model and Monte Carlo simulation. Landslides 12:757–772. https://doi.org/10.1007/s10346-014-0503-z

Macciotta R, Martin CD, Cruden DM et al (2017b) Rock fall hazard control along a section of railway based on quantified risk. Georisk Assess Manag Risk Eng Syst Geohazards 11(3):272–284. https://doi.org/10.1080/17499518.2017.1293273

Macciotta R, Martin CD, Edwards T et al (2015a) Quantifying weather conditions for rock fall hazard management. Georisk 9(3):171–186. https://doi.org/10.1080/17499518.2015.1061673

Mardia KV (1972) Statistics of directional data. Elsevier, London, New York

McGreevy JP, Whalley WB (1982) The geomorphic significance of rock temperature variations in cold environments: A discussion. Arct Alp Res 14(2):157–162. https://doi.org/10.2307/1551114

Meinshausen M, Smith SJ, Calvin K et al (2011) The RCP greenhouse gas concentrations and their extensions from 1765 to 2300. Clim Change 109:213–241. https://doi.org/10.1007/s10584-011-0156-z

Monger JWH (1970) Hope map-area, west half (92H W1/2), British Columbia, Paper 69-47. Ottawa, ON.

Porter M, Hove J Van, Barlow P et al (2019) The estimated economic impacts of prairie landslides in western Canada. In: Proceedings of the 72nd Canadian geotechnical conference. St. John's,Newfoundland and Labrador, p 8

Pratt C, Macciotta R, Hendry M (2019) Quantitative relationship between weather seasonality and rock fall occurrences north of Hope, BC, Canada. Bull Eng Geol Environ 78:3239–3251. https://doi.org/10.1007/s10064-018-1358-7

White RH, Anderson S, Booth JF et al (2023) The unprecedented Pacific Northwest heatwave of June 2021. Nat Commun 14:727. https://doi.org/10.1038/s41467-023-36289-3

WMO (2019) Technical regulations, basic documents No. 2 volume I – General meteorological standards and recommended practices (WMO-No. 49). Geneva, Switzerland

CHAPTER 6

Regional Scale Evaluation of Landslide Activity and its Relation to Climate

Contribution of this chapter to the overall study

The third main objective of this thesis is to develop a methodology to evaluate the changes in regional landslide hazards due to different climate conditions. The challenges associated with regional-scale studies are different from local-scale studies. This study investigates the long-term effects of climate on the formation of landslides and compares landslide activity among three river valleys in Alberta, Canada. A modified version of the research presented in this chapter was submitted to the Canadian Geotechnical Journal in August 2023 with the following citation:

Mirhadi N, Macciotta R, Regional scale evaluation of landslide activity and its relation to climate in southern Alberta, Canada. Submitted to "Canadian Geotechnical Journal" on August 28, 2023

Abstract

This work illustrates a semi-quantitative approach to evaluate changes in regional landslide activity as a consequence of forecasted climate change, which can be adopted in other regions. I evaluate the relationship between climate conditions and landslide activity at a regional scale. In this paper, landslides on parts of the Battle, Red Deer, and Bow Rivers that are located within the Bearpaw geological Formation in southern Alberta, Canada were mapped, and their characteristics were compared. In order to find a relationship between the climate conditions and the mapped landslides, 30-year annual precipitation and other factors such as slope aspect and geology were compared between the river valleys. Results show that climatic conditions and the size and shape of the landslides are different in the Battle River area compared to the Red Deer and Bow Rivers

regions. The weak Bearpaw overconsolidated shale and the bentonite layer throughout the region are sensitive to moisture and create favourable conditions for landslides in the river valleys. Further investigations into the long-term impact of climate on the formation of river valleys and the Bearpaw Formation support the argument that climate is the main factor in causing variations in landslide activity across the study areas. These findings provide insight into possible changes in regional landslide activity as a consequence of climate change.

6.1 Introduction

Slope processes and the distribution of landslide activity can be attributed to several main factors. These factors include the type of rock or soil (lithology), the prevailing climate conditions, the extent of weathering, the presence and movement of groundwater, the type and density of vegetation covering the slopes, the history and evolution of the valley, and the erosion occurring at the base of the slope (toe erosion). Although understanding the direct relationship between climate and slope processes can be problematic, it is undeniable that climate plays a significant role in shaping the Earth's landforms (Atkinson et al. 1976; Liang 1999).

Investigating the effects of climate on landslides has consistently remained an interesting and complex subject in geologic sciences and engineering which results provide valuable insights into managing the risks associated with landslide hazards. Numerous studies including statistical analysis, numerical modelling, laboratory experiments, and qualitative investigations, have been conducted around the world in the regions susceptible to landslides. As explained by Cruden and Varnes (1996), weather-related factors, notably precipitation, freeze-thaw cycles, and weathering are recognized as primary factors in landslide occurrences. In this regard, many researchers have investigated the effect of weather-related factors on landslide activity. (Godt et al. 2006; Guzzetti et al. 2008; Macciotta et al. 2015a; Rosi et al. 2016; Macciotta et al. 2017a; Brunetti et al. 2018; Martinović et al. 2018; Pratt et al. 2019; Leyva et al. 2022; Mirhadi and Macciotta 2023).

The challenges associated with regional-scale studies are different from local-scale studies. Among the differences, the lack of information regarding the exact time of landslide occurrences makes it impossible to investigate the impact of factors such as antecedent cumulative rainfall or

freeze-thaw cycles on each individual landslide. Moreover, due to the limited availability of weather stations within a large geographical area which are continuously operational over a large period of time, it is necessary to rely on modern and paleoclimate models to simulate conditions for different time periods. Despite these challenges, the study of climate impact on landslides at the regional scale remains feasible, even if in a qualitative manner.

In this paper, I develop a methodology to examine the influence of climate conditions at a regional scale on landslide occurrences within three regions located in southern Alberta, Canada. The study area covers parts of the Battle, Red Deer, and Bow Rivers, with a total length of 182 kilometres. To ensure that the geological factors have the least effect on the results, the study area has been chosen entirely within the Bearpaw Formation, a geological formation known for its vulnerability to landslides due to its structurally weak nature (Thomson and Morgenstern 1977).

6.2 Study area

6.2.1 Location

Large parts of Western Canada are made up of rock formations that were formed during the Late Cretaceous period, around 75 million years ago. One of these formations is called the Bearpaw Formation, which is a sedimentary deposit composed primarily of silt and clay particles that have been subjected to consolidation loads more than those provided by the present overburden. The interparticle bonds of these materials can break when they come into contact with water (Brooker and Scott 1968).

The Bearpaw Formation covers large regions of Alberta and Saskatchewan in Canada, as well as the state of Montana in the United States. The extent of the Bearpaw formation in Alberta is shown in Figure 6-1. Three rivers in the southern part of the province pass through this formation.

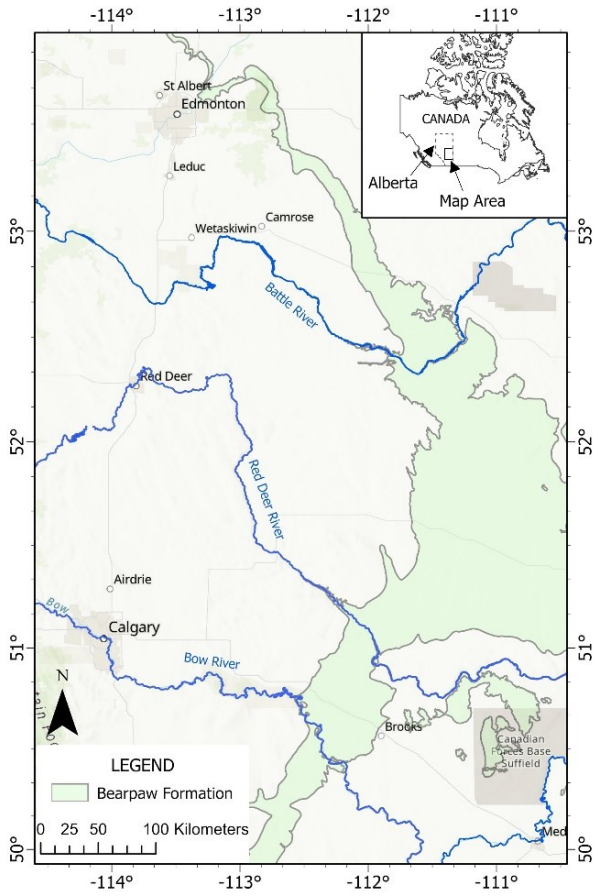

Figure 6-1: The extent of the Bearpaw Formation in Alberta (after Prior et al. 2013)

As a river stream gradually erodes the surrounding land, it carves out a valley and exposes the underlying geological structures. This makes river valleys an ideal location for studying geological formations. The Bearpaw Formation is particularly weak and prone to landslides. The combination of this vulnerable geological structure and the presence of river valleys creates favourable conditions for landslides to occur.

This study focuses on the parts of the Battle, Red Deer, and Bow Rivers, along with parts of their tributary channels, which lie entirely within the Bearpaw Formation to make sure that all of the mapped landslides are located within the same geological context. Figure 6-2 shows the study area along each river. In total, 54.5 km of the Battle River, 70.6 km of the Red Deer River, and 56.9 km of the Bow River were selected for this study. The geometrical characteristics of the study areas are presented in Table 6-1.

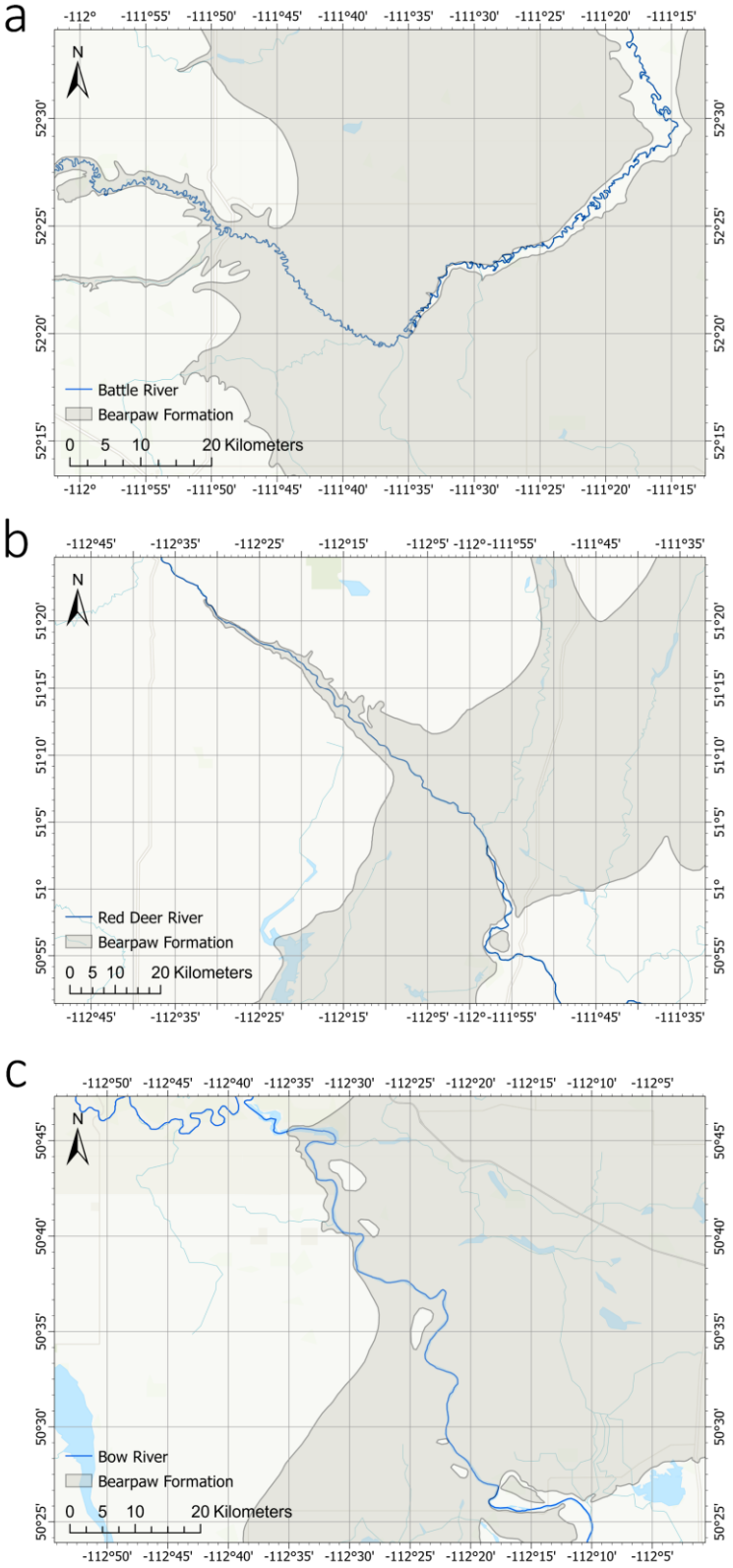

Figure 6-2: The study areas along Battle (a), Red Deer (b), and Bow Rivers (c)

The mean valley slope in the Red Deer and Bow Rivers regions is comparable and notably higher compared to the Battle River area. The Battle River has a lower flow compared to the Red Deer and Bow Rivers. The Red Deer River exhibits moderate river flow, while the Bow River has a higher flow. Geographically, the Red Deer River and Bow River are situated near each other and share several common characteristics.

Table 6-1: Overview of the rivers' characteristics. All parameters were calculated for the parts of the rivers that are located inside the study areas. The rivers' mean discharge rates were calculated for the period of 2011-2020 from the available historical hydrometric data (Environment and Climate Change Canada Historical Hydrometric Data website 2023).

	Length through the Bearpaw Fm. (km)	Total valley area (km^2)	Mean valley slope (deg.)	Valley width (km)	Valley height (m)	Mean River bed slope (deg.)	10-year Mean Discharge in Spring (m^3/s)	10-year Mean Discharge in Summer (m^3/s)
Battle River	54.5	86.6	11.3	1.0 - 3.0	45 - 100	3.2	16.9	6.6
Red Deer River	70.6	113.1	17.8	1.2 - 3.9	40 - 155	0.6	87.6	99.5
Bow River	56.9	47.7	15.7	0.3 - 2.2	20 - 100	0.2	109.6	167.5

Note: Spring months are March, April, and May. Summer months are June, July, and August.

According to Brooker and Scott (1968), the current river valleys in the area were formed during the retreat phase of the latest continental glaciation 12,000 to 25,000 years ago. In another study, Matheson and Thomson (1973) showed that the deep, steep-sided channels which were frequently ice-marginal or glacial lake spillways, were rapidly eroded by the large volumes of glacier meltwater and formed the current river valleys. They also stated that the existing river valleys have relatively steep valley walls except where landslide activity has flattened them.

6.2.2 Surficial Geology and Geomorphology

The geomorphology and surficial geology (to a depth of approximately 2 m) of the study areas are shown in Figure 6-3. As expected, all three river valleys are mostly covered superficially by fluvial and colluvial deposits. Generally, stagnant ice moraine is the most common material found in the region. However, there are some distinct differences in the surficial geology in the study areas. For example, although fluted moraine can be found widely right along the Battle River valley, it is not common in the Red Deer and Bow Rivers area. On the other hand, glaciolacustrine deposits are more commonly found in the Red Deer and Bow Rivers area compared to the Battle River area.

The Geomorphology maps of the study areas show similar patterns in the Red Deer and Bow Rivers areas. Hummocky, ridged, plain, and gullied patterns are the most common patterns along these two rivers. The Battle River area is covered mostly with a reticulated pattern.

6.2.3 Ecoregion

The map of the ecoregions of Alberta is shown in Figure 6-4. According to this map, the study area along the Battle River lies within the Central Parkland ecoregion, but the study areas in the Red Deer and Bow Rivers are located within the Dry Mixedgrass ecoregion. In comparison to the Dry Mixedgrass subregion which has hot summers, intense sunshine, high evaporation and long, cold winters with low snow cover, Central Parkland lies between the cold, snowy northern forests and the warm, dry southern prairies and receives more rainfall during summer (Alberta Parks 2015).

The surficial geology and geomorphology data with the information associated with the ecoregions - as well as the vegetation type and cover on the river valleys and the surrounding area - show that the climate regime in the Battle River area is different from the Red Deer and Bow Rivers areas.

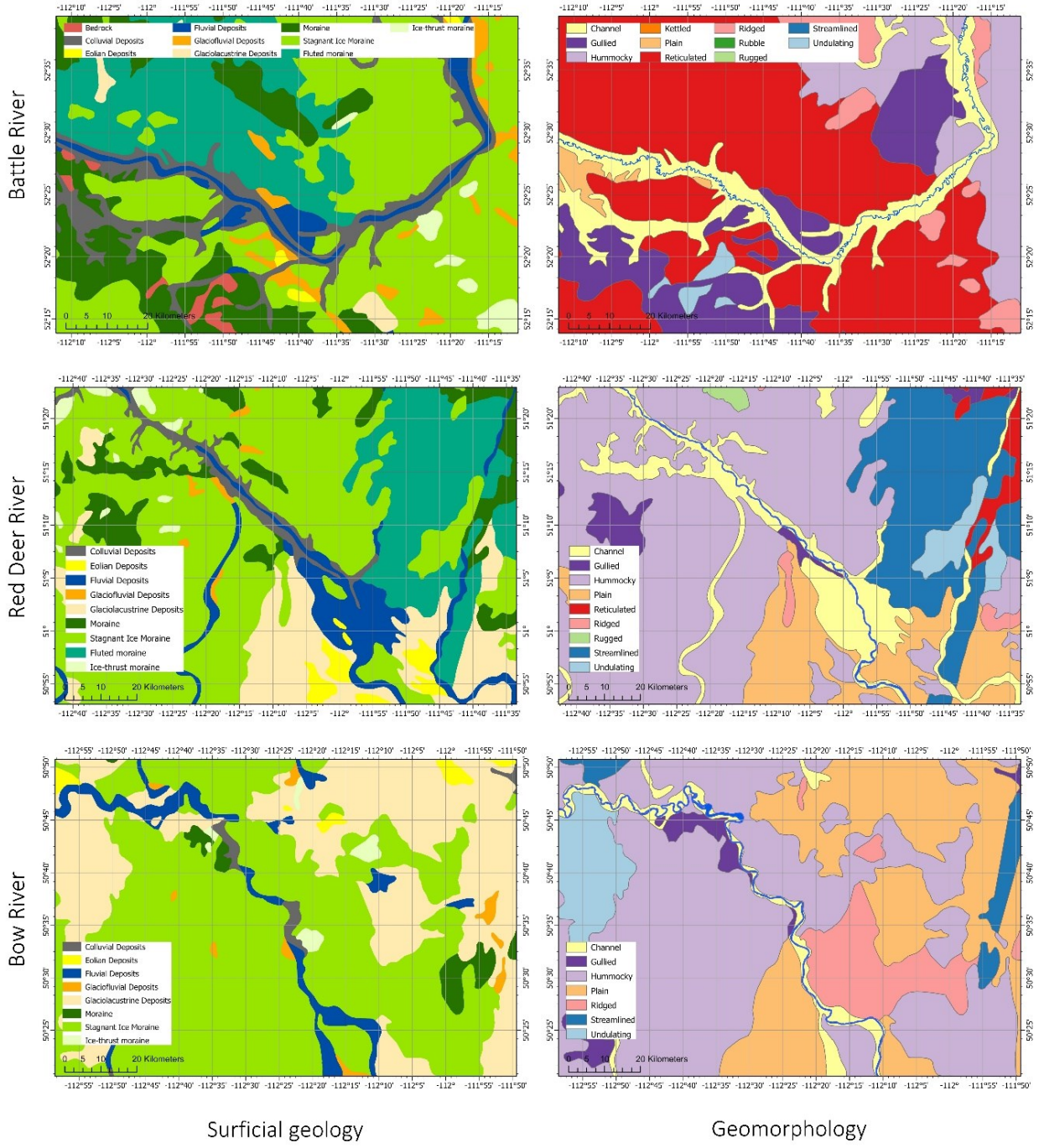

Figure 6-3: Surficial geology and geomorphology of the study areas (Fenton et al. 2013)

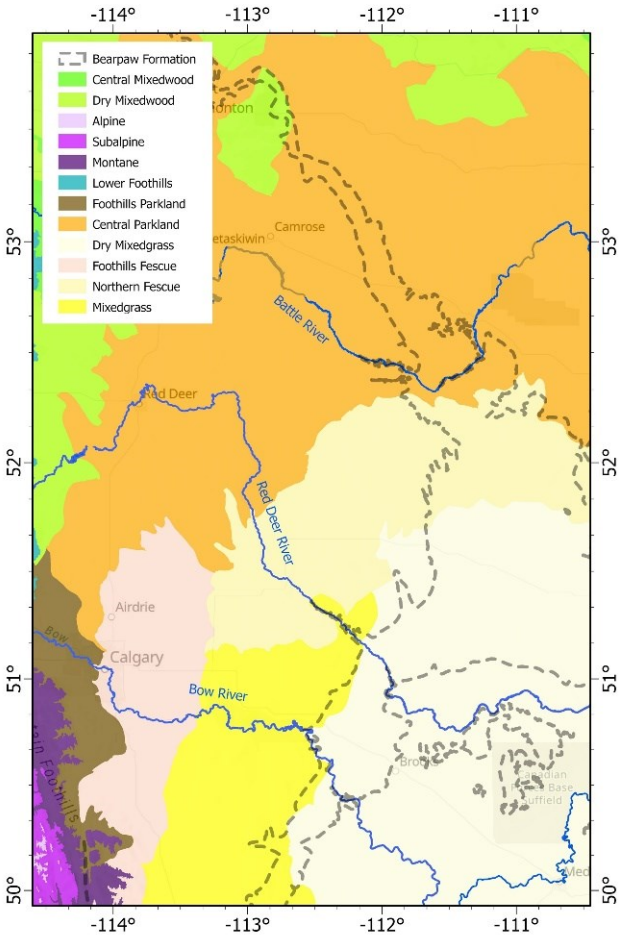

Figure 6-4: Ecoregions of southern Alberta (Downing and Pettapiece 2006; Alberta Parks 2015)

6.3 The Bearpaw Formation

The Bearpaw Formation was named after the Bearpaw Mountains in Montana, USA, where marine shales of this formation were first identified (Hatcher and Stanton 1903). The Bearpaw Formation extends throughout central and southern Alberta, with varying thicknesses in different areas. According to Allan and Sanderson (1945), the formation is estimated to be between 120 and 150 m thick along the Red Deer River east of Drumheller. In southern Alberta, Russell (1932) measured 223 m of the formation along St. Mary River south of Lethbridge.

Around 75 million years ago, during the Late Cretaceous Epoch, sediments were deposited in a broad shallow sea called Bearpaw Sea, which was bounded by the Cordillera highlands on the west and by the Canadian Shield on the east (Brooker and Scott 1968). Most of the sediment that constitutes the Bearpaw Formation came from the Cordillera highlands during a period when the sea level was fluctuating but gradually retreating (Brooker and Scott 1968). According to Reeside (1957), Bearpaw sediments accumulated slowly in calm waters. Radiometric dating of sedimentary sequences in the Alberta and Peace River basins suggests that the sediment accumulated at a rate of approximately 30 cm every 7000 years (Folinsbee et al. 1961).

During the time when the sediments were being deposited, volcanic activity was taking place in what is now southwestern Montana, USA. This volcanic activity led to the deposition of layers of volcanic ash within the sedimentary sequence of the Bearpaw Formation, which over time, resulted in the formation of bentonite layers throughout the formation (Brooker and Scott 1968). According to the stratigraphy sections provided in Lines (1963), thin seams of bentonite are distributed at different levels throughout the Bearpaw Formation resulting in bentonitic shale and sandstone zones. Bentonite and bentonitic layers, which will be explained in the Results and discussion section, are common geological causes of deep-seated landslides in southern Alberta.

Millions of years later during the Pleistocene Epoch (2.6 million - 11700 cal yr B.P.), which was the Earth's most recent period of glaciations, southern Alberta was covered by a thick ice sheet called Laurentide, reaching approximately 1220 m in the Red Deer Valley east of Drumheller and 670 m in the Lethbridge area (Stalker 1965). Generally, glaciation can affect the area in three ways: erosion and reshaping the landscape as it moves; deposition of new materials as it melts or recedes; and crustal depression under the influence of the ice load. The sediments of the Bearpaw Formation experienced loading from the deposition of younger sediments and unloading through erosion during uplift periods, followed by further cycles of loading and unloading due to glaciation. This process led to the formation of overconsolidated shales and widespread drifts, including till, throughout Alberta. It should be noted that according to (Brooker and Scott 1968), the preglacial load in Alberta was not enough to create a permanent cohesive bonding in the shale. As a result, the shale can still disaggregate when exposed to water.

As Fulton (1989) stated, clay shale in the region appears to have undergone prolonged and deep weathering during the Tertiary period. Because of the presence of smectite clay minerals in

the Bearpaw Formation (Dubbin et al. 1993), the bentonite-rich sediment is prone to softening if sheared (Fulton 1989). These shearing processes occurred during glacial periods and continued as postglacial cutting of deep valleys released earth pressure. Present-day instability further contributes to pressure release along the backscarps of slides and results in a progressive reduction in strength (Fulton 1989).

Figure 6-5 shows an outcrop section of the Bearpaw Formation near the hamlet of Dorothy which is located inside the study area and along the Red Deer River. Dorothy is known for its 10-13 m thick bentonite layer which can be traced for 20 km along the Red Deer River (Scafe 1975). According to Brooker and Scott (1968), landslides in Western Canada often occur in thin seams of bentonitic material or other geological discontinuities.

The Bearpaw Formation shown in Figure 6-5 is approximately 180 m thick and consists mostly of mudstone and shale, with layers of sandstone. Bearpaw Formation is sub-horizontal, dipping west into the Alberta syncline at an inclination of approximately seven feet per mile (1.3 m per km) (Allan and Sanderson 1945).

6.4 Climate

According to ClimateData.ca (2023), the highest levels of rainfall in the region happen between May and September, which lead to the erosion of the river banks and increased water flow. The 30-year average annual precipitation from 1991 to 2020 in the Battle, Red Deer and Bow Rivers areas are 399, 330, and 333 mm, respectively. Harsh winters with daily lows reaching -30 °C are also a climatic characteristic of Alberta. According to the 30-year mean monthly temperatures between 1991 and 2020, the mean temperature can be as low as -13.9 °C in the Battle River area, -12.7 °C in the Red Deer River, and -11.2 °C in the Bow River area (ClimateData.ca 2023). The total annual precipitation and mean monthly temperatures were calculated for a 30-year time period and do not reflect the extreme recorded values.

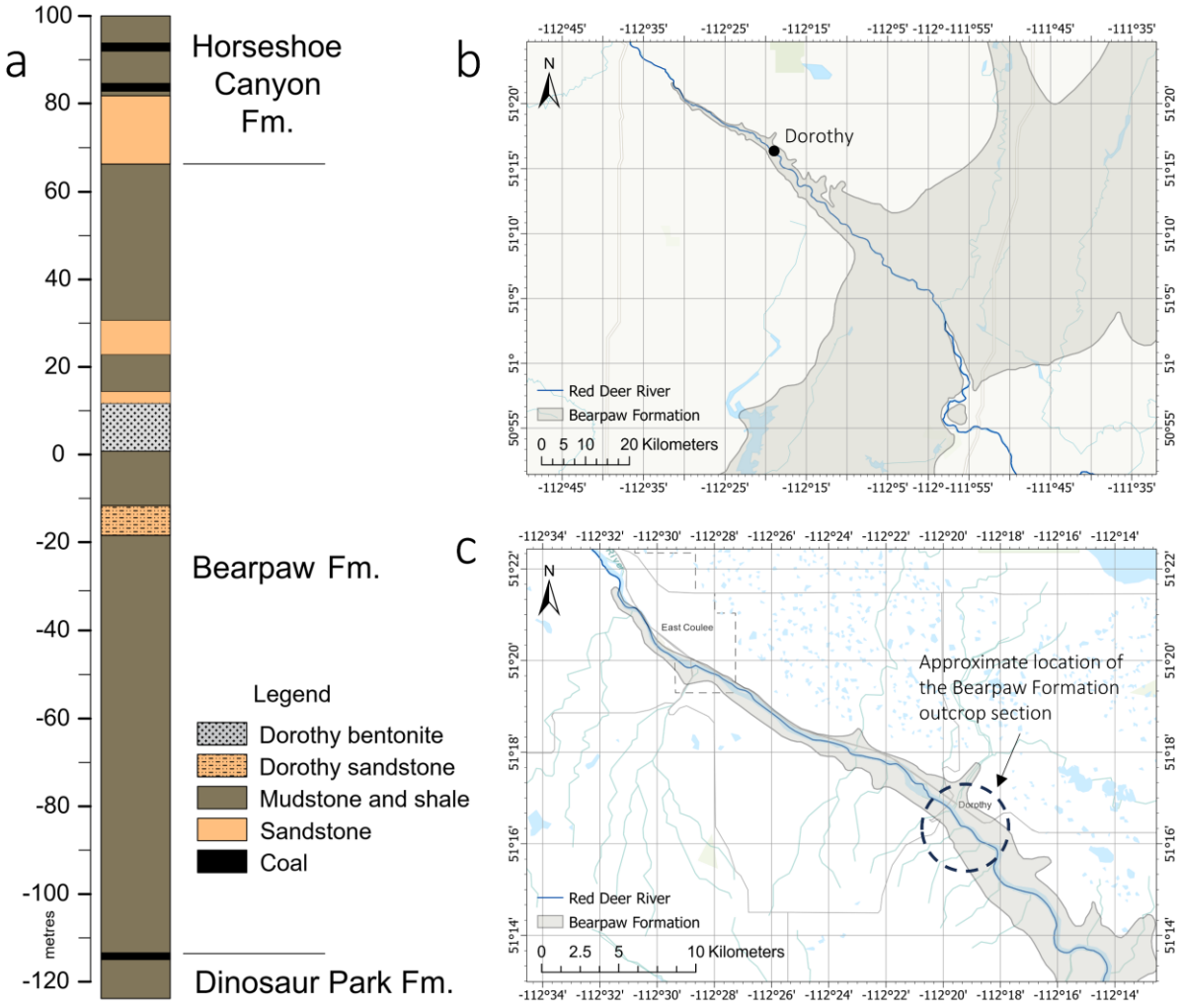

Figure 6-5: Geology section of the Bearpaw Formation near Dorothy, AB (after Lerbekmo 2002) (a), and the location of the outcrop (b) and (c)

Frost may occur in some areas provided that all conditions are present. These conditions include moisture content, ambient air temperature, and thermal properties of soil (Penner 1962). According to Brooker and Scott (1968), frost can penetrate the ground to a depth of about 3 meters in the region, with the maximum penetration usually happening in late March or early April. Frost penetration and its impact on fractures are other factors that contribute to landslides in overconsolidated shales.

Slopes are influenced not only by present climate conditions but also by past climatic regimes that have shaped the landscape over long periods of time. Western Canada has experienced

changes in precipitation and temperature due to climatic variations since the last deglaciation. However, it is unlikely that the precipitation gradient over relatively short north-south distances in the study area has been significantly altered. This is because the topographic influence of the Rocky Mountains has remained constant over time (Liang 1999b). Therefore, the northern part of the study area (Battle River) would have been experiencing more precipitation than the southern part of the study area (Red Deer and Bow Rivers) since the last glaciation (Campbell and Campbell 1997).

Moreover, Campbell and Campbell (1997) stated that the long deglaciation period which occurred approximately 20,000 – 12,000 cal yr B.P. is the source of the emergence of several major rivers in Central and Southern Alberta, all of which originate from the Rocky Mountains or the foothills. According to the radiocarbon dates of proglacial lakes in the region, deglaciation itself was probably complete prior to 15,000 cal yr B.P. However, the runoff originating from the mountains continued shaping the landscape until approximately 13,000–12,000 cal yr B.P. The final postglacial period was associated with landscape instability in the region, extending from ca. 10,000 cal yr B.P. to the present (Campbell and Campbell 1997).

Vance et al. (1995) conducted an extensive paleoecological study in the Canadian Prairies to compare the climatic conditions throughout the region approximately 6000 cal yr B.P. with today's climatic conditions and found that mean annual temperature was 0.5°C to 1.5°C higher than today with summer temperature up to 3°C higher. Also, the mean annual precipitation was reduced by 65 mm (summer precipitation was reduced by 50 mm) compared to today. This suggests that 1) it is reasonable to use the current modern climate models to investigate the differences in the climate conditions between the study areas as their relative differences would have been similar in the past, and 2) because the climate has not changed significantly since the slope instability period, it can be concluded that the difference between the climatic conditions at the study areas has remained approximately the same and therefore, it is reasonable to study the effect of climate on landslides and compare the landslide activities among the study areas.

6.5 Methods and materials

6.5.1 Climate data

I collected the annual precipitation from the ClimateData.ca (2023) database to determine the climate conditions from 1950 to 2100 considering the RCP4.5 emission scenario. The average 30-year annual precipitation was calculated for every 10 km by 10 km grid of southern Alberta. Ultimately, three 30-year weather databases were created for 1950-1979, 2010-2039, and 2070-2099 by interpolating the weather data using the Empirical Bayesian Kriging (EBK) method in ArcGIS Pro v2.8.0 software (Krivoruchko 2012).

6.5.2 Landslides

The geometric characteristics of river valleys and landslides including size, aspect, and the degree of slope were calculated using the digital elevation models generated from lidar data in ArcGIS Pro v2.8.0 software. The resolution of the lidar data used in this study is 15 m, which makes it difficult to locate landslides smaller than 15 m long. Therefore, the location of landslides on the river valley and its tributary channels was mapped through the interpretation of aerial photos, satellite images, and the hillshades derived from the digital elevation models.

To determine the extent of the study area in each region, the general river path was marked with a simple polyline and two parallel lines 2 km away from the river path on each side were drawn. Subsequently, the locations of landslides on the river valley and its tributary channels were mapped. It should be noted that since different failure mechanisms are involved in landslides occurring in the floodplains, only landslides on the river valley slopes were mapped in this study.

Since most of the landslides in the area are prehistoric to several hundred years in age, and no records of their occurrence are available, identifying the crown and main scarp of the landslides is challenging due to the erosion processes over time. Similarly, observation of the displaced materials is commonly not possible as they have been eroded or washed away over time. To create as comprehensive a database as possible, I did a multipass search on the river valleys and in each pass, I looked for identifiable characteristics of landslides including crown, main scarp, transverse cracks, flanks, and displaced material on aerial photos, satellite images, and hillshades

simultaneously. Once a justifiable landslide property is found, the extent of the landslide is delineated in the ArcGIS software.

The final landslide database was partially validated through direct comparisons with databases provided by Liang (1999) and Pawley et al. (2017).

6.5.3 Geological data

Geological data at the regional scale were gathered from scientific articles as referenced in the previous sections and publicly accessible databases published by the governments of Alberta and Canada (Downing and Pettapiece 2006; Fenton et al. 2013; Prior et al. 2013; Alberta Parks 2015). The local geological data were extracted from water wells and coal test drilling reports near each landslide (Government of Alberta 2021). It is worth noting that most of these wells were initially drilled for water access purposes, and therefore, the reported geological information may not be entirely accurate. However, the closest boreholes with the most complete and reliable data were used, and their data were checked for consistency with the other boreholes in the vicinity. Additionally, due to the lack of denser geological information and detailed geological context in the area, I assumed horizontal stratigraphy for the analysis which is consistent with the nature of the Bearpaw Formation.

6.5.4 Relationship between climate data and landslides

The relationship between climate and mapped landslides was analyzed semi-qualitatively in ArcGIS. This analysis was done by overlaying landslide-prone areas with climate data and direct comparison of the average annual climate data with the location and geometrical properties of the river valleys and mapped landslides. The choice of the software platform allowed for the efficient handling and visualization of geographic and numerical data. It is important to note that due to the nature of the study and limitations in the available input data, conducting a complex statistical analysis was not feasible.

6.6 Results and discussion

6.6.1 Climate

The average annual precipitation in the region for three 30-year time periods is shown in Figure 6-6. This figure shows how measured and projected precipitation changes over time throughout the region as a result of climate change.

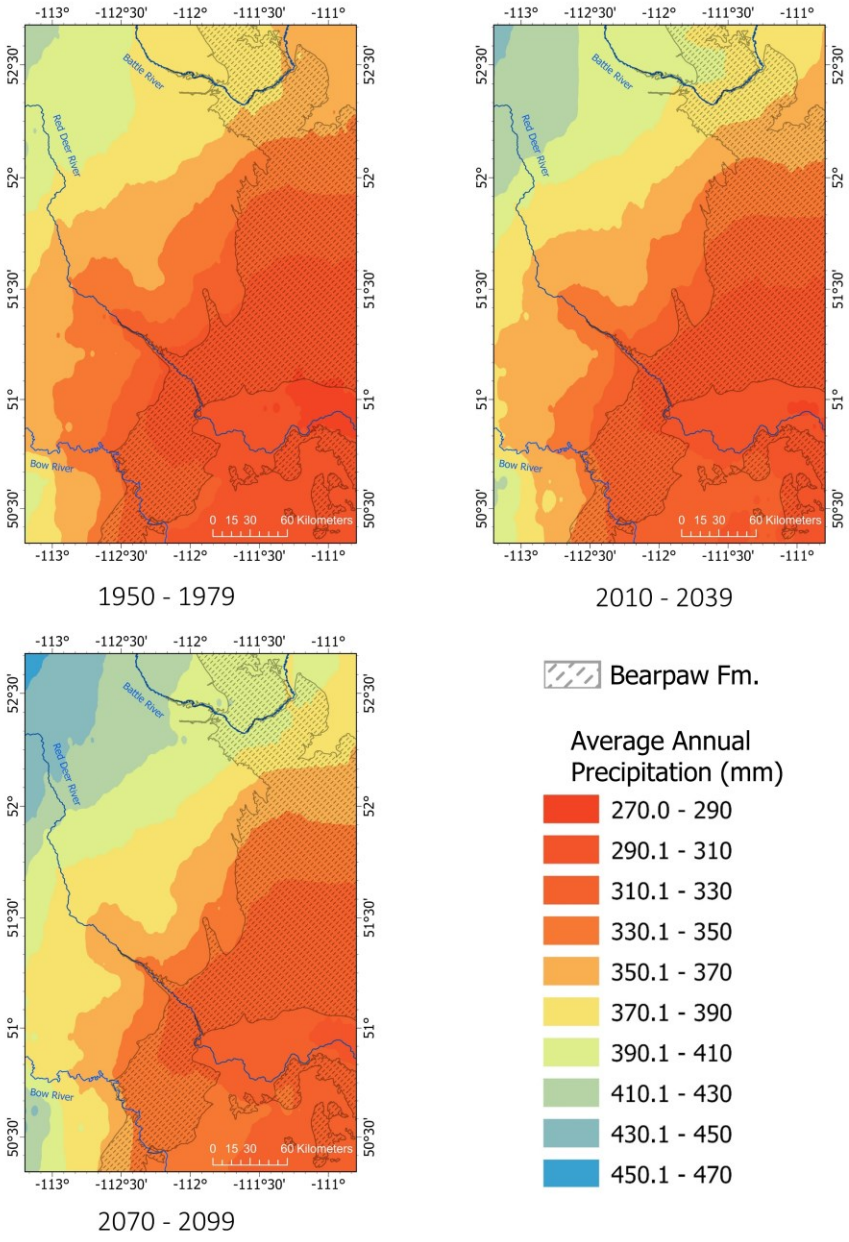

Figure 6-6: Average annual precipitation in different time periods

According to Table 6-2 which shows the average annual precipitation within each river valley in the Bearpaw Formation, annual precipitation relative to the base period of 1950 – 1979 is expected to increase over time. The percentage changes relative to 1950 – 1979 vary across the regions. The Red Deer and Bow Rivers are projected to experience greater changes compared to the Battle River with up to 3.1% in 2010 – 2039 and 8.4% in 2070 – 2099. Although annual precipitation is estimated to increase, the difference in the precipitation between the areas will remain approximately the same over time meaning that the Battle River will continue to receive more precipitation than Red Deer and Bow Rivers. Therefore, although climate change may impact the current rate of landslide activity in the river valleys, the difference in landslide activity between the river valleys could remain unchanged.

Table 6-2: Average annual precipitation (mm) in each river valley in different time periods. The percentage changes relative to 1950 – 1979 are shown in parentheses

	1950 - 1979	2010 - 2039	2070 - 2099
Battle River	377	386 (+2.4%)	402 (+6.6%)
Red Deer River	309	318 (+2.9%)	335 (+8.4%)
Bow River	319	329 (+3.1%)	345 (+8.2%)

6.6.2 Landslides

Figure 6-7 shows the mapped landslides in the three regions. Contrasting landslide sizes are observed in the Battle River area in comparison to the Red Deer and Bow Rivers. The differences in the land cover and density of agricultural activities are also visible in the satellite images. These variations come from the different ecoregion where the Battle River is located and show the differences in the moisture content between the study areas.

As previously mentioned, the resolution limitation of the lidar data and satellite images made it difficult to detect small landslides. The smallest landslide recorded in this study is 28 m wide and 10.5 m long and located along the Bow River.

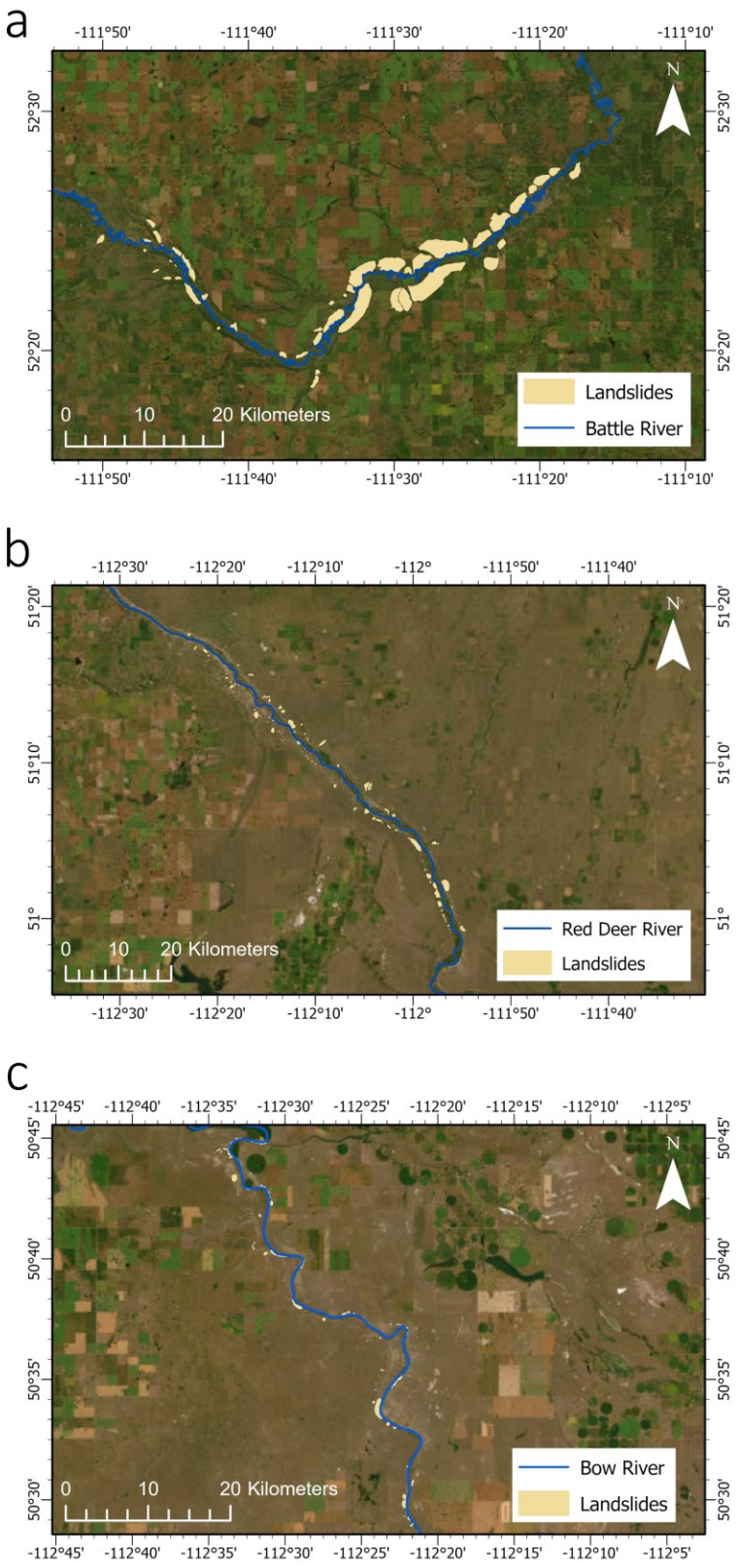

Figure 6-7: Mapped landslides along the Battle (a), Red Deer (b), and Bow Rivers (c)

Figure 6-8 and Figure 6-9 show the distributions of the area and mean degree of slope of the mapped landslides, respectively. The mapped landslides' statistics are presented in Table 6-3.

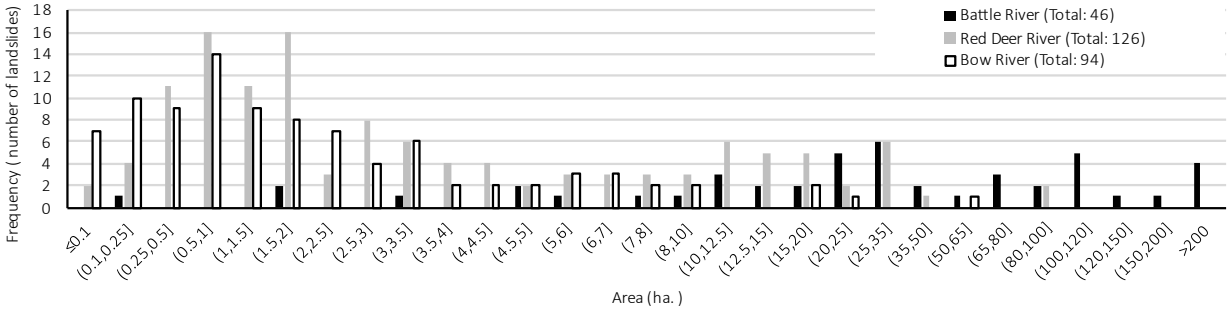

Figure 6-8: Distribution of the landslides area. Note the different bin sizes.

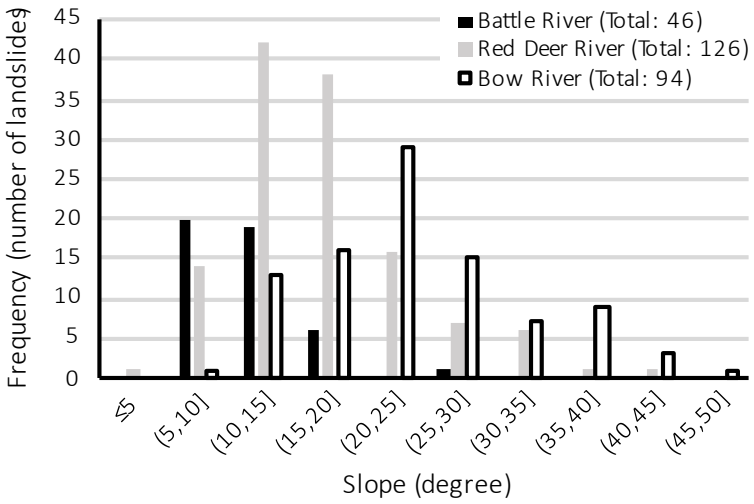

Figure 6-9: Distribution of the mean degree of slope for the mapped landslides

Based on the mean area values, the landslides along the Battle River are approximately 10 times larger than those in the Red Deer River area and 23 times larger than the landslides mapped along the Bow River.

Table 6-3: Landslides' information

	Number	Landslide area (m^2)		Landslide slope (degree)		Total area of landslides per unit length of the river (km^2/km)	Number of Landslides per unit length of the river (1/km)	Total area of landslides/Total area of the river valley
		Mean	Median	Mean	Median			
Battle River	46	714,332	284,383	11.5	10.9	0.60	0.84	0.38
Red Deer River	126	70,836	24,546	16.8	15.6	0.13	1.78	0.08
Bow River	94	30,766	13,721	23.9	22.5	0.05	1.65	0.06

According to Table 6-3, The median area values in all three rivers are less than half of the mean values. This indicates that a few larger landslides in each river valley are causing a positive skew in the dataset. However, this will not change the general interpretation of the landslide areas, as the median landslide area in the Battle River is still significantly higher than that in the Red Deer and Bow Rivers.

On the other side, while the Battle River has the lowest degree of slope with an average of 11.5 degrees, landslides in the Bow River area are steeper than the other two regions with an average of 23.9 degrees.

Table 6-3 also shows higher landslide activity in the Battle River area with 0.6 km^2 landslide per one kilometre length of the river which is 4.6 and 12 times higher than the landslide activity along the Red Deer and Bow Rivers, respectively. This is consistent with the findings of (Liang 1999). In terms of the number of landslides per unit length of the river, due to the smaller size of the landslides, the Red Deer and Bow rivers show similar activity rates with 1.78 and 1.65 landslides per one kilometre of the river which is almost 2 times the rate in the Battle River area.

The ratios of total landslide area over total valley area show a higher activity in the Battle River area with 38% of the total river valley within the Bearpaw Formation involved in landslide activity. In comparison, only 8% and 6% of the Red Deer and Bow valleys are involved in landslide activity, respectively. According to Thomson and Morgenstern (1977), the proximity of the preglacial bedrock channels to the southern part of the study area in Bow River resulted in a lower groundwater level, thereby reducing the landslide activity.

Figure 6-10 illustrates the hillshade samples along each river, providing enhanced visualization of the valleys' shape, the surrounding terrain, and the typical landslides. These hillshades, generated from the digital elevation models, effectively highlight the bare ground and landslides, aiding in a more precise identification of landslide locations, especially in vegetated regions like the Battle River valley.

As shown in Figure 6-10, there are clear differences in the shape of the valleys, channels, and morphology in the Red Deer and Bow Rivers regions compared to the Battle River area. Landslides on the Red Deer and Bow Rivers valleys are similar in size and type and are different from the landslides on the Battle River.

Figure 6-11, Figure 6-12, and Figure 6-13 show landslide examples along with the geological data retrieved from the nearby boreholes. Note that all the landslides shown in these figures are sub-horizontal and the vertical scale was set 7 times the horizontal scale only to get a better visualization of the slopes and landslides. Shale and sandstone are the most common materials found in the region and make up most of the landslide bodies.

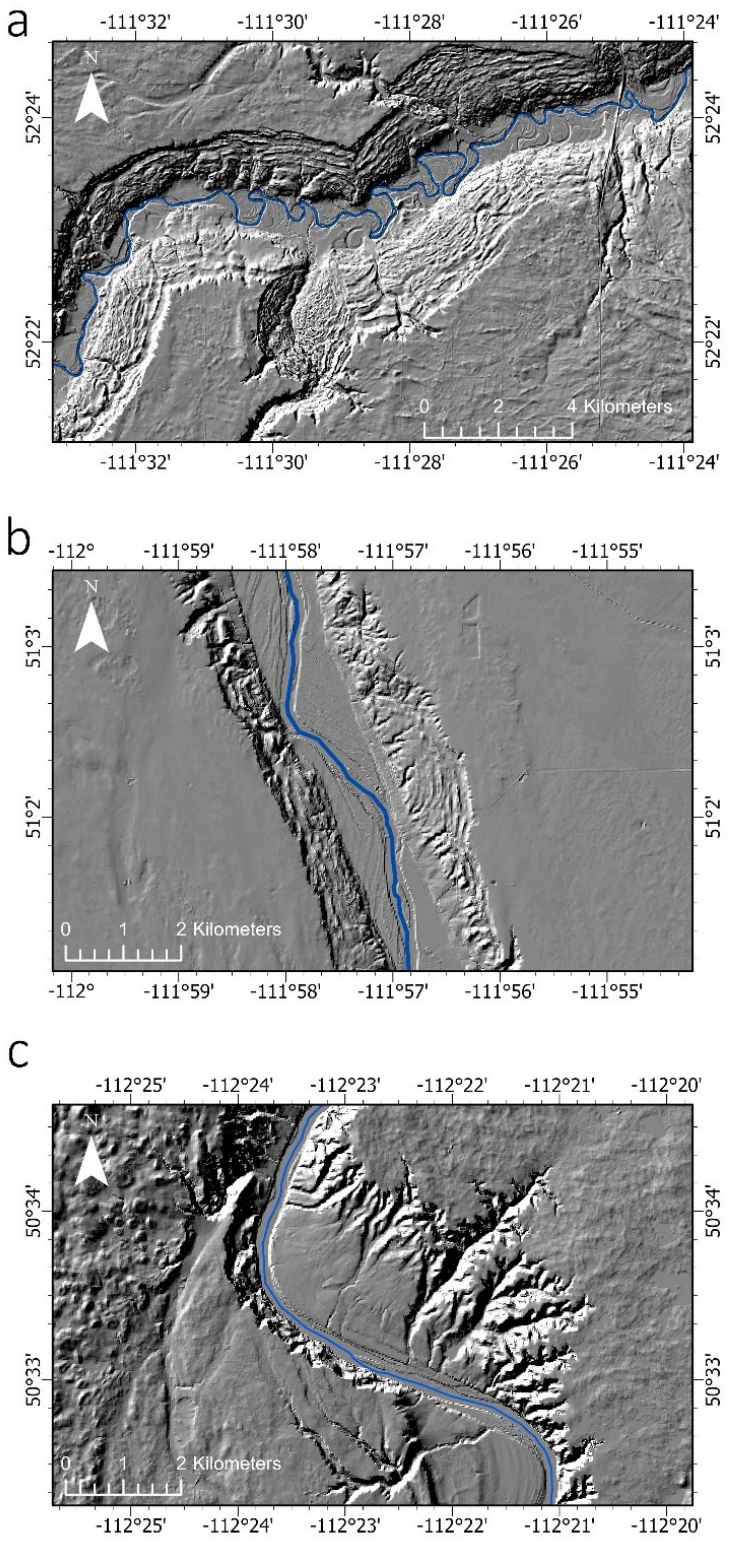

Figure 6-10: Hillshades showing the typical valley shape along the Battle (a), Red Deer (b), and Bow Rivers (c)

The geological sections shown in the figures are consistent with the geological characteristics of the Bearpaw Formation. Although there might be some spatial differences in the formation at the location of the three rivers, their depositional environment suggests that these differences would be minor. Any variations in the water-well logs could be attributed to simplified descriptions, as these boreholes were not intended to provide detailed geological descriptions.

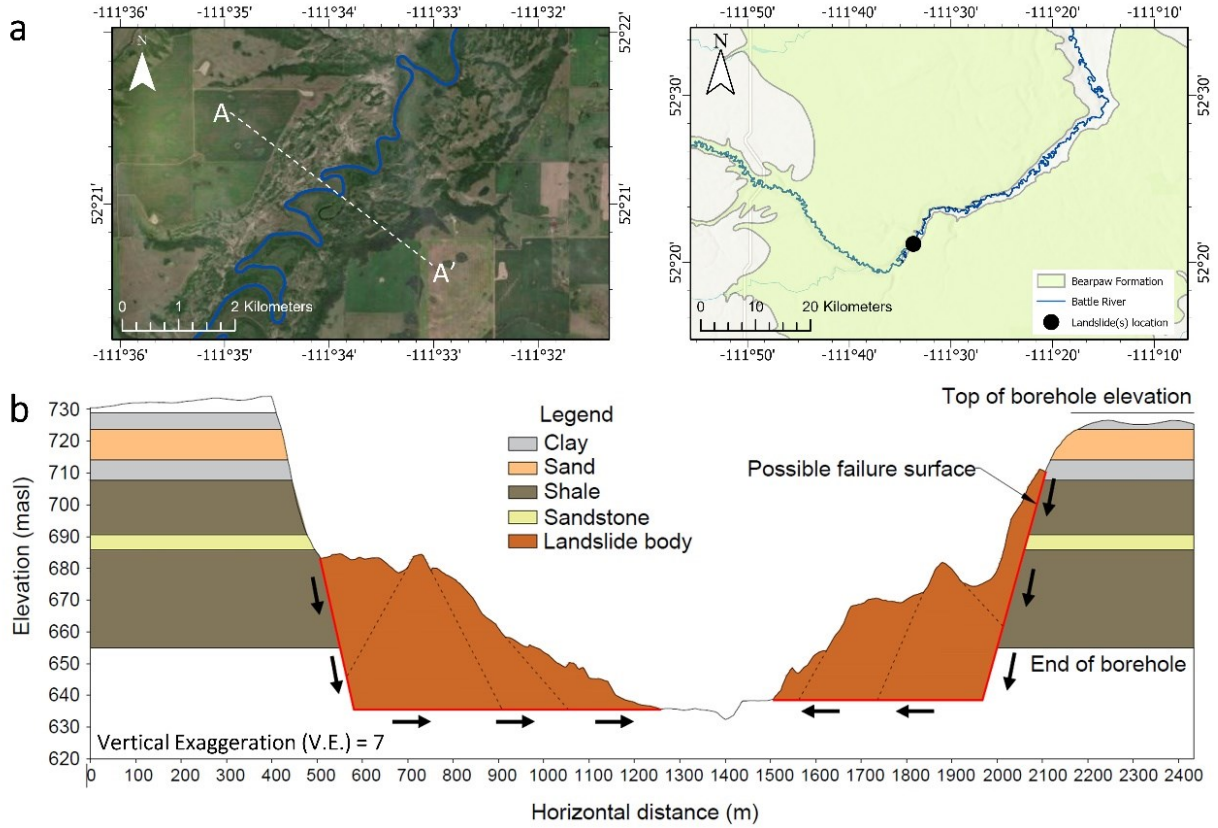

Figure 6-11: Map of the selected landslide along the Battle River (a), and the geologic cross section of Section A-A' (b). Vertical exaggeration is the ratio of the vertical scale to the horizontal scale. The inferred internal shear is based on surface features and is intended for illustration purposes.

The majority of landslides in the region are categorized as translational and compound landslides, which are intermediate between rotational and translational slide types. Translational slides in the area are controlled by sub-horizontal weak layers composed of bentonite and coal. These weak

layers, as described by Lines (1963), occur in the form of thin seams at various levels between the sandstone and shale of the Bearpaw Formation.

There may be controlling structures that lead to differences in landslide intensity, but it is expected that these influences would be localized to specific regions and depths, and not affect the entire river section under analysis.

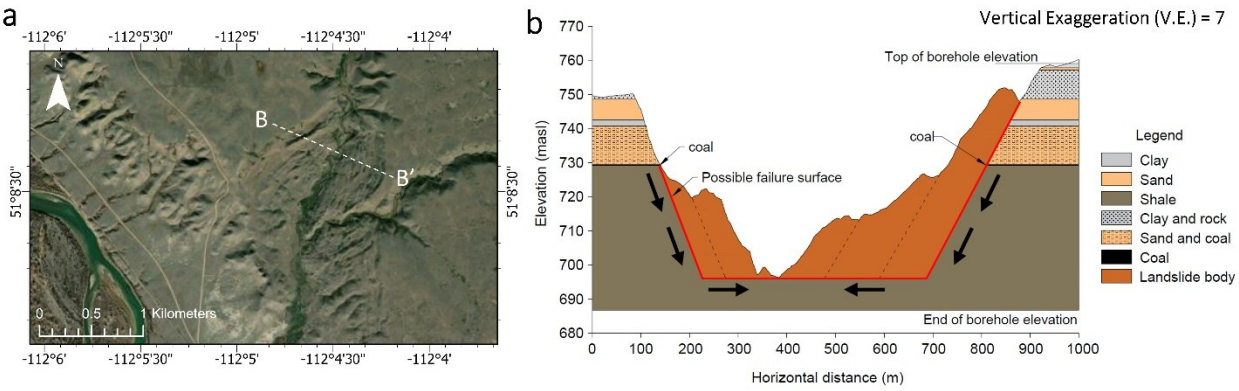

Figure 6-12: Map of the selected landslide along the Red Deer River (a), and the geologic cross section of Section B-B' (b). The inferred internal shear is based on surface features and is intended for illustration purposes.

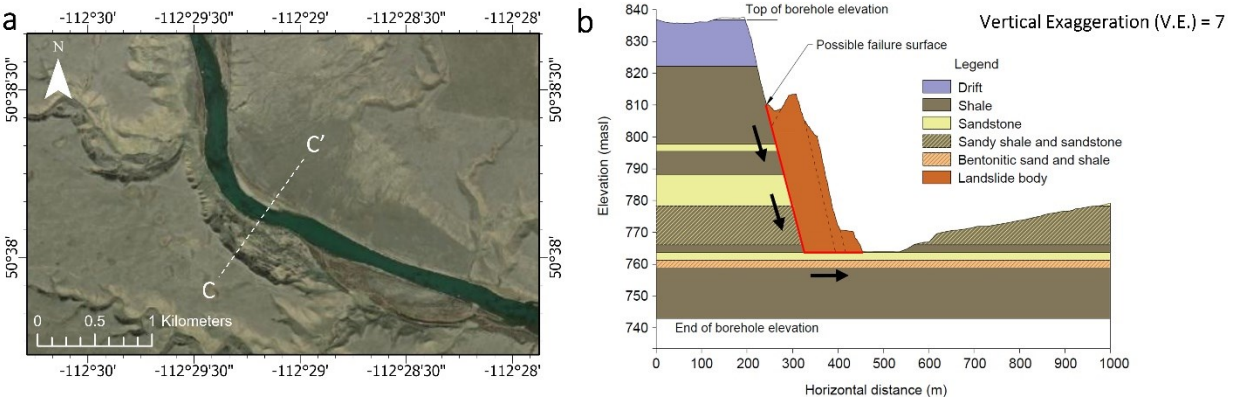

Figure 6-13: Map of the selected landslide along the Bow River (a), and the geologic cross section of Section C-C' (b). The inferred internal shear is based on surface features and is intended for illustration purposes.

Based on the observations made from the geologic cross sections and according to Brooker and Scott (1968), the landslide process often begins with rotational movement until it encounters a weak sub-horizontal surface. Once this surface is found, the landslide transitions into a translational slide, continuing to slide on this weaker layer. This is consistent with the previous studies in the area by Thomson and Morgenstern (1977, 1979), Liang (1999), and Biagini et al. (2022). The possible slip surfaces and the direction of movement of the mapped landslides are shown in Figure 6-11, Figure 6-12, and Figure 6-13.

According to Fulton (1989), landslides in the Canadian Prairies move down the slope at a slow rate, and as the slope toe advances, there is subsidence of individual blocks of material behind. Every few decades, sufficient subsidence and translation occur in front of the backscarp, causing a new block of material to fail and the landslide's crown to retrogress. The retrogression of landslides along the Battle and Red Deer Rivers can be seen in the hillshades of Figure 6-10.

The orientation of the landslide with respect to the North is called the aspect. The slope aspect plays an important role in local microclimate and, therefore, in plant cover and soil stability (Fulton 1989). The percentage distributions of the mean aspect of the mapped landslides are shown in Figure 6-14. The results indicate that 50% of the landslides along the Red Deer River and 50% along the Bow River face north, northeast, or northwest. In contrast, 61% of the landslides along the Battle River face southeast, south, or southwest. Since north-facing slopes receive less direct solar radiation than south-facing slopes, it is expected that the north-facing slopes are wetter and subject to less frequent and intense episodes of drying and wetting (Churchill 1981).

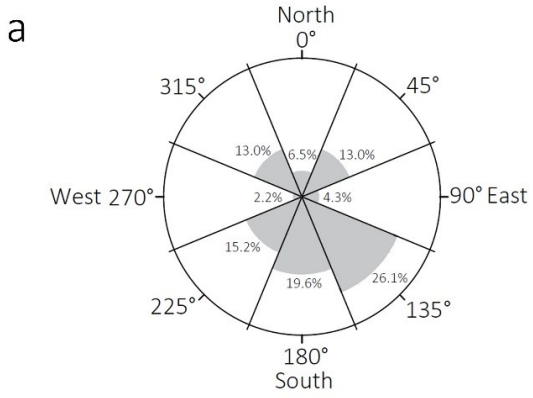

Figure 6-14: Percentage distributions of the mean aspect for the mapped landslides along the Battle River (a), Red Deer River (b), and Bow River (c)

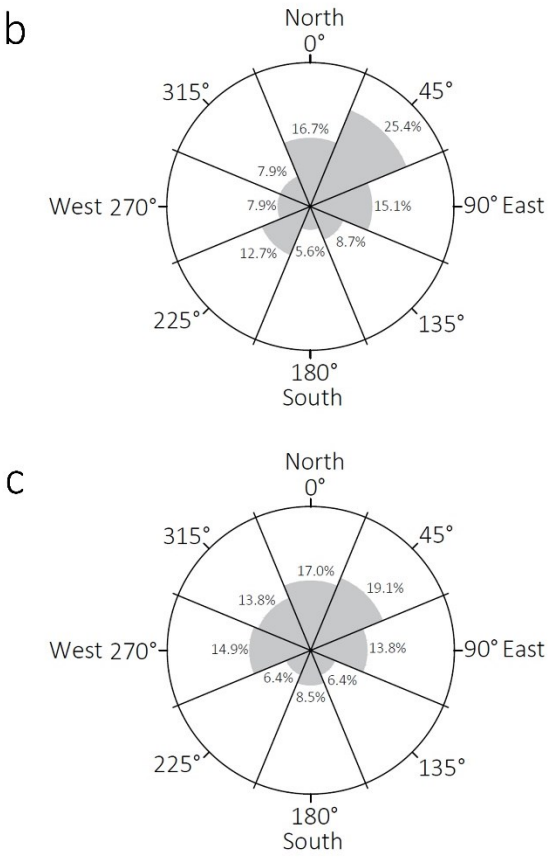

Figure 6-14 (continued).

6.6.3 Effect of climate on the landslides in the Bearpaw Formation

One objective of this study is to examine the regional impact of climatic conditions on landslides. As indicated previously, there are notable differences in the geometric attributes of landslides, such as size, aspect, and average slope between the Battle River region and the Red Deer and Bow Rivers regions. I also showed that the study area along the Battle River lies within the Central Parkland ecoregion with higher average annual precipitation than the study areas along the Red Deer and Bow Rivers which are located in the Dry Mixedgrass ecoregion. These findings, in conjunction with previous research on long-term climatic conditions in the region, provide evidence of contrasting climatic conditions between the Battle River and the other two rivers which highlights the influence of climatic conditions on the formation of river valleys and the occurrence of landslides in the region.

Although the regional geological maps show some differences in the surficial materials throughout the study areas, the sections in Figure 6-11 to Figure 6-13 show that the landslides are deep-seated and primarily occur within the Bearpaw Formation. Consequently, considering the consistency in the geological structure observed within the landslide bodies, and the fact that all three rivers originate from the Rocky Mountains in the west with a similar formation history, it can be concluded that a main driver in the difference in the current shape of the valleys, including the slope, height, and width of the valleys, can be considered as a result of the difference in climatic conditions and their prolonged impact on the valley's formation.

In simple terms, the long-term impact of climatic conditions on landslide activity in the study areas can be observed in three ways:

1- More precipitation and moisture within a particular region alter the shape of the river valley. In other words, as the water level rises and the flow velocity increases, potential floods intensify toe erosion and wash away slope materials. On a time scale of hundreds to thousands of years, downcutting and in particular lateral migration of river channels both lead to slope steepening and are major causes of slope instability (Fulton 1989). Figure 6-15 compares the average annual precipitation with the landslide activity in each study area for 1950-1979, 2010-2039, and 2070-2099. The average annual precipitation and the ratio of total landslide area over total valley area are approximately the same in the Red Deer and Bow Rivers as they are both located in the same ecoregion with similar climate conditions. On the other hand, the landslide activity in the Battle River is significantly higher compared to the Red Deer and Bow Rivers. This is while the average annual precipitation is only about 20% higher in the Battle River area. This could be a sign of how climate can impact landslide activity in the long term.

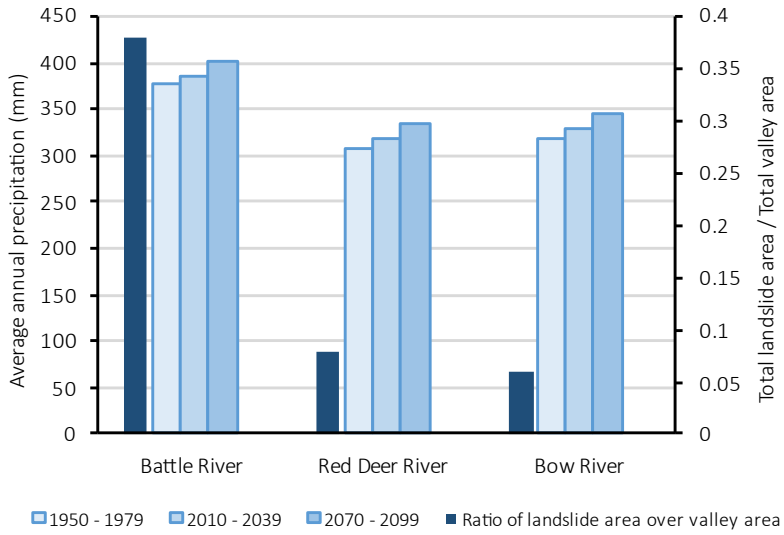

Figure 6-15: Comparison of average annual precipitation in different time periods with landslide activity

Climate models predict more precipitation in all three rivers until 2100. However, according to Table 6-2, the amount of increase is less than the 20% gap in the average annual precipitation between the Battle River and the Red Deer and Bow Rivers which shows that the landslide activity in the Red Deer and Bow Rivers is not expected to transition to those characteristics in the Battle River in the short term. Therefore, although more landslide activity is expected in all three river valleys until 2100 because of the increase in the average annual precipitation (especially in the case of intense seasonal rainfalls), the landslide activity difference between the river valleys is expected to remain the same. Predicting changes in landslide activity in the long term, however, is more complicated and depends not only on the climatic conditions but also on human activity and residential development.

2- Frost penetration and precipitation infiltration into the ground and the valley walls through opened tension cracks lead to the erosion and weathering of materials. In the case of moisture-sensitive materials like the Bearpaw overconsolidated shale, increased moisture content results in a higher degree of disintegration. The amount and rate of infiltration of precipitation into the surrounding soils at a regional scale is unknown as it is dependent on

factors such as surficial permeability, soil porosity, air temperature, etc. However, even small amounts of infiltration into overconsolidated shales may lead to the generation of high swelling with consequent decreases in the shear resistance of the soil mass (Brooker and Scott 1968).

3- Aspect plays a significant role in determining the amount of solar radiation received by the valley walls. In the northern hemisphere, surfaces facing south (south, southeast, and southwest) generally receive more solar energy compared to those facing north (north, northeast, and northwest). As a result, moisture content, and therefore landslide activity, are expected to be lower on the south-facing slopes. I showed in Figure 6-14 that a higher percentage of recorded landslides in the Red Deer and Bow areas face north, while 61% of recorded landslides along the Battle River face south. According to Fulton (1989), South-facing slopes are more susceptible to soil erosion due to the presence of scattered shrubs and bunchgrass compared to north-facing slopes, which have a moister environment and a denser plant cover. They also noted that this distinction is lost in the moister Cordilleran valleys where precipitation is greater than about 500 mm annually. Although the annual precipitation in the Battle River area is less than 500 mm, it is possible that due to the higher moisture, the effect of solar radiation on landslides is negligible.

It is worth mentioning that according to the 30-year climate data, the annual precipitation is not constant throughout each river valley with some parts of each river receiving up to 2.5% more precipitation annually. However, this difference was not considered significant and did not show a direct correlation with higher landslide activity along a given river valley.

6.7 Conclusion

This work illustrated a semi-quantitative approach to evaluate changes in regional landslide activity as a consequence of forecasted climate change, which can be adopted in other regions. This paper presented the characterization of landslides along three river valleys in Alberta, Canada, within the same geologic formation. It is observed that Battle River has less steep valleys than the Red Deer and Bow Rivers valleys with landslides that are larger in size and the mean degree of

slope of the landslides being lower in the Battle River region. The higher landslide activity along Battle River has flattened the valley in the long term.

According to previous studies, Battle River has been experiencing more precipitation than Red Deer and Bow Rivers since the slope instability period in the last deglaciation. My study shows that the current annual precipitation is higher in the Battle River and will remain higher until at least 2100. Therefore, climate and its long-term effects are one of the main factors for the different landslide activities across the study regions. Based on the climate predictions, I expect more landslide activity in all three river valleys in the short-term (i.e., until 2100) because of the increase in the average annual precipitation. However, the landslide activity difference between the river valleys is expected to remain the same at least until 2100.

The Bearpaw overconsolidated shale and the bentonitic layer throughout the region are weak and prone to landslides. These materials can soften and lose their strength when sheared. Moreover, due to the sensitivity to moisture, the Bearpaw shale can disaggregate when exposed to water.

Aspect plays an important role in local climate, and therefore soil stability, as the north-facing slopes are wetter and subject to less frequent and intense episodes of drying and wetting. I showed that 50% of the landslides along the Red Deer River and 50% along the Bow River face north, northeast, or northwest. In contrast, 61% of the landslides along the Battle River face southeast, south, or southwest. It is possible that due to the higher moisture in the Battle River region, the effect of aspect and therefore solar radiation on landslides is negligible.

These findings, in conjunction with previous research on long-term climatic conditions in the region, provide evidence of contrasting climatic conditions between the Battle River and the other two rivers which highlights the influence of climatic conditions on the formation of river valleys and the occurrence of landslides in the region. On a regional scale, long-term climate conditions appear to be one main factor in landslide activity where the geologic formation is the same. Forecasted changes in climate, however, indicate that the landslide activity in the Red Deer River and the Bow River will not reach the activity levels (in terms of aerial extent) mapped at the Battle River by 2100.

6.8 Acknowledgement

This study was supported financially by Transport Canada (contract No. T8009-210202) under the umbrella of the Canadian Rail Research Laboratory (CaRRL) and the (Canadian) Railway Ground Hazard Research Program (RGHRP) at the University of Alberta, financially supported by Canadian National Railway (CN) and Canadian Pacific Kansas City Railway (CPKC) and the Natural Sciences and Engineering Research Council of Canada (NSERC).

6.9 References

Alberta Parks (2015) Natural regions and subregions of Alberta; A Framework for Alberta's parks. Alberta Tourism, Parks and Recreation. Edmonton, Alberta.

Allan JA, Sanderson JOG (1945) Geology of Red Deer and Rosebud Sheets, Alberta. Research council of Alberta, Report number 13.

Atkinson TC, Carson MA, Curtis CD, Derbyshire E, Douglas I, Evans IS, Gregory KJ, Kennedy BA, Kirkby MJ, Morgan RCP, Ollier CD, Smith DI, Thomas MF, Trudgill ST (1976) Geomorphology and climate. John Wiley & Sons Ltd.

Biagini L, Macciotta R, Gräpel C, Tappenden K, Skirrow R (2022) Characteristics, kinematics and contributing factors of compound and translational landslides in the interior plains of Canada. Geosciences (Switzerland) 12. https://doi.org/10.3390/geosciences12080289

Brooker EW, Scott JS (1968) Geological and engineering aspects of Upper Cretaceous shales in western Canada. Geological Survey of Canada, Paper 66-3. https://doi.org/10.4095/100958

Brunetti MT, Melillo M, Peruccacci S, Ciabatta L, Brocca L (2018) How far are we from the use of satellite rainfall products in landslide forecasting? Remote Sensing of Environment, 210: 65–75. Elsevier. https://doi.org/10.1016/j.rse.2018.03.016

Campbell C, Campbell IA (1997) Calibration, review, and geomorphic implications of postglacial radiocarbon ages in southeastern Alberta, Canada. Quaternary Research 47:37–44. https://doi.org/10.1006/qres.1996.1873

Churchill RR (1981) Aspect-related differences in badlands slope morphology. Annals of the Association of American Geographers 71:374–388. http://www.jstor.org/stable/2562897

ClimateData.ca (2022) Climate data for a resilient Canada. https://climatedata.ca/

Cruden DM, Varnes DJ (1996) Landslide types and processes. In: Turner AK. and Shuster RL (eds) Landslides: Investigation and Mitigation. Transportation Research Board Special Report 247, Wasington, DC, pp 36-75

Downing DJ, Pettapiece WW (2006) Natural regions and subregions of Alberta. Government of Alberta, publication No. T/852. https://doi.org/10.5962/bhl.title.115367

Dubbin WE, Mermut AR, Rostad HPW (1993) Clay mineralogy of parent materials derived from uppermost Cretaceous and Tertiary sedimentary rocks in southern Saskatchewan. Canadian Journal of Soil Science 73: 447–457. https://doi.org/10.4141/cjss93-046

Environment and climate change Canada historical hydrometric data (2023). Government of Canada. Available from https://wateroffice.ec.gc.ca/mainmenu/historical_data_index_e.html. [accessed 18 July 2023].

Fenton MM, Waters EJ, Pawley SM, Atkinson N, Utting DJ, Mckay K (2013) Surficial geology of Alberta. Alberta Energy Regulator, AER/AGS Map 601. https://ags.aer.ca/publication/map-601

Folinsbee RE, Baadsgaard H, Lipson J (1961) Potassium-argon dates of upper cretaceous ash falls, Alberta, Canada. Annals of the New York Academy of Sciences 91:352–359. https://doi.org/10.1111/j.1749-6632.1961.tb35475.x

Fulton RJ (1989) Quaternary geology of Canada and Greenland. Geological Survey of Canada. https://doi.org/10.4095/127905

Godt JW, Baum RL, Chleborad AF (2006) Rainfall characteristics for shallow landsliding in Seattle, Washington, USA. Earth Surface Processes and Landforms 31:97–110. https://doi.org/10.1002/esp.1237

Alberta Water Well Information Database (2021) Government of Alberta. Available from http://groundwater.alberta.ca/WaterWells/d/. [accessed 15 May 2021].

Guzzetti F, Peruccacci S, Rossi M, Stark CP (2008) The rainfall intensity-duration control of shallow landslides and debris flows: An update. Landslides, 5: 3–17. doi: https://doi.org/10.1007/s10346-007-0112-1.

Hatcher JB, Stanton TW (1903) The Stratigraphic position of the Judith River beds and their correlation with the Belly River beds. Science 18:211–212. https://doi.org/10.1126/science.18.450.211

Krivoruchko K (2012) Empirical Bayesian Kriging implemented in ArcGIS Geostatistical Analyst. ArcUser Fall 2012.

Lerbekmo JF (2002) The Dorothy bentonite: an extraordinary case of secondary thickening in a late Campanian volcanic ash fall in central Alberta. Canadian Journal of Earth Sciences 39(12):1745–1754. https://doi.org/10.1139/e02-079

Leyva S, Cruz-Pérez N, Rodríguez-Martín J, Miklin L, Santamarta JC (2022) Rockfall and rainfall correlation in the Anaga Nature Reserve in Tenerife (Canary Islands, Spain). Rock Mechanics and Rock Engineering. Springer Vienna. https://doi.org/10.1007/s00603-021-02762-y

Liang L (1999) Landslide incidence and its relationship with climate in three river valleys in the Bearpaw Formation in southern Alberta. PhD Dissertation, University of Alberta. Edmonton. https://doi.org/10.7939/R34T6FB7W.

Lines FG (1963) Stratigraphy of Bearpaw Formation of southern Alberta. Bulletin of Canadian Petroleum Geology 11:212–227.

Macciotta R, Hendry M, Cruden DM, Blais-Stevens A, Edwards T (2017a) Quantifying rock fall probabilities and their temporal distribution associated with weather seasonality. Landslides 14(6):2025–2039. https://doi.org/10.1007/s10346-017-0834-7

Macciotta R, Martin CD, Edwards T, Cruden DM, Keegan T (2015a) Quantifying weather conditions for rock fall hazard management. Georisk: Assessment and Management of Risk for Engineered Systems and Geohazards 9:171–186. https://doi.org/10.1080/17499518.2015.1061673

Martinović K, Gavin K, Reale C, Mangan C (2018) Rainfall thresholds as a landslide indicator for engineered slopes on the Irish Rail network. Geomorphology 306:40–50. https://doi.org/10.1016/j.geomorph.2018.01.006

Matheson DS, Thomson S (1973) Geological Implications of Valley Rebound. Canadian Journal of Earth Sciences 10:961–978. https://doi.org/10.1139/e73-085

Mirhadi N, Macciotta R (2023) Quantitative correlation between rock fall and weather seasonality to predict changes in rock fall hazard with climate change. Landslides. https://doi.org/10.1007/s10346-023-02105-8

Pawley SM, Hartman GMD, Chao DK (2017) AER/AGS Information Series 148: Examples of landslides and the geological, topographic, and climatic factors that contribute to landslide susceptibilities in Alberta; A cross-reference to the explanatory notes for AGS Map 605. Alberta Energy Regulator, AER/AGS Information Series 148, 26 p.

Penner E (1962) Ground freezing and frost heaving. National Research Council of Canada. Division of Building Research. https://doi.org/10.4224/40000788

Pratt C, Macciotta R, Hendry M (2019) Quantitative relationship between weather seasonality and rock fall occurrences north of Hope, BC, Canada. Bulletin of Engineering Geology and the Environment 78:3239–3251. https://doi.org/10.1007/s10064-018-1358-7

Prior GJ, Hathway B, Glombick PM, Pana DI, Banks CJ, Hay DC, Schneider CL, Grobe M, Elgr R, Weiss JA (2013) Bedrock geology of Alberta. Alberta Enery Regulator, AER/AGS Map 600, scale 1:1 000 000.

Reeside JB (1957) Chapter 18: Paleoecology of the cretaceous seas of the western interior of the united states. In: Treatise on marine ecology and paleoecology. pp. 505–542. https://doi.org/10.1130/MEM67V2-p505

Rosi A, Peternel T, Jemec-Auflič M, Komac M, Segoni S, Casagli N (2016) Rainfall thresholds for rainfall-induced landslides in Slovenia. Landslides 13:1571–1577. https://doi.org/10.1007/s10346-016-0733-3.

Russell LS (1932) Stratigraphy and structure of the eastern portion of the Blood Indian Reserve, Alberta. Geological Survey of Canada, Summary report, Part B. Ottawa, ON. https://publications.gc.ca/collections/collection_2017/rncan-nrcan/M41-2-1931-B-eng.pdf

Scafe DW (1975) Alberta bentonites. Alberta Research Council. Economic geology report No. 2. https://static.ags.aer.ca/files/document/ECO/ECO_2.pdf

Stalker AM (1965) Pleistocene ice surface, Cypress Hills area. In: Cypress Hills plateau Alberta and Saskatchewan. Alberta society of petroleum geologists 15th annual field conference guidebook, Part 1, Cypress Hills plateau. pp. 116–130.

Thomson S, Morgenstern NR (1977) Factors affecting distribution of landslides along rivers in southern Alberta. Canadian Geotechnical Journal 14:508–523. https://doi.org/doi:10.1139/t77-052

Thomson S, Morgenstern NR (1979) Landslides in argillaceous rock, prairie provinces, Canada. Developments in Geotechnical Engineering 14: 515–540. https://doi.org/10.1016/B978-0-444-41508-0.50022-3

Vance RE, Beaudoin AB, Luckman BH (1995) The paleoecological record of 6 ka BP climate in the Canadian prairie provinces. Géographie physique et Quaternaire 49:81–98. https://doi.org/10.7202/033031ar

CHAPTER 7

Conclusion and Future Research

This research introduced various methodologies to investigate changes in landslide hazard for different weather conditions and climate change scenarios. The proposed methodologies can be utilized by future researchers to study the effects of past and future weather conditions, especially precipitation and temperature, on landslides in other parts of the world. Moreover, the findings of this research can help decision-makers in strategically allocating monitoring resources for risk mitigation and enhancing the resilience of infrastructure during periods when landslide hazards are the highest.

This chapter brings an end to this thesis by summarizing each study, recapping the findings, and suggesting possibilities for further research. The following sections provide the key findings derived from each study conducted in this research.

7.1 Chapter 3: Effect of antecedent precipitation and freeze-thaw cycles on landslide occurrences

A probabilistic analysis was employed to investigate the relationship between weather conditions and the documented landslides at the C018 site. This study revealed a correlation between the antecedent weather conditions and the recorded landslides between 2000 and 2021 at this site. Furthermore, the climatic predictions for the 2050s and 2080s were used to assess the potential impacts of climate change on landslide risk and to quantify the increase in landslide hazard over the upcoming decades. This study may assist the highway agency in prioritizing sites for climate resiliency interventions. The following remarks were derived from this study:

- Evaluating the 4-month antecedent weather conditions preceding each landslide showed that except for the May 2013 landslide, all other eight landslides that occurred in spring and summer occurred shortly after a period of rainfall. Results showed that an average of 6.9 mm of rain had fallen in the previous three days. Precipitation data also showed that at least 4.4 mm of rainfall had occurred during the 14 days before the landslide.
- Analyses showed that if there is more than 10 mm of rainfall in a 7-day period, there will be an approximately 3% probability of a landslide, with around 0.1% probability that a landslide occurs if there is less than 10 mm of rainfall in 7 days. The values for a 20 mm rainfall in a 14-day period are a 6% probability of a landslide if the threshold is exceeded, and approximately 0.1% probability that a landslide occurs if there is less than 20 mm of rainfall in 14 days. Based on these findings, 10 mm rainfall in 7 days and 20 mm rainfall in 14 days can be considered useful thresholds for landslide hazard monitoring and risk reduction strategies at this site.
- The ACCESS1.0-RCP4.5 global climate model forecasts an increase in the mean spring precipitation at the C018 site of 12% over the next 65 years. Moreover, mean seasonal temperatures are also expected to increase in the future, which means that more freeze-thaw cycles could be anticipated in winter. These findings also suggest that the probability of landslides at the C018 site during winter months could increase as a result of climate change because the two winter landslide events (December 2017 and January 2021) occurred when the air temperature fluctuated around 0°C, and freeze-thaw cycles were more likely to occur.

- The expected landslide probabilities in the 2050s and 2080s were calculated and the results showed increases in landslide probabilities in the future. Landslide probability is expected to rise about 13% in the 2050s compared to 2000-2021. Results also revealed that the landslide probability increases by 13% and 7% in the 2050s and 2080s, respectively, when the total precipitation is more than 20 mm in 14 days.

7.2 Chapter 4: Influence of precipitation on landslide volume

The relationship between the annual precipitation and the volume of landslides was investigated on the records between 2018 and 2022 at the C018 site. This study showed that in a slope, there is a direct relationship between the cumulative precipitation and the associated landslide volumes. The correlation between the landslide volumes and the annual precipitation was then used to assess the effects of climate change on the landslide volumes in the future. The following remarks were derived from this study:

- Based on the available data, a linear correlation was found by the comparison between annual precipitation and the corresponding landslide volume at the study site.
- Results showed that with 20% more precipitation than the maximum observed precipitation between 2018 and 2022, the annual landslide volume can increase up to 1044-1222 m^3 with 85% confidence, which is 16-35% more than the highest observed volume (903 m^3) in 2018.
- Based on the climate predictions and using the linear relationship found between the annual precipitation and landslide volumes, up to 81% more annual landslide volume could be expected in future years of above-average precipitation.

7.3 Chapter 5: Quantitative correlation between rock fall and weather seasonality to predict changes in rock fall hazard with climate change

A statistical method was employed to quantify the relationship between monthly weather averages and rock fall frequencies in a section of CN's Yale subdivision along the Fraser River in British Columbia, Canada. von Mises distributions were used to find the best-fitted models to the monthly precipitation and freeze-thaw cycles, and proper relative weights were applied to the models in order to calibrate them to the rock fall monthly frequency. Subsequently, the calibrated model was used with input data from climatic predictions for 2041-2070 and 2071-2100 to see how rock fall distribution will be affected due to climate change in the future decades. The following remarks were derived from this study:

- At least 13% more rock fall activity is expected in winter (December to February) for the period of 2041-2070. The maximum increase in the rock fall events in the period of 2041-2070 is predicted to occur in January.
- The increase in rock fall activity in the period of 2071-2100 is greatest in December and reaches 19% relative to the reference period of 1990-2019.
- Rock fall predictions indicate fewer events in the fall and spring, which could be caused by the expected shorter period in which freeze-thaw cycles occur. Based on the results, it is anticipated that the number of rock fall events will decrease by 24% on average in October, November, March, and April. Based on these findings, the average annual number of rock falls is expected to decrease by 2.31% in 2041-2070 (i.e., from 28.64 events per year to 27.98), and by 2.15% in 2071-2100 (i.e., from 28.64 events per year to 28.03).
- The rate of increase in rock fall events is greatest between the present time and 2041-2070, with a reduced rate of increase between 2041-2070 and 2071-2100 considering the RCP 4.5 emission scenario.

7.4 Chapter 6: Regional scale evaluation of landslide activity and its relation to climate

A semi-qualitative analysis was conducted to study the relationship between climate conditions and landslide activity at a regional scale in parts of the Battle, Red Deer, and Bow Rivers that are located within the Bearpaw geological Formation in southern Alberta, Canada. Possible changes in regional landslide activity as a consequence of climate change were also studied. The following remarks were derived from this study:

- Based on the mean area values, the landslides along the Battle River are approximately 10 times larger than those in the Red Deer River area and 23 times larger than the landslides mapped along the Bow River.
- While the Battle River has the lowest degree of slope with an average of 11.5 degrees, landslides in the Bow River area are steeper than the other two regions with an average of 23.9 degrees.
- Results showed higher landslide activity in the Battle River area with 0.6 km^2 landslide per one kilometre length of the river which is 4.6 and 12 times higher than the landslide activity along the Red Deer and Bow Rivers, respectively. The higher landslide activity along Battle River has flattened the valley in the long term.
- In terms of the number of landslides per unit length of the river, due to the smaller size of the landslides, the Red Deer and Bow rivers show similar activity rates with 1.78 and 1.65 landslides per one kilometre of the river which is almost 2 times the rate in the Battle River area.
- Battle River has been experiencing more precipitation than Red Deer and Bow Rivers since the slope instability period in the last deglaciation. On a regional scale, long-term climate conditions appear to be one main factor in landslide activity where the geologic formation is the same.

- Forecasted changes in climate, however, indicate that the landslide activity in the Red Deer River and the Bow River would not reach the activity levels (in terms of aerial extent) mapped at the Battle River.

7.5 General conclusions

This research provided different methodologies for investigating the relationship between landslides and weather data, particularly precipitation and freeze-thaw cycle. Importantly, it demonstrated that, while it is possible to use past landslide behaviour with weather to predict future behaviour from a statistical perspective, uncertainties remain due to climate forecasting.

This research showed that the study of landslides at a regional scale is more challenging due to the limited information about the occurrence time of the landslides. However, it showed that it is possible to study the impact of precipitation on landslides by comparing different study areas with similar geological backgrounds.

In summary, considering current climate change scenarios, temperatures in western Canada are expected to increase in the future decades. Depending on the location, this temperature increase may result in more or fewer freeze-thaw cycles. Precipitation, however, is projected to increase in western Canada, although some southern areas may experience decreased summer rainfall under a high-emission scenario. This research showed that the increase in precipitation will change the volume and number of landslides in the study areas over the 21st century. Weather extremes resulting from climate change, including intense rainfalls, will trigger more severe landslides in the future. Due to the natural uncertainties in predicting the timing, magnitude, and location of these weather extremes, forecasting landslides resulting from weather extreme events remains challenging.

Ultimately, it is worth noting that there are multiple challenges associated with this type of study, among them, uncertainties in climate forecasting and the completeness of the landslide records are the most important ones. This highlights the importance of maintaining adequate landslide records along transportation corridors for future studies.

7.6 Recommendations for future work

This section outlines several directions for further research that can enhance our understanding of the subject and contribute to the development of more comprehensive strategies for managing landslide risks in the face of evolving climate conditions.

- A Bayesian Updating method is recommended to be used on the results obtained from the studies conducted on the C018 site. Updated results can reduce the errors in estimating periods with higher landslide activity and provide more accurate estimates for the landslide volumes.
- Design an effective notification system for risk management along transportation corridors. This notification system can work based on landslide probabilities, defined weather thresholds; providing notification to highway users and maintenance crews of the period of time with increased landslide hazard such that driving attitudes are adequate (e.g., attention for possible blocked sections of road) and inspections are efficiently programmed.
- The methodology outlined in Chapter 4 has the potential to be utilized in other study areas as a means of measuring the impact of climate change on landslide volumes. It is recommended to update the relationship identified between the annual landslide volume and precipitation at the C018 provided that new data become available. The updated relationship can subsequently be applied to obtain more accurate estimations of landslide volumes in the future.
- The circular distribution method described in Chapter 5 can be used to develop more accurate rock fall hazard monitoring and risk reduction strategies in other areas where there is a direct relationship between weather-related factors and recorded landslides.

References

ADAM Technology (2021) 3DM Analyst. Available at: https://www.adamtech.com.au

Aditian A, Kubota T, Shinohara Y (2018) Comparison of GIS-based landslide susceptibility models using frequency ratio, logistic regression, and artificial neural network in a tertiary region of Ambon, Indonesia. Geomorphology 318:101–111. https://doi.org/10.1016/j.geomorph.2018.06.006

Alberta Climate Information Service (2020) Current and Historical Alberta Weather Station Data Viewer. http://agriculture.alberta.ca/acis/weather-data-viewer.jsp. Accessed 11 August 2021

Alberta Parks (2015) Natural regions and subregions of Alberta; A Framework for Alberta's parks. Alberta Tourism, Parks and Recreation. Edmonton, Alberta.

Alberta Transportation (2021) Annual Landslides Assessments for Central Region (CMA511-516). https://www.transportation.alberta.ca/PlanningTools/GMS/Annual Landslides Assessments/Reg-Central Region (CMA511-516)/Inspection Sites/837_02 (C18) - Red Deer River Scour 1.9km from SH575/Reports/. Accessed 23 August 2021

Alberta Water Well Information Database (2021) Government of Alberta. Available from http://groundwater.alberta.ca/WaterWells/d/. [accessed 15 May 2021].

Allan JA, Sanderson JOG (1945) Geology of Red Deer and Rosebud Sheets, Alberta. Research council of Alberta, Report number 13.

Arabameri A, Pradhan B, Rezaei K et al (2019) GIS-based landslide susceptibility mapping using numerical risk factor bivariate model and its ensemble with linear multivariate regression and boosted regression tree algorithms. J Mt Sci 16:595–618. https://doi.org/10.1007/s11629-018-5168-y

Arosio D, Longoni L, Mazza F et al (2013) Freeze-Thaw Cycle and Rockfall Monitoring. In: Margottini C, Canuti P, Sassa K (eds) Landslide Science and Practice. Springer, Berlin, Heidelberg. https://doi.org/10.1007/978-3-642-31445-2_50

Atkinson TC, Carson MA, Curtis CD, Derbyshire E, Douglas I, Evans IS, Gregory KJ, Kennedy BA, Kirkby MJ, Morgan RCP, Ollier CD, Smith DI, Thomas MF, Trudgill ST (1976) Geomorphology and climate. John Wiley & Sons Ltd.

Barredo JI, Benavides A, Hervás J, Van Westen CJ (2000) Comparing heuristic landslide hazard assessment techniques using GIS in the Tirajana basin, Gran Canaria Island, Spain. Int J Appl Earth Obs Geoinf 2000:9–23. https://doi.org/10.1016/s0303-2434(00)85022-9

Bhardwaj A, Wasson RJ, Ziegler AD et al (2019) Characteristics of rain-induced landslides in the Indian Himalaya: A case study of the Mandakini Catchment during the 2013 flood. Geomorphology 330:100–115. https://doi.org/10.1016/j.geomorph.2019.01.010

Bi D, Dix M, Marsland S et al (2013) The ACCESS coupled model: description, control climate and evaluation. Aust Meteorol Oceanogr J 63:41–64. https://doi.org/10.22499/2.6301.004

Biagini L, Macciotta R, Gräpel C, Tappenden K, Skirrow R (2022) Characteristics, kinematics and contributing factors of compound and translational landslides in the interior plains of Canada. Geosciences (Switzerland) 12. https://doi.org/10.3390/geosciences12080289

Bjerrum L (1967) The Third Terzaghi Lectures; Progressive failure in slopes of overconsolidated plastic clay and clay shales. J Soil Mech Found Div 93:1–49. https://doi.org/10.1061/JSFEAQ.0001017

Bjerrum L, Jørstad F (1968) Stability of rock slopes in Norway. Nor Geotech Inst Publ 79:1–11

Blais-Stevens, A. (2019) Historical landslides in Canada resulting in fatalities (1771- 2018). In: GeoSt.John's 2019, the 72nd Canadian Geotechnical Conference. St. John's, Newfoundland and Labrador. https://doi.org/10.1130/abs/2020AM-354152

Bovis MJ, Jones P (1992) Holocene history of earthflow mass movements in south-central British Columbia: the influence of hydroclimatic changes. Can J Earth Sci 29:1746–1755. https://doi.org/10.1139/e92-137

Brooker EW, Scott JS (1968) Geological and engineering aspects of Upper Cretaceous shales in western Canada. Geological Survey of Canada. Paper 66-3. https://doi.org/10.4095/100958

Brooks SM, Crozier MJ, Glade TW, Anderson MG (2004) Towards Establishing Climatic Thresholds for Slope Instability: Use of a Physically-based Combined Soil Hydrology-slope Stability Model. Pure Appl Geophys 161:881–905. https://doi.org/10.1007/s00024-003-2477-y

Brunetti MT, Melillo M, Peruccacci S, Ciabatta L, Brocca L (2018) How far are we from the use of satellite rainfall products in landslide forecasting? Remote Sensing of Environment, 210: 65–75. Elsevier. https://doi.org/10.1016/j.rse.2018.03.016

Bush E, Lemmen DS (2019) Canada's changing climate report. Environment and Climate Change Canada, Government of Canada, Ottawa, ON.

Campbell C, Campbell IA (1997) Calibration, review, and geomorphic implications of postglacial radiocarbon ages in southeastern Alberta, Canada. Quaternary Research 47:37–44. https://doi.org/10.1006/qres.1996.1873

Cannon AJ, Sobie SR, Murdock TQ (2015) Bias correction of GCM precipitation by quantile mapping: How well do methods preserve changes in quantiles and extremes? J Clim 28:6938–6959. https://doi.org/10.1175/JCLI-D-14-00754.1

Chen W, Panahi M, Tsangaratos P et al (2019) Applying population-based evolutionary algorithms and a neuro-fuzzy system for modeling landslide susceptibility. Catena 172:212–231. https://doi.org/10.1016/j.catena.2018.08.025

Chen W, Pourghasemi HR, Panahi M et al (2017) Spatial prediction of landslide susceptibility using an adaptive neuro-fuzzy inference system combined with frequency ratio, generalized additive model, and support vector machine techniques. Geomorphology 297:69–85. https://doi.org/10.1016/j.geomorph.2017.09.007

Chi Y, Lee Y (2013) Assessment of landslide volume for Alishan Highway based on database of rainfall-induced slope failure. Int J Environ Chem Ecol Geol Geophys Eng 7:693–698

Churchill RR (1981) Aspect-related differences in badlands slope morphology. Annals of the Association of American Geographers 71:374–388. http://www.jstor.org/stable/2562897

ClimateData.ca (2022) Climate data for a resilient Canada. https://climatedata.ca

CloudCompare (version 2.10.2) [GPL software] (2022) Retrieved from: http://www.cloudcompare.org

Coe JA, Godt JW (2012) Review of approaches for assessing the impact of climate change on landslide hazards. In: Eberhardt E, Froese C, Turner AK, and Leroueil S (eds) Landslides and Engineered Slopes, Protecting Society Through Improved Understanding: Proceedings of the 11th International and 2nd North American Symposium on Landslides and Engineered Slopes, Banff, Canada, 3-8 June, Taylor & Francis Group, London, pp 371-377

Collins M, Knutti R, Arblaster J et al (2013) Long-term Climate Change: Projections, Commitments and Irreversibility. In: Climate Change 2013: The Physical Science Basis. Contribution of Working Group I to the Fifth Assessment Report of the Intergovernmental Panel on Climate Change. Cambridge University Press, Cambridge, United Kingdom and New York, NY, USA, pp 1029–1136

Corominas J, van Westen C, Frattini P et al (2014) Recommendations for the quantitative analysis of landslide risk. Bull Eng Geol Environ 73:209–263. https://doi.org/10.1007/s10064-013-0538-8

Crozier MJ (2010) Deciphering the effect of climate change on landslide activity: A review. Geomorphology 124:260–267. https://doi.org/10.1016/j.geomorph.2010.04.009

Crozier MJ (2017) A proposed cell model for multiple-occurrence regional landslide events: Implications for landslide susceptibility mapping. Geomorphology 295:480–488. https://doi.org/10.1016/j.geomorph.2017.07.032

Cruden DM, Varnes DJ (1996) Landslide types and processes. In: Turner AK. and Shuster RL (eds) Landslides: Investigation and Mitigation. Transportation Research Board Special Report 247, Wasington, DC, pp 36-75

Cui Y, Miller D, Schiarizza P, Diakow LJ (2017) British Columbia digital geology. British Columbia Ministry of Energy, Mines and Petroleum Resources, British Columbia Geological Survey Open File 2017-8, p 9

Curtis Engineering Associates (2009) Geotechnical investigation - proposed residential subdivision SE 27-29-21W4M - MD of Kneehill, Alberta

Dai F, Lee C (2001) Frequency–volume relation and prediction of rainfall-induced landslides. Eng Geol 59:253–266. https://doi.org/10.1016/S0013-7952(00)00077-6

Dehnavi A, Nasiri Aghdam I, Pradhan B, Morshed Varzandeh MH (2015) A new hybrid model using step-wise weight assessment ratio analysis (SWARA) technique and adaptive neuro-fuzzy inference system (ANFIS) for regional landslide hazard assessment in Iran. Catena 135:122–148. https://doi.org/10.1016/j.catena.2015.07.020

Dikau R, Schrott L (1999) The temporal stability and activity of landslides in Europe with respect to climatic change (TESLEC): main objectives and results. Geomorphology 30:1–12. https://doi.org/10.1016/S0169-555X(99)00040-9

DJI (2021) Phantom 4 - Product Information - DJI. https://www.dji.com/ca/phantom-4/info. Accessed 26 Dec 2021

Downing DJ, Pettapiece WW (2006) Natural regions and subregions of Alberta. Government of Alberta, publication No. T/852. https://doi.org/10.5962/bhl.title.115367

Dubbin WE, Mermut AR, Rostad HPW (1993) Clay mineralogy of parent materials derived from uppermost Cretaceous and Tertiary sedimentary rocks in southern Saskatchewan. Canadian Journal of Soil Science 73: 447–457. https://doi.org/10.4141/cjss93-046

Durgin PB (1977) Landslides and the weathering of granitic rocks. In: Coates DR, Landslides. Geological Society of America. pp 125–132

Environment and climate change Canada historical hydrometric data (2023). Government of Canada. Available from https://wateroffice.ec.gc.ca/mainmenu/historical_data_index_e.html. [accessed 18 July 2023].

Fahey BD, Lefebure TH (1988) The freeze-thaw weathering regime at a section of the Niagara escarpment on the Bruce Peninsula, Southern Ontario, Canada. Earth Surf Process Landforms 13:293–304. https://doi.org/10.1002/esp.3290130403

Fan L, Lehmann P, Zheng C, Or D (2020) Rainfall intensity temporal patterns affect shallow landslide triggering and hazard evolution. Geophys Res Lett 47:1–9. https://doi.org/10.1029/2019GL085994

Fenton MM, Waters EJ, Pawley SM, Atkinson N, Utting DJ, Mckay K (2013) Surficial geology of Alberta. Alberta Energy Regulator, AER/AGS Map 601. https://ags.aer.ca/publication/map-601

Folinsbee RE, Baadsgaard H, Lipson J (1961) Potassium-argon dates of upper cretaceous ash falls, Alberta, Canada. Annals of the New York Academy of Sciences 91:352–359. https://doi.org/10.1111/j.1749-6632.1961.tb35475.x

Fulton RJ (1989) Quaternary geology of Canada and Greenland. Geological Survey of Canada. https://doi.org/10.4095/127905

Gariano SL, Guzzetti F (2016) Landslides in a changing climate. Earth-Science Rev 162:227–252. https://doi.org/10.1016/j.earscirev.2016.08.011

Girardeau-Montaut D, Roux M, Marc R, Thibault G (2005) Change detection on points cloud data acquired with a ground laser scanner. Int Arch Photogramm Remote Sens Spat Inf Sci 36:30–35

Godt JW, Baum RL, Chleborad AF (2006) Rainfall characteristics for shallow landsliding in Seattle, Washington, USA. Earth Surface Processes and Landforms 31:97–110. https://doi.org/10.1002/esp.1237

Government of Canada (2020) Historical weather data. https://climate.weather.gc.ca/historical_data/search_historic_data_e.html. Accessed 10 August 2021

Guo Y, Shan W, Jiang H et al (2014) The Impact of Freeze–thaw on the Stability of Soil Cut Slope in High-latitude Frozen Regions. In: Shan W, Guo Y, Wang F, Marui H, Strom A (eds) Landslides in Cold Regions in the Context of Climate Change. Environ Sci Eng, pp 85–98. https://doi.org/10.1007/978-3-319-00867-7_7

Guzzetti F, Peruccacci S, Rossi M, Stark CP (2008) The rainfall intensity-duration control of shallow landslides and debris flows: An update. Landslides 5:3–17. https://doi.org/10.1007/s10346-007-0112-1

Hamblin AP (2004) The Horseshoe Canyon Formation in southern Alberta: surface and subsurface stratigraphic architecture, sedimentology, and resource potential. Geological Survey of Canada, Bulletin no. 578. https://doi.org/10.4095/215068

Hardy R (1957) Engineering problems involving pre-consolidated clay shales. In: Tenth Canadian Soil Mechanics Conference, December 17-18, 1956. Ottawa, Ontario, Canada

Hatcher JB, Stanton TW (1903) The Stratigraphic position of the Judith River beds and their correlation with the Belly River beds. Science 18:211–212. https://doi.org/10.1126/science.18.450.211

Hong H, Pourghasemi HR, Pourtaghi ZS (2016) Landslide susceptibility assessment in Lianhua County (China): A comparison between a random forest data mining technique and bivariate and multivariate statistical models. Geomorphology 259:105–118. https://doi.org/10.1016/j.geomorph.2016.02.012

Huang AB, Lee JT, Ho YT et al (2012) Stability monitoring of rainfall-induced deep landslides through pore pressure profile measurements. Soils Found 52:737–747. https://doi.org/10.1016/j.sandf.2012.07.013

Huang F, Yao C, Liu W et al (2018) Landslide susceptibility assessment in the Nantian area of China: A comparison of frequency ratio model and support vector machine. Geomatics, Nat Hazards Risk 9:919–938. https://doi.org/10.1080/19475705.2018.1482963

Huang F, Zhang J, Zhou C et al (2020) A deep learning algorithm using a fully connected sparse autoencoder neural network for landslide susceptibility prediction. Landslides 17:217–229. https://doi.org/10.1007/s10346-019-01274-9

Hungr O, Evans SG, Hazzard J (1999) Magnitude and frequency of rock falls and rock slides along the main transportation corridors of southwestern British Columbia. Can Geotech J 36:224–238. https://doi.org/10.1139/t98-106

IPCC (2014) Climate Change 2014: Synthesis Report. Contribution of Working Groups I, II and III to the Fifth Assessment Report of the Intergovernmental Panel on Climate Change. Gian-Kasper Plattner, Geneva, Switzerland

IPCC (2021) Climate Change 2021: The physical science basis. Contribution of working group I to the sixth assessment report of the intergovernmental panel on climate change. Cambridge University Press. In Press.

Iverson RM (2000) Landslide triggering by rain infiltration. Water Resour Res 36:1897–1910. https://doi.org/10.1029/2000WR900090

Iverson RM, Major JJ (1987) Rainfall, ground-water flow, and seasonal movement at Minor Creek landslide, northwestern California: physical interpretation of empirical relations. Geol Soc Am Bull 99:579–594. https://doi.org/10.1130/0016-7606(1987)99<579:RGFASM>2.0.CO;2

Jakob M, Lambert S (2009) Climate change effects on landslides along the southwest coast of British Columbia. Geomorphology 107:275–284. https://doi.org/10.1016/j.geomorph.2008.12.009

Jakob M, Owen T (2021) Projected effects of climate change on shallow landslides, North Shore Mountains, Vancouver, Canada. Geomorphology 393. https://doi.org/10.1016/j.geomorph.2021.107921

Jolliffe IT, Cadima J (2016) Principal component analysis: a review and recent developments. Philosophical Transactions of the Royal Society A 374:20150202. https://doi.org/10.1098/rsta.2015.0202

Kavzoglu T, Sahin EK, Colkesen I (2014) Landslide susceptibility mapping using GIS-based multi-criteria decision analysis, support vector machines, and logistic regression. Landslides 11:425–439. https://doi.org/10.1007/s10346-013-0391-7

Kayastha P, Dhital MR, De Smedt F (2013) Application of the analytical hierarchy process (AHP) for landslide susceptibility mapping: A case study from the Tinau watershed, west Nepal. Comput Geosci 52:398–408. https://doi.org/10.1016/j.cageo.2012.11.003

Klohn Crippen Berger (2000) Central Region Landslide Assessment SH837:02 River Scour @ km 1.9 Emergency Geotechnical Inspection Report, July 25, 2000

Klohn Crippen Berger (2018) CON0017608 Central Region GRMP – Call-Out Report C018 Hwy 837:02 Call-Out Report January 19, 2018. Red Deer

Klohn Crippen Berger (2019) 2019 C018 Inspection Photos. Alberta Transportation Central Region GRMP. Document number A05115A02. October 2019.

Krautblatter M, Moser M (2009) A nonlinear model coupling rockfall and rainfall intensity based on a four year measurement in a high Alpine rock wall (Reintal, German Alps). Nat Hazards Earth Syst Sci 9:1425–1432. https://doi.org/10.5194/nhess-9-1425-2009

Krivoruchko K (2012) Empirical Bayesian Kriging implemented in ArcGIS Geostatistical Analyst. ArcUser Fall 2012.

Lague D, Brodu N, Leroux J (2013) Accurate 3D comparison of complex topography with terrestrial laser scanner: Application to the Rangitikei canyon (N-Z). ISPRS J Photogramm Remote Sens 82:10–26. https://doi.org/10.1016/j.isprsjprs.2013.04.009

Laherrère J (2019) Are there enough fossil fuels to generate the IPCC CO2 baseline scenario? https://aspofrance.files.wordpress.com/2019/08/ipccco2rcp.pdf. Accessed 18 March 2021

Lerbekmo JF (2002) The Dorothy bentonite: an extraordinary case of secondary thickening in a late Campanian volcanic ash fall in central Alberta. Canadian Journal of Earth Sciences 39(12):1745–1754. https://doi.org/10.1139/e02-079

Leyva S, Cruz-Pérez N, Rodríguez-Martín J, Miklin L, Santamarta JC (2022) Rockfall and rainfall correlation in the Anaga Nature Reserve in Tenerife (Canary Islands, Spain). Rock Mechanics and Rock Engineering. Springer Vienna. https://doi.org/10.1007/s00603-021-02762-y

Liang L (1999) Landslide incidence and its relationship with climate in three river valleys in the Bearpaw Formation in southern Alberta. PhD Dissertation, University of Alberta. https://doi.org/10.7939/R34T6FB7W

Lines FG (1963) Stratigraphy of Bearpaw Formation of southern Alberta. Bulletin of Canadian Petroleum Geology 11:212–227.

Liu KF, Wu YH, Chen YC et al (2013) Large-scale simulation of watershed mass transport: A case study of Tsengwen reservoir watershed, southwest Taiwan. Nat Hazards 67:855–867. https://doi.org/10.1007/S11069-013-0611-4

Lucieer A, Jong SM, Turner D (2014) Mapping landslide displacements using Structure from Motion (SfM) and image correlation of multi-temporal UAV photography. Prog Phys Geogr 38:97–116. https://doi.org/10.1177/0309133313515293

Macciotta R, Cruden DM, Martin CD, Morgenstern NR (2011) Combining geology , morphology and 3D modelling to understand the rock fall distribution along the railways in the Fraser River valley, between Hope and Boston Bar, B.C. In: Slope Stability 2011: International symposium on rock slope stability in open pit mining and civil engineering. Vancouver, Canada

Macciotta R, Cruden D, Martin D et al (2013) Spatial and temporal aspects of slope hazards along a railroad corridor in the Canadian Cordillera. In: Proceedings of the 2013 international symposium on slope stability in open pit mining and civil engineering. Australian Centre for Geomechanics, Perth, pp 1171–1185

Macciotta R, Martin CD, Edwards T, Cruden DM, Keegan T (2015a) Quantifying weather conditions for rock fall hazard management. Georisk Assess Manag Risk Eng Syst Geohazards 9:171–186. https://doi.org/10.1080/17499518.2015.1061673

Macciotta R, Martin CD, Cruden DM (2015b) Probabilistic estimation of rockfall height and kinetic energy based on a three-dimensional trajectory model and Monte Carlo simulation. Landslides 12:757–772. https://doi.org/10.1007/s10346-014-0503-z

Macciotta R, Hendry M, Roghani A (2016) Developing Hazard Management Strategies based on Tolerable Risk to Railway Operations. In: Pombo J (ed) Proceedings of the Third International Conference on Railway Technology: Research, Development and Maintenance. Civil-Comp Press, Stirlingshire, Scotland. https://doi.org/10.4203/ccp.110.282

Macciotta R, Hendry M, Cruden DM, Blais-Stevens A, Edwards T (2017a) Quantifying rock fall probabilities and their temporal distribution associated with weather seasonality. Landslides 14(6):2025–2039. https://doi.org/10.1007/s10346-017-0834-7

Macciotta R, Martin CD, Cruden DM et al (2017b) Rock fall hazard control along a section of railway based on quantified risk. Georisk Assess Manag Risk Eng Syst Geohazards 11(3):272–284. https://doi.org/10.1080/17499518.2017.1293273

Macciotta R (2019) Review and latest insights into rock fall temporal variability associated with weather. Proc Inst Civ Eng Geotech Eng 172(6):556–568. https://doi.org/10.1680/jgeen.18.00207

Mardia KV (1972) Statistics of directional data. Elsevier, London, New York

Martinović K, Gavin K, Reale C, Mangan C (2018) Rainfall thresholds as a landslide indicator for engineered slopes on the Irish Rail network. Geomorphology 306:40–50. https://doi.org/10.1016/j.geomorph.2018.01.006

Mateos RM, García-Moreno I, Azañón JM (2012) Freeze-thaw cycles and rainfall as triggering factors of mass movements in a warm Mediterranean region: The case of the Tramuntana Range (Majorca, Spain). Landslides 9:417–432. https://doi.org/10.1007/s10346-011-0290-8

Matheson DS, Thomson S (1973) Geological Implications of Valley Rebound. Canadian Journal of Earth Sciences 10:961–978. https://doi.org/10.1139/e73-085

Matsuoka N, Murton J (2008) Frost weathering: recent advances and future directions. Permafr Periglac Process 19:195–210. https://doi.org/10.1002/ppp.620

Mbogga M, Wang T, Hansen C, Hamann A (2010) A comprehensive set of interpolated climate data for Alberta. Government of Alberta, Publication Number: Ref. T/235.

McColl ST (2022) Landslide causes and triggers. In: Shroder JF, Davies T, Rosser N (eds) Landslide Hazards, Risks, and Disasters. Elsevier, pp 13–41. https://doi.org/10.1016/B978-0-12-818464-6.00011-1

McGreevy JP, Whalley WB (1982) The geomorphic significance of rock temperature variations in cold environments: A discussion. Arct Alp Res 14(2):157–162. https://doi.org/10.2307/1551114

Meinshausen M, Smith SJ, Calvin K et al (2011) The RCP greenhouse gas concentrations and their extensions from 1765 to 2300. Clim Change 109:213–241. https://doi.org/10.1007/s10584-011-0156-z

Mirhadi N, Macciotta R (2023) Quantitative correlation between rock fall and weather seasonality to predict changes in rock fall hazard with climate change. Landslides. https://doi.org/10.1007/s10346-023-02105-8

Mirhadi N, Macciotta R, Gräpel C et al (2022) Antecedent weather signatures for various landslide failure modes at a 60-m-high rock slope near Drumheller, AB. In: Geohazards8, 8th Canadian Conference on Geotechnique and Natural Hazards: Innovative geoscience for tomorrow. Québec City, pp 447–455

Mollard JD (1977) Regional landslide types in Canada. In: Coates DR, Landslides. Geological Society of America. pp 29–56

Monger JWH (1970) Hope map-area, west half (92H W1/2), British Columbia, Paper 69-47. Ottawa, ON.

Natural hazards learning resources at EOAS (2022) Porteau Cove rockfall. https://blogs.ubc.ca/eoashazards/porteau-cove-rockfall/. Accessed 5 Apr 2022

Natural Resources Canada (2017) Landslides. Government of Canada. https://www.nrcan.gc.ca/science-and-data/science-and-research/natural-hazards/landslides/10661. Accessed 9 Aug 2021

Niethammer U, James MR, Rothmund S et al (2012) UAV-based remote sensing of the Super-Sauze landslide: Evaluation and results. Eng Geol 128:2–11. https://doi.org/10.1016/J.ENGGEO.2011.03.012

Pawley SM, Hartman GMD, Chao DK (2017) AER/AGS Information Series 148: Examples of landslides and the geological, topographic, and climatic factors that contribute to landslide susceptibilities in Alberta; A cross-reference to the explanatory notes for AGS Map 605. Alberta Energy Regulator, AER/AGS Information Series 148, 26 p.

Penner E (1962) Ground freezing and frost heaving. National Research Council of Canada. Division of Building Research. https://doi.org/10.4224/40000788

Pomeroy JW, Stewart RE, Whitfield PH (2016) The 2013 flood event in the South Saskatchewan and Elk River basins: Causes, assessment and damages. Can Water Resour J / Rev Can des ressources hydriques 41:105–117. https://doi.org/10.1080/07011784.2015.1089190

Popescu ME (1994) A suggested method for reporting landslide causes. Bull Int Assoc Eng Geol 50:71–74. https://doi.org/10.1007/BF02594958

Porter M, Hove J Van, Barlow P et al (2019) The estimated economic impacts of prairie landslides in western Canada. In: Proceedings of the 72nd Canadian Geotechnical Conference. St. John's, Newfoundland and Labrador, p 8

Pratt C, Macciotta R, Hendry M (2019) Quantitative relationship between weather seasonality and rock fall occurrences north of Hope, BC, Canada. Bulletin of Engineering Geology and the Environment 78:3239–3251. https://doi.org/10.1007/s10064-018-1358-7

Prior GJ, Hathway B, Glombick PM, Pana DI, Banks CJ, Hay DC, Schneider CL, Grobe M, Elgr R, Weiss JA (2013) Bedrock geology of Alberta. Alberta Enery Regulator, AER/AGS Map 600, scale 1:1 000 000.

Rahardjo H, Li XW, Toll DG, Leong EC (2001) The effect of antecedent rainfall on slope stability. Geotech Geol Eng 19:371–399. https://doi.org/10.1023/A:1013129725263

Reeside JB (1957) Chapter 18: Paleoecology of the cretaceous seas of the western interior of the united states. In: Treatise on marine ecology and paleoecology. pp. 505–542. https://doi.org/10.1130/MEM67V2-p505

Reid LM, Page MJ (2003) Magnitude and frequency of landsliding in a large New Zealand catchment. Geomorphology 49:71–88. https://doi.org/10.1016/S0169-555X(02)00164-2

Rhinehart RR, Bethea RM (2021) Applied Engineering Statistics. (2nd ed.). CRC Press. https://doi.org/10.1201/9781003222330

Rodriguez J, Macciotta R, Hendry MT et al (2020) UAVs for monitoring, investigation, and mitigation design of a rock slope with multiple failure mechanisms—a case study. Landslides 17:2027–2040. https://doi.org/10.1007/s10346-020-01416-4

Rodriguez-Caballero E, Rodriguez-Lozano B, Segura-Tejada R et al (2021) Landslides on dry badlands: UAV images to identify the drivers controlling their unexpected occurrence on vegetated hillslopes. J Arid Environ 187:104434. https://doi.org/10.1016/j.jaridenv.2020.104434

Rosi A, Peternel T, Jemec-Auflič M, Komac M, Segoni S, Casagli N (2016) Rainfall thresholds for rainfall-induced landslides in Slovenia. Landslides 13:1571–1577. https://doi.org/10.1007/s10346-016-0733-3.

Roustaei M, Macciotta R, Hendry M et al (2020) Characterisation of a rock slope showing three weather-dominated failure modes. In: Proceedings of the 2020 International Symposium on Slope Stability in Open Pit Mining and Civil Engineering. Australian Centre for Geomechanics, Perth, pp 427–438

Russell LS (1932) Stratigraphy and structure of the eastern portion of the Blood Indian Reserve, Alberta. Geological Survey of Canada, Summary report, Part B. Ottawa, ON. https://publications.gc.ca/collections/collection_2017/rncan-nrcan/M41-2-1931-B-eng.pdf

Russell LS, Landes RW (1940) Geology of the southern Alberta plains. Geol Surv Canada, Memoir 221. https://doi.org/10.4095/101619

Saito H, Korup O, Uchida T et al (2014) Rainfall conditions, typhoon frequency, and contemporary landslide erosion in Japan. Geology 42:999–1002. https://doi.org/10.1130/G35680.1

Scafe DW (1975) Alberta bentonites. Alberta Research Council. Economic geology report No. 2. https://static.ags.aer.ca/files/document/ECO/ECO_2.pdf

Shu H, Hürlimann M, Molowny-Horas R et al (2019) Relation between land cover and landslide susceptibility in Val d'Aran, Pyrenees (Spain): Historical aspects, present situation and forward prediction. Sci Total Environ 693:1–14. https://doi.org/10.1016/j.scitotenv.2019.07.363

Song Y, Gong J, Gao S et al (2012) Susceptibility assessment of earthquake-induced landslides using Bayesian network: A case study in Beichuan, China. Comput Geosci 42:189–199. https://doi.org/10.1016/j.cageo.2011.09.011

Sowers GB, Sowers GF (1970) Introductory soil mechanics and foundations, 3rd ed. Macmillan, London

Stalker AM (1965) Pleistocene ice surface, Cypress Hills area. In: Cypress Hills plateau Alberta and Saskatchewan. Alberta society of petroleum geologists 15th annual field conference guidebook, Part 1, Cypress Hills plateau. pp. 116–130.

Stalker AM (1973) Surficial geology of the Drumheller area, Alberta. Geological Survey of Canada, Memoir 370. https://doi.org/10.4095/103298

Tappenden KM, Skirrow RK (2020) Vision for Geotechnical Asset Management at Alberta Transportation. In: GeoVirtual 2020, Resilience and Innovation, 14-16 September

Thomson S, Morgenstern NR (1977) Factors affecting distribution of landslides along rivers in southern Alberta. Canadian Geotechnical Journal 14:508–523. https://doi.org/doi:10.1139/t77-052

Thomson S, Morgenstern NR (1979) Landslides in argillaceous rock, prairie provinces, Canada. Developments in Geotechnical Engineering 14: 515–540. https://doi.org/10.1016/B978-0-444-41508-0.50022-3

Turner D, Lucieer A, Jong SM (2015) Time series analysis of landslide dynamics using an Unmanned Aerial Vehicle (UAV). Remote Sens 2015, Vol 7, Pages 1736-1757 7:1736–1757. https://doi.org/10.3390/RS70201736

Uchiogi T (1971) Landslides due to one continual rainfall. Japan Soc Eros Control Eng 23:21–34. https://doi.org/https://doi.org/10.11475/sabo1948.23.4_21

Vance RE, Beaudoin AB, Luckman BH (1995) The paleoecological record of 6 ka BP climate in the Canadian prairie provinces. Géographie physique et Quaternaire 49:81–98. https://doi.org/10.7202/033031ar

Varnes DJ (1978) Slope movement types and processes. In: Landslide analysis and national academy of sciences. Special Report 176. Transportation Research Board, pp 11–33

Vincent LA, Zhang X, Brown RD et al (2015) Observed trends in Canada's climate and Influence of low-frequency variability modes. J Clim 28:4545–4560. https://doi.org/10.1175/JCLI-D-14-00697.1

Wang T, Hamann A, Mbogga M (2008) ClimateAB v3.21 software package. available at http://tinyurl.com/ClimateAB

Weidner L, DePrekel K, Oommen T, Vitton S (2019) Investigating large landslides along a river valley using combined physical, statistical, and hydrologic modeling. Eng Geol 259:105169. https://doi.org/10.1016/j.enggeo.2019.105169

White RH, Anderson S, Booth JF et al (2023) The unprecedented Pacific Northwest heatwave of June 2021. Nat Commun 14:727. https://doi.org/10.1038/s41467-023-36289-3

Wieczorek GF (1996) Landslide triggering mechanisms. In: Turner AK. and Shuster RL (eds) Landslides: Investigation and Mitigation. Transportation Research Board Special Report 247, Wasington, DC, pp 76–90

Wieczorek GF, Jäger S (1996) Triggering mechanisms and depositional rates of postglacial slope-movement processes in the Yosemite Valley, California. Geomorphology 15:17–31. https://doi.org/10.1016/0169-555X(95)00112-I

Witte, R. S. and Witte, J. S. (2016) Statistics (11th ed.). John Wiley & Sons.

WMO (2019) Technical regulations, basic documents No. 2 volume I – General meteorological standards and recommended practices (WMO-No. 49). Geneva, Switzerland

Wolter A, Ward B, Millard T (2010) Instability in eight sub-basins of the Chilliwack River valley, British Columbia, Canada: A comparison of natural and logging-related landslides. Geomorphology 120:123–132. https://doi.org/10.1016/j.geomorph.2010.03.008

Wu C-Y, Chou P-K (2021) Prediction of total landslide volume in watershed scale under rainfall events using a probability model. Open Geosci 13:944–962. https://doi.org/10.1515/geo-2020-0284

Wu T, Lu Y, Fang Y et al (2019) The Beijing Climate Center Climate System Model (BCC-CSM): the main progress from CMIP5 to CMIP6. Geosci Model Dev 12:1573–1600. https://doi.org/10.5194/gmd-12-1573-2019

Wyllie DC (2014) Rock fall engineering. CRC Press. https://doi.org/10.1201/b17470

Wyllie DC (2017) Rock slope engineering. CRC Press, fifth edition. Taylor & Francis, CRC Press

Yang Z, Lv J, Shi W et al (2021) Experimental study of the freeze thaw characteristics of expansive soil slope models with different initial moisture contents. Sci Rep 11:23177. https://doi.org/10.1038/s41598-021-02662-9

Yuan G, Che A, Tang H (2021) Evaluation of soil damage degree under freeze–thaw cycles through electrical measurements. Eng Geol 293:106297. https://doi.org/10.1016/j.enggeo.2021.106297

Zhu AX, Miao Y, Wang R et al (2018) A comparative study of an expert knowledge-based model and two data-driven models for landslide susceptibility mapping. Catena 166:317–327. https://doi.org/10.1016/j.catena.2018.04.003